

Multispectral Determination of
Vegetative Cover in Corn Crop Canopies¹

E. R. Stoner
M. F. Baumgardner

June, 1972

Published by the
Laboratory for Applications of Remote Sensing (LARS)
and the
School of Agriculture
Purdue University
West Lafayette, Indiana 47906

¹This work was supported by the National Aeronautics and Space Administration under Grant No. NGL 15-005-112.

TABLE OF CONTENTS

	Page
LIST OF TABLES	vi
LIST OF FIGURES	viii
ABSTRACT	xi
INTRODUCTION	1
CHAPTER I - REVIEW OF LITERATURE	3
Crop Canopy Considerations in Remote Sensing	3
Plant Reflectance Properties	4
Reflective Properties of Background -- Soil, Shadows, and Non-Green Vegetation.	8
Incident Solar Spectral Properties	10
Methods of Estimating Percent Vegetative Cover	11
Direct Measurements	11
Photographic Methods	14
Spectrum Matching	15
Ratio Techniques	17
Theoretical Formulations	17
CHAPTER II - MATERIALS AND METHODS	21
Plot Location	21
Plot Design	22
Data Collection	24
CHAPTER III - LOW ALTITUDE PHOTOGRAPHY OF CORN CANOPIES	25
Problem Definition	25
Procedures	26
Photographic Data Collection and Ground Measurements	26

TABLE OF CONTENTS
(Continued)

	Page
Estimation of Percent Ground Cover by	
Point Grid System	27
Analysis of Digitized Photography	27
Characteristics of Color Infrared Film	27
Color Separation	29
Microdensitometry	31
Reformatting and Data Registration	33
Digital Display Imagery	34
Training Class Analysis - Clustering	36
Classification	40
Results and Discussion	42
Relating Estimated Percent Ground Cover to	
Leaf Area Index	42
Results of Classifications Using Three Color	
Separations	44
Evaluation of Color and Color Infrared Film in	
Determining Ground Cover	49
Need for More Quantifiable Information	51
Summary and Conclusions	51
 CHAPTER IV - AIRBORNE MULTISPECTRAL SCANNER DATA FROM	
CORN CANOPIES	53
Problem Definition	53
Procedures	54
Multispectral Scanner Data Collection	54
Digital Display Imagery	57
Locating Plots and Obtaining Mean Scanner Data	
Values	59
Ratio Techniques for Relating Scanner Response	
Ratios to Leaf Area Index	61
Results and Discussion	66
Visual Comparisons of Digital Display Imagery	66
Scanner Response Ratios and Leaf Area Index	
for Two Flight Dates	67
Problems in Evaluating Scanner Data Over Time	71
Summary and Conclusions	72
 CHAPTER V - NORMALIZED SPECTRAL RESPONSE OF CORN CANOPIES	
FROM AIRBORNE MULTISPECTRAL SCANNER DATA	73
Problem Definition	73
Procedures	74
Internal Calibration - Black Level and	
Calibration Lamp	74

TABLE OF CONTENTS
(Continued)

	Page
External Calibration - Ground Reflectance	
Panels	76
Locating Panels and Obtaining Mean	
Scanner Data Values	76
Laboratory Measurements of Spectral	
Reflectance of Panels	79
Evolving Prediction Equations for Relative	
Reflectance from Scanner Data Values	85
Determining Relative Reflectance of Plots	
Normalized to Panels	93
Ratio Techniques for Relating Normalized	
Reflectance to Leaf Area Index	93
Results and Discussion	93
Evaluation of Normalized Reflectance Curves	
of Corn Plots	93
Relative Reflectance Ratios and Leaf Area	
Index for Two Flight Dates.. . . .	106
Summary and Conclusions	109
BIBLIOGRAPHY	111

LIST OF TABLES

Table	Page
1. Assignment of planting dates to field plots	23
2. Point grid estimates and leaf area index measurements for 30 ground cover plots	28
3. Spectral bands from color separation of color and color infrared film	32
4. Percent ground cover determinations from 4 classifications of Chalmers plot 12	47
5. Percent ground cover determinations from classifications of three Chalmers plots in the near infrared	50
6. The 12 channels and corresponding wavelength bands for the University of Michigan multi- spectral scanner	56
7. Uncalibrated mean scanner data values for 12 Russell plots in 11 reflective wavelength bands for two flight dates	62
8. Ratios of uncalibrated scanner data values and leaf area indices for 12 Russell plots for two flight dates	65
9. Internal calibration values for two flight dates	77
10. Scanner data values for ground reflectance panels, calibrated to C0 and C1	80

LIST OF TABLES
(Continued)

Table	Page
11. DK-2 percent reflectance for two sets of color panels in the wavelength regions corresponding to channels of the multi-spectral scanner	86
12. Reflectance panels selected for regression analysis on two flight dates	87
13. Prediction equations for percent reflectance (relative to ground reflectance panels) from scanner data values calibrated to C0 and C1	91
14. Mean scanner data values calibrated to C0 and C1 for 12 Russell plots for two flight dates	94
15. Normalized reflectance (relative to ground reflectance panels) of Russell ground cover plots for two flight dates	96
16. Ratios of normalized reflectance in channels 8/7 and 9/7 for Russell plots on two flight dates	98

LIST OF FIGURES

Figure	Page
1. Solar energy spectrum; incremented in wave-length units and wave numbers (Gates, 1962, 1963, 1965)	12
2. "Mixing" of spectral response curves for green vegetation and soil for prediction of canopy response (Miller, 1969)	16
3. Energy absorbed by a plant canopy as a function of exposed soil (Gates, 1965)	19
4. Spectral sensitivity curves for Kodak Ektachrome Infrared film type 2443, and the spectral transmittance of Kodak Wratten filter No. 12 (Fritz, 1971)	30
5. Digital display images from 3 color separations of color IR film taken over 3 Chalmers plots	35
6. Color prints from color and color infrared photographs taken over 3 Chalmers plots	37
7. Coincident spectral plot for 5 cluster classes from digitized photography of Chalmers plot 12	41
8. Percent ground cover plotted against leaf area index for 30 observations	43
9. Computer display maps for 4 ground cover classifications of Chalmers plot 12	45

LIST OF FIGURES
(Continued)

Figure	Page
10. Computer display maps for ground cover classifications of Chalmers plots 9, 11, and 12, using near infrared color separations for classification	48
11. Ground reflectance panel placement at the Purdue University Agronomy Farm Weather Station, August 17, 1971	55
12. Digital display imagery of Russell plots and panels, July 12 scanner flight	58
13. Black and white scanner coincident photograph filtered to the red wavelength region, taken July 21, 1971 over the Purdue University Agronomy Farm Weather Station	60
14. Leaf area index versus the ratio of scanner data values in channels 9/7 for two flight dates	68
15. Leaf area index versus the ratio of scanner data values in channels 8/7 for two flight dates	70
16. DK-2 spectral reflectance for red, green, and blue LARS color panels	83
17. DK-2 spectral reflectance for 5 LARS gray scale panels	84
18. Percent reflectance versus scanner data values in channel 7 for 5 panels, July 21 scanner flight	88
19. Percent reflectance versus scanner data values in channel 9 for 8 panels, July 21 scanner flight	90
20. DK-2 spectral reflectance of corn leaves and two soils in air dry and saturated conditions	100
21. Uncalibrated scanner response curves for 3 Russell plots, July 12	102

LIST OF FIGURES
(Continued)

Figure	Page
22. Normalized spectral response curves for 3 Russell plots, July 12	104
23. Normalized spectral response curves for 3 Russell plots, July 21	105
24. Leaf area index versus the ratio of normalized reflectance in channels 9/7 for two flight dates	107
25. Leaf area index versus the ratio of normalized reflectance in channels 8/7 for two flight dates	108

ABSTRACT

This research was designed to study the relationship between different amounts of vegetative ground cover and the energy reflected by corn canopies. Low altitude photography and an airborne multispectral scanner were used to measure this reflected energy.

Field plots were laid out, representing four growth stages of corn. Two plot locations were chosen -- on a very dark and a very light surface soil. Color and color infrared photographs were taken from a vertical distance of 10 m. Estimates of ground cover were made from these photographs and were related to field measurements of leaf area index. Ground cover could be predicted from leaf area index measurements by a second order equation.

Color infrared photography proved helpful in determining ground cover on dark soil backgrounds. Color photography was useful for determining ground cover on light soil backgrounds, as long as the ground cover did not exceed about 75%.

Microdensitometry and digitization of the three separated dye layers of color infrared film showed that the near infrared dye layer is most valuable in ground cover determinations. Computer analysis of the digitized photography provided an accurate method of determining percent ground cover.

Multispectral scanner data were collected in two flights over the light soil background plots at an altitude of 305 m. Energy in eleven reflective wavelength bands from 0.46 to 2.6 μm was recorded by the scanner. A set of eight ground reflectance panels was in close proximity to the ground cover plots and was used to try to normalize the scanner data over time.

Ratio techniques were used to relate uncalibrated scanner response to leaf area index. The ratios of scanner data values for the 0.72 to 0.92 μm band over the 0.61 to 0.70 μm band and the 1.0 to 1.4 μm band over the 0.61 to 0.70 μm band were calculated for each plot. The ratios related very well to leaf area index for a given scanner flight date, but could not be generalized between flights because of uncertainty in scanner response over time.

Ground reflectance panels were used to relate laboratory reflectance measurements to scanner response. Separate prediction equations were obtained for both flight dates for all eleven reflective wavelength bands of the multispectral scanner. In this way, scanner response was normalized to ground panel reflectance. Ratios of normalized scanner data could be related to leaf area index over time.

The normalized scanner response was used to plot relative reflectance versus wavelength for the ground cover plots. Spectral response curves resulted which were similar to those for bare soil and green vegetation as determined by laboratory measurements. The spectral response of different ground cover plots represented a "mixing" of the spectral response curves for the bare soil and green vegetation components of the scene.

The spectral response curves from the normalized scanner data indicated that reflectance in the 0.72 to 1.3 μm wavelength range increased as leaf area index increased. A decrease in reflectance was observed in the 0.65 μm chlorophyll absorption band as leaf area index increased. This confirmed the validity of using the ratio of the response from a near infrared wavelength band to that of the red wavelength band in relating multispectral scanner data to leaf area index in corn.

INTRODUCTION

Properties of reflectance and emittance of energy have been studied for many natural earth surface features in connection with research in the field of remote sensing. Usually the spectral properties of individual samples of soils or plant materials are determined in the laboratory, and their properties are generalized to the field situation. Very little work has been done in measuring the spectral properties of the green vegetation - bare soil complex in the field.

An understanding of the component spectral properties of bare soil and green vegetation is a first step in determining the spectral properties of a crop canopy. Incident solar spectral properties also must be taken into account in the field situation.

In this study, photography and a multispectral scanner were used to determine some of the spatial, spectral, and temporal aspects of increasing ground cover in corn crop canopies. The corn canopy was chosen because of the prevalence of the corn crop in the Midwestern United States, and because of the interesting geometrical complexity of the canopy. Percent ground cover has always been most difficult to measure in corn canopies and has been a measurement of questionable value to the agronomist. Leaf area index could also be considered a measurement of

vegetative cover, and is of great value to the agronomist in determining the extent of utilization of energy from the sun in photosynthesis.

The potential for measuring vegetative cover from the spectral properties of a canopy holds promise in determining the above ground biomass of a crop by remote sensing techniques. In a general way the above ground biomass could then be related to crop yield.

Future efforts in remote sensing from orbital altitudes such as are proposed for the Earth Resources Technology Satellite (ERTS) and SKYLAB will be concerned with general views of agricultural crops. With the extremely high altitude and coarse resolution from space platforms, it is likely that any discrimination of healthy green agricultural crops will be on the basis of differences in vegetative cover, and not on individual plant spectral properties. Vegetative cover may well reflect disease infestations, drought stress, and other physiological stresses within a given crop type.

CHAPTER I

REVIEW OF LITERATURE

Crop Canopy Considerations in Remote Sensing

Remote sensing has been developing in recent years into a useful tool for the agronomist in characterizing the spectral, spatial, and temporal aspects of soils and plant communities (Hoffer, 1967; LARS, 1967; LARS, 1968; LARS, 1970). The extent of vegetative cover has been an important consideration to the crop and soil scientist in viewing agricultural land from a remote position. Multispectral scanner data from fields of bare, uniformly cultivated soil have been useful in delineating soil boundaries of interest to the soil mapper. Scanner data from full crop covers have been useful in general crop inventory and detection of physiological stress in plants. A partial ground cover tends to complicate the interpretation of the scene for both the crop and soil scientist. Knowledge of the extent of vegetative cover will be necessary as agronomists attempt to refine their interpretation of remotely sensed data.

Remote sensing has potential utility in the determination of the amount of vegetative cover in the above ground portion of the crop biomass. Miller and Pearson (1971) attempted to measure spectrally the

standing crop biomass of a shortgrass prairie vegetation. They reasoned that a measure of percent vegetative cover or leaf area index would relate to the carrying capacity for grazing in an area. It is reasonable to assume that the same principle could be used to relate vegetative cover in corn canopies to the above ground biomass of corn and, perhaps, in a relative way to corn yield.

Spectral response data obtained with an airborne multispectral scanner over a particular crop represent an integration of the radiation from both plants and soils in the instantaneous field of view of the scanner. Many variables come into play which affect the intensity and wavelength of radiation from both plants and soil. Leaf angle, leaf moisture content, leaf area index, plant geometry, variety or species, and planting technique will affect the spectral response from plants in a field situation. Moisture content, texture, surface crusting, organic matter content, surface residue, and color will affect the spectral response from surface soil. In order to understand the soil-crop complex it is first necessary to look at the individual factors which have an effect on intensity and wavelength of the energy radiating from plants and soils.

Plant Reflectance Properties

The spectral response from an individual plant leaf in the 0.4 to 2.6 μm wavelength reflective range can be broken up into three portions (Hoffer and Johannsen, 1969): 1. The visible wavelengths where pigment absorption predominates, 2. The 0.72 to 1.3 μm wavelength region where very little absorption takes place and almost all the incident light is

transmitted or reflected, and 3. The 1.3 to 3.0 μm wavelength region where prominent water absorption takes place at 1.45 μm and 1.95 μm . Chlorophyll, carotene, anthocyanin, and xanthophyll absorb at 0.445 μm in the blue, while chlorophyll alone absorbs at 0.645 μm in the red portion of the spectrum (Gates, et al., 1965). Reflectance in the visible peaks at 0.540 μm in the green region for green leaves and accounts for the green color of plants perceived by the human eye. According to Knipling (1970) about 40 to 60 percent of the infrared radiation in the wavelength range from 0.7 to 1.3 μm is scattered upward through the surface of incidence and is designated as reflected radiation, whereas the remainder is scattered downward and transmitted. The strong absorption by a leaf in the infrared beyond 1.3 μm is due to water, as supported by theoretical considerations of the equivalent water thickness of leaves (Knipling, 1970). Absorption of radiation in plants is very high in the visible portion of the spectrum where energy is needed for photosynthesis and drops quite low from 0.7 to 1.1 μm where most of the energy of the solar spectrum is concentrated. Absorption rises again in the 1.3 to 3.0 μm region. Thus, a plant's spectral properties allow it to absorb energy where it is needed for growth, and reflect and transmit energy where it is detrimental.

Leaf moisture content has a consistent effect on reflectance in all reflective wavelength regions. Johannsen (1969), working with corn and soybeans, found a high negative correlation between DK-2 spectrophotometric leaf reflectance and leaf moisture in the chlorophyll absorption band at 0.64 μm , and concluded that leaf moisture may be changing leaf pigments in short periods of time. Johannsen also found high

negative correlation between leaf reflectance and leaf moisture in the water absorption bands at 1.43 μm and 1.94 μm and in the green peak at 0.53 μm . He concluded that reflectance measurements from corn and soybean leaves showed a steady increase in all reflective wavelengths with decreasing leaf moisture. Johannsen reported diurnal effects on leaf moisture content. Leaf moisture seemed to increase with increasing soil moisture. Scanner data from corn canopies gave decreasing reflectance with increasing plant and soil moisture.

Leaf structural parts exhibit varying effects on reflectance properties of plants. Gausman, Allen, and Cardenas (1969), working with salinity stressed cotton, reported that changes in reflectance in the 0.75 to 1.3 μm range were primarily due to changes in internal structure and not leaf moisture content. They associated increased reflectance with thicker leaves having stronger palisade cell development, loosely arranged spongy mesophyll, and hence, more intercellular space or interfaces. Sinclair (1968) found that the greatest reflectance in the shorter infrared wavelengths came from the internal leaf structure which had the greatest amount of cell wall material perpendicular to the incident radiation. Thus, he found that the palisade tissue was more reflective in dorsiventral leaves (typical of dicotyledonous plants like the soybean) since it provided greater barriers of cell walls to impinging radiation than did spongy mesophyll tissue. Sinclair also reported that the cuticle probably contributes a relatively small portion of the total leaf reflectance observed in the wavelength bands highly reflected by leaves. In the highly absorbed bands, though, he found that cuticular reflectance may contribute nearly all of the leaf reflectance observed.

Plant leaves may be diffuse or specular reflectors depending on the wavelength of interest. Sinclair (1968) reasoned that in order to obtain high levels of reflectance in the shorter infrared wavelengths, the cell walls must be diffuse reflectors of incident radiation. Breece and Holmes (1971), in a study of the bidirectional scattering characteristics of corn and soybean leaves, found that for wavelengths beyond $0.75\ \mu\text{m}$, reflectance was nearly Lambertian in character. They reported that the more strongly absorbed visible wavelengths showed a tendency to reflect specularly the radiation incident upon the leaf.

When the spectral response from stacked leaves or leaves in a canopy is considered, the idealized single leaf spectral reflectance becomes much more complicated. Myers et al. (1966), in an experiment with stacked leaves, reported that no difference in reflectance occurred in the visible wavelengths for any combination of stacked leaves, but a 17% increase in the reflectance occurred in the near infrared for two leaf layers. As the number of leaf layers increased up to six layers, the reflectance increased in the near infrared except in the $1.45\ \mu\text{m}$ and $1.95\ \mu\text{m}$ water absorption bands. The probable explanation for this enhanced reflectance with multiple leaf layers in the near infrared is a retransmission of infrared radiation back through the canopy from lower layer reflection. Myers (1970) reasoned that the leaf layers could be related to an actual measure of leaf density or leaf area index (LAI). Leaf area index is the ratio of leaf area to soil area in a plant canopy. Myers reported that Kodak Ektachrome Infrared Aero film, which is sensitive in the wavelength interval from 0.4 to $0.9\ \mu\text{m}$, could be used to record variations in reflectance associated with leaf area index.

For the real situation of leaves in a crop canopy, reflectance is considerably less than for a single leaf because of general attenuation of radiation by variations in illumination angle, leaf orientation, shadows, and non foliage background (soil in most cases). Vinogradov (1969) concludes that the reflectance for vegetation decreases with an increase in the roughness of the surface geometry of the plant canopy. He states that the reflectivity for the soil-plant system decreases with the increase in leaf area index, but that beyond an LAI of 3 or 4, a further decrease in the reflectance practically does not occur. Vinogradov, however, reports that reflectance in the 0.72 to 0.98 μm wavelength band is augmented with an increase in ground cover, height, and leaf area index. Knipling (1969) estimates that the visible and near infrared reflectance from a complete canopy may be 3% to 5% and 35% respectively versus 10% and 50% for a single leaf. This would be a 60% reduction in reflectance in the visible and a 30% reduction in reflectance in the near infrared. The relatively smaller reduction in the near infrared is accounted for by enhanced reflectance in the multiple leaf layered-canopy.

Reflective Properties of Background --

Soil, Shadows, and Non-Green Vegetation

Baumgardner et al. (1970) found that organic matter plays an important role in bestowing spectral properties to soils when the organic matter content is above 2%. As the organic matter content drops below 2% it may be less effective in masking out the effects of other soil constituents such as iron oxides.

Bouyoucos (1913) showed that different types of soil tended to radiate heat energy differently when dry and about the same or more when well moistened and in their natural condition. Hoffer and Johannsen (1969) showed that moist soils had an overall lower reflectance than their dry counterpart in the 0.4 to 2.6 μm wavelength region. They also found, however, that crusting of surface soil can make a soil appear dry when it is actually wet. Cipra et al. (1971) found that crusted surfaces gave higher reflectance values in the 0.43 to 0.73 μm wavelength region than did soils with the crust broken. They attributed the lower reflectance of the disturbed soil to the rough surface which presumably caused scattering of light as well as a shadowing effect. Because of this crusting effect the emissive wavelengths in combination with the reflective wavelengths could give the best clues to soil moisture content. Bowers and Hanks (1965) estimated that an additional 14% to 18% of the direct solar energy was absorbed by a silt loam due to an increase in moisture content.

Differences in soil texture may account for differences in spectral response. Bowers and Hanks (1965) found differences in reflectance as large as 24% evident for soil particles ranging from 22 μm to 2680 μm in size (coarse clay to sand size fractions). They found a rapid exponential increase in reflectance with decreasing particle size. The field situation may not be very similar since surface soil aggregates of varying sizes will predominate.

Soil color may be related to organic matter content, the presence of oxidized or reduced iron compounds, and the internal drainage characteristics of the soil. Lighter colored soils may have lower organic

matter contents, higher percentages of oxidized iron compounds, and good natural drainage. Darker soils may have high organic matter contents, reduced iron compounds, and poor natural drainage. For the 0.3 to 1.0 μm wavelength region, Condit (1970) studied the spectral properties of many surface soils having a wide variety of colors and textures.

Factors whose effects on the spectral reflectance of surface soils are most important, yet more difficult to quantitize, are soil surface roughness, shadowing, and non-green crop residue. Tillage effects and the resulting clod size of cultivated soil will impart varying spectral characteristics to bare soil. As for shadow effects, Miller and Pearson (1971) felt that shadows might be considered a spectrally separate material upon first investigation, but that shadows would more accurately be described in terms of modified spectral properties of the materials upon which the shadows fall. Shadows in a canopy are certainly elusive and hard to measure at ground level. Non-green crop residue will have to be considered as part of the background scene when it is present in large enough amounts to affect the spectral properties of the canopy. Although this component may play a large part in grassland canopy considerations, non-green vegetation should not be too complicating a factor in cultivated crops.

Incident Solar Spectral Properties

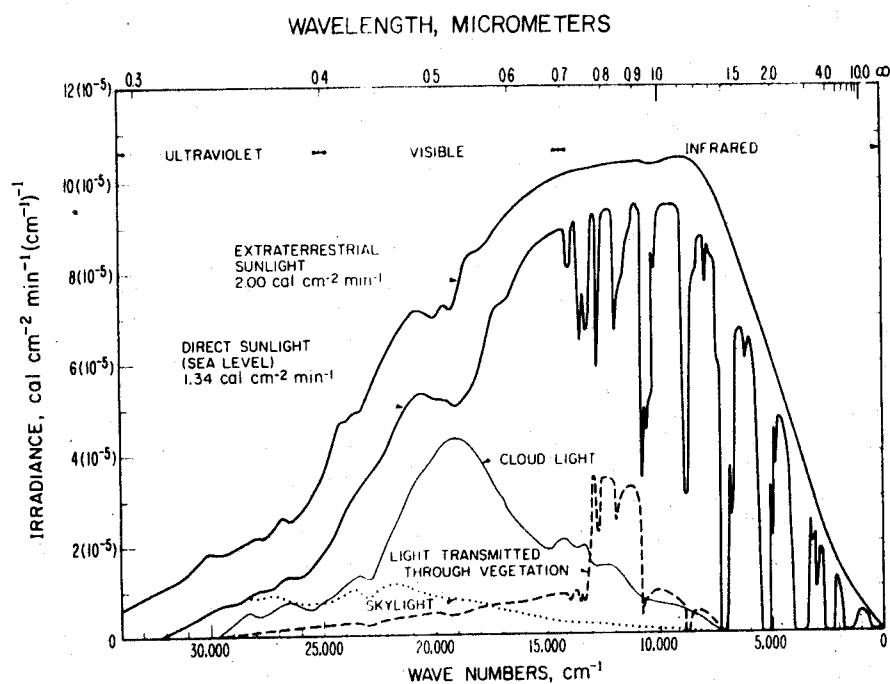
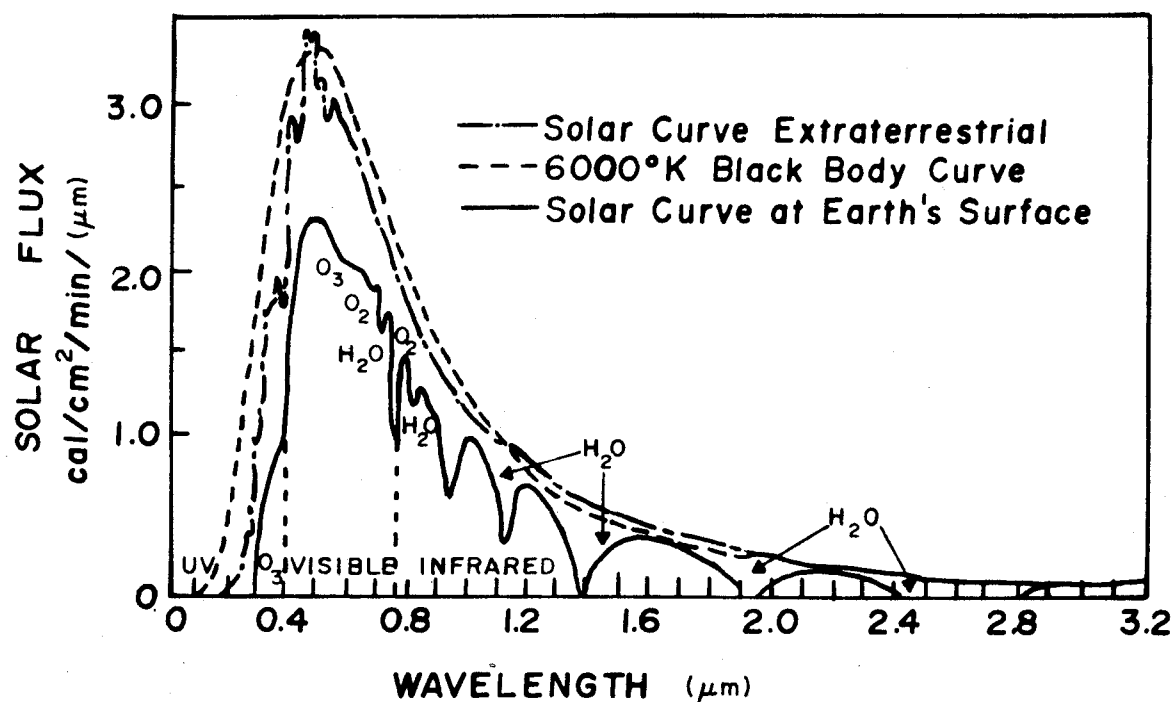
The character of reflected and emitted light from a plant canopy will depend on the nature of the surface and the intensity and spectral quality of the radiation incident upon the surface. The plant canopy may be irradiated by direct sunlight, scattered skylight, and thermal radiation from the surroundings. Idso, Baker, and Gates (1966) reported that

scattered or diffuse radiation (skylight) makes up as much as 10% to 15% of the direct sunlight on a clear day. Cloud light, or the diffuse radiation which is the result of a complete overcast, is another type of solar radiation which may be present. Idso (1966) also lists two other types of solar energy: 1. that transmitted through the leaves of a canopy, and 2. that radiation reflected from other plants (which is usually rich in the green and near infrared wavelengths). Figure 1 from Gates (1962, 1963, 1965) shows the distribution of solar energy at the earth's surface with the accompanying absorption bands for O_2 , O_3 , and H_2O . Figure 1a. is in the familiar increments of wavelength while Figure 1b. is incremented in wave numbers. The various absorption bands are evident, and the great variation between the intensity and quality of direct sunlight, cloud light, and skylight is made evident. The choice of spectral bands for analysis of a vegetated surface would have to be made with reference to the incident solar energy as well as the soil and plant spectral characteristics.

Methods of Estimating Percent Vegetative Cover

Direct Measurements

According to Miller and Pearson (1971) there is no rapid method which has been found practical for measuring percent ground cover from the ground location of the observer. Estimates of percent ground cover can be made by individual research workers and checked for consistency with estimates of other researchers. The subjectivity involved in ground level estimation of percent ground cover is even further increased in a complex canopy such as the corn canopy where view angle effects, height



b. wave number increments

Figure 1. Solar energy spectrum; incremented in wavelength units and wave numbers (Gates, 1962, 1963, 1965).

effects, and shadowing complicate the scene. Nevertheless, ground measurement methods for percent ground cover have been attempted, and Cuellar (1971) suggests methods for two different canopy structures:

1. Solid canopy with bare soil exposed only in the furrows: The "bare soil width" and row width are measured, the bare soil width being the amount of bare soil showing between the canopies of adjacent rows. Percent crop cover is calculated as:

$$\left(\frac{RW - BW}{RW} \right) \times 100 = \text{percent cover}$$

where

RW = row width in cm.

BW = bare soil width in cm.

2. Open canopy with bare soil exposed through the canopy and furrow: The open canopy is considered as being "solid," and the formula above is used. A subjective estimate is made of the open spaces in the canopy, and this amount is subtracted from the assumed cover to obtain actual cover.

In the second method, used for corn crop canopies, the subjectivity involved can be readily seen. Cuellar found it especially difficult to estimate cover as ground cover approached 100%, especially in tall crop canopies such as corn where ground observers were unable to look down at the crop.

A more quantitative measure for characterizing the extent of vegetative cover would be that of leaf area index (LAI). Although leaf area index has not yet been found to relate directly to percent ground cover, its usage is consistent with multi-layer models of plant canopies, as discussed earlier. Leaf area index, of itself, should certainly be a valuable measure of above ground biomass. In the case of the corn

canopy, the LAI is easily calculated by measuring the length and width of each leaf of a corn plant, multiplying these together times a factor of 0.73 to account for the non-rectangular form of the corn leaf (McKee, 1964), and multiplying this times the plant population per unit area of soil.

For shortgrass prairie vegetation the point-quadrat method has proved valuable for measuring percent ground cover (Miller and Pearson, 1971). This method would be impractical for canopies of considerable height. Equally unsuitable would be destructive sampling methods of the canopy vegetation when additional measurements are desired over time.

Photographic Methods

Various photographic approaches have been used to arrive at an estimate of the amount of surface covered by a vegetative canopy. Perhaps the most unusual approach was that of McCree (1968) who chose to view the plant canopy from the ground level looking vertically upwards. He used a 180° mirror to photograph the canopy of willow trees and was able to relate tonal response on color infrared film with sunlit leaves, clear sky, shade light, and sunlight. Similar photographs have been taken of corn canopies (LARS, 1968) from a ground position with a wide angle lens. The resultant photographs give a qualitative view of the canopy cover and the amount of transmitted light.

In viewing the plant canopy from a vertical position, Miller (1969) found that dark colored soils and dark, wet soils had a suitably low reflectance in the 0.7 to 0.9 μ m wavelength band so that response in the instantaneous field of view of a crop canopy would be approximately equal to percent cover of vegetation. Hoffer (1967) also found the

photographic infrared wavelengths useful in estimating ground cover on dark soils and noted that increasing canopy resulted in higher response on infrared film. For light soils, with high reflectance relative to plants, the visible photographic wavelengths were best for determining percent vegetative cover. On light soils the 0.7 to 0.9 μm band showed a blending of soil and highly reflective vegetation resulting in a relatively uniform response despite variations in ground cover. In the visible wavelengths, however, the light colored soil did not blend with the vegetation and the density of vegetative cover was proportional to the decrease in response registered on film.

A sampling method was used by Null (1969) to measure canopy density from photography. He used a point grid system to estimate the percent of film area represented by vegetation.

Spectrum Matching

For estimating percent green vegetation on light colored soils, Miller (1969) suggests a technique of "spectrum matching" in which pure samples of vegetation and soil are "mixed" to form a set of test spectra representing various levels of percent vegetative cover. The spectral response values from the instantaneous field of view of the remote sensing device could be matched with these test spectra to estimate percent ground cover. Figure 2 (Miller, 1969) illustrates this procedure for low, medium, and high percent ground cover situations.

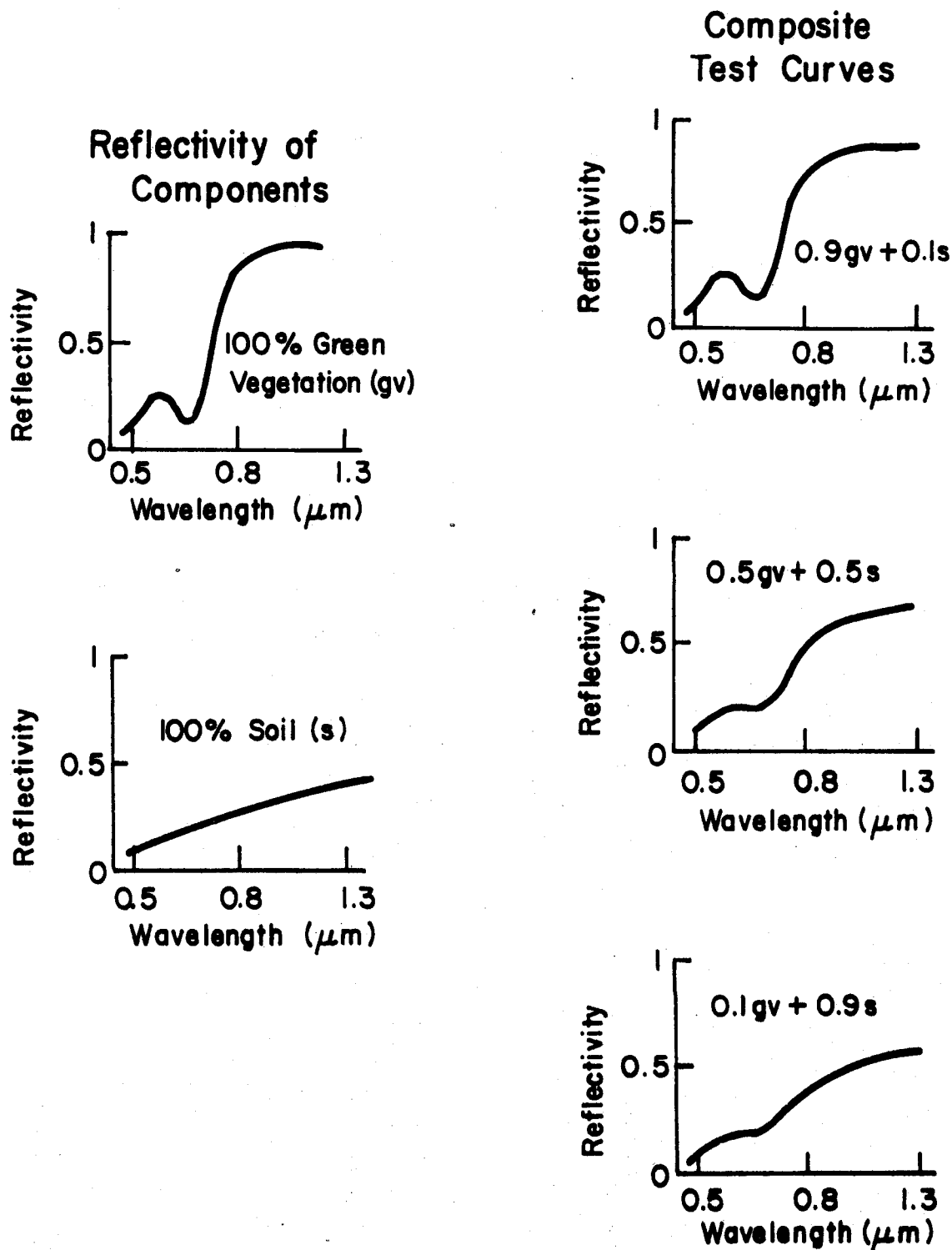


Figure 2. "Mixing" of spectral response curves for green vegetation and soil for prediction of canopy response (Miller, 1969).

Ratio Techniques

Kristof and Baumgardner (1970) found that a decrease in radiation in the visible and an increase in the reflective infrared region occurred in comparing multispectral scanner data over crop cover from April to late June. Disregarding complications of row structure and direction which may produce a "stove pipe effect" (LARS, 1968) in corn canopies, the increase in ground cover could be detected by establishing a ratio of the relative reflectance in the chlorophyll absorption band to the relative reflectance in the near infrared. Kristof and Baumgardner (1970) used the ratio of relative reflectance in the 0.58 to 0.62 μm band to the relative reflectance in the 0.80 to 1.00 μm band to observe increases in ground cover. With the increased reflectance in the near infrared and the increased chlorophyll absorption with increasing crop cover, this ratio would decrease with increasing crop canopy. For a given crop and soil type an estimate of the percent ground cover could possibly be made from the value of the ratio of the relative reflectance from two channels of a multispectral scanner.

Theoretical Formulations

Various investigators have attempted theoretical models for estimating the radiation response from the soil background and plant components of a plant canopy. Allen and Richardson (1968) used the two parameter Kubelka-Munk theory to arrive at theoretical values for reflectance and transmittance of a plant canopy from the leaf area, an absorption coefficient, a scattering coefficient, and the background reflectivity. The two coefficients are based on crop geometry and the

optical properties of the individual leaves. The validity of this theory in an actual situation is doubtful, since it assumes a uniform distribution of leaf inclinations and assumes infinite lateral extension to the canopy.

Idso and deWit (1970) improved on the Kubelka-Munk theory by including a factor called the leaf distribution function, which characterizes the frequency distribution of plant leaf inclination from the horizontal. The so-called deWit-Idso theory introduces leaf area index and canopy density to consider the extinction of the solar beam as it penetrates the canopy foliage. The deWit-Idso theory gives information on the fraction of leaves in each layer receiving diffuse and direct light at various angles of inclination to the sun's radiation.

Gates (1965) arrived at a formula for the total radiation absorbed by a stand of vegetation and soil. Figure 3 from Gates (1965) shows that the energy absorbed by a plant canopy increases with exposed soil up to a point (about 40% ground cover) but then declines in a parabolic manner. Gates found that the reflected solar component has only a fairly strong dependence upon the amount of plant cover on dark soils.

Holmes and MacDonald (1969) arrived at a formula for the integrated radiance vector for crop canopies as follows:

$$\text{total radiation} = \alpha_{r_{BL}} + \beta_{r_{SL}} + \gamma_{r_{BS}} + \delta_{r_{SS}}$$

where r = the radiation vector for: BL (bright leaves)
SL (shaded leaves)
BS (bright soil)
SS (shaded soil)

$\alpha, \beta, \gamma, \delta$ are terms for the ratios of the projected areas of the four component scenes to the projected viewed scene area, on a plane normal to the line-of-sight.

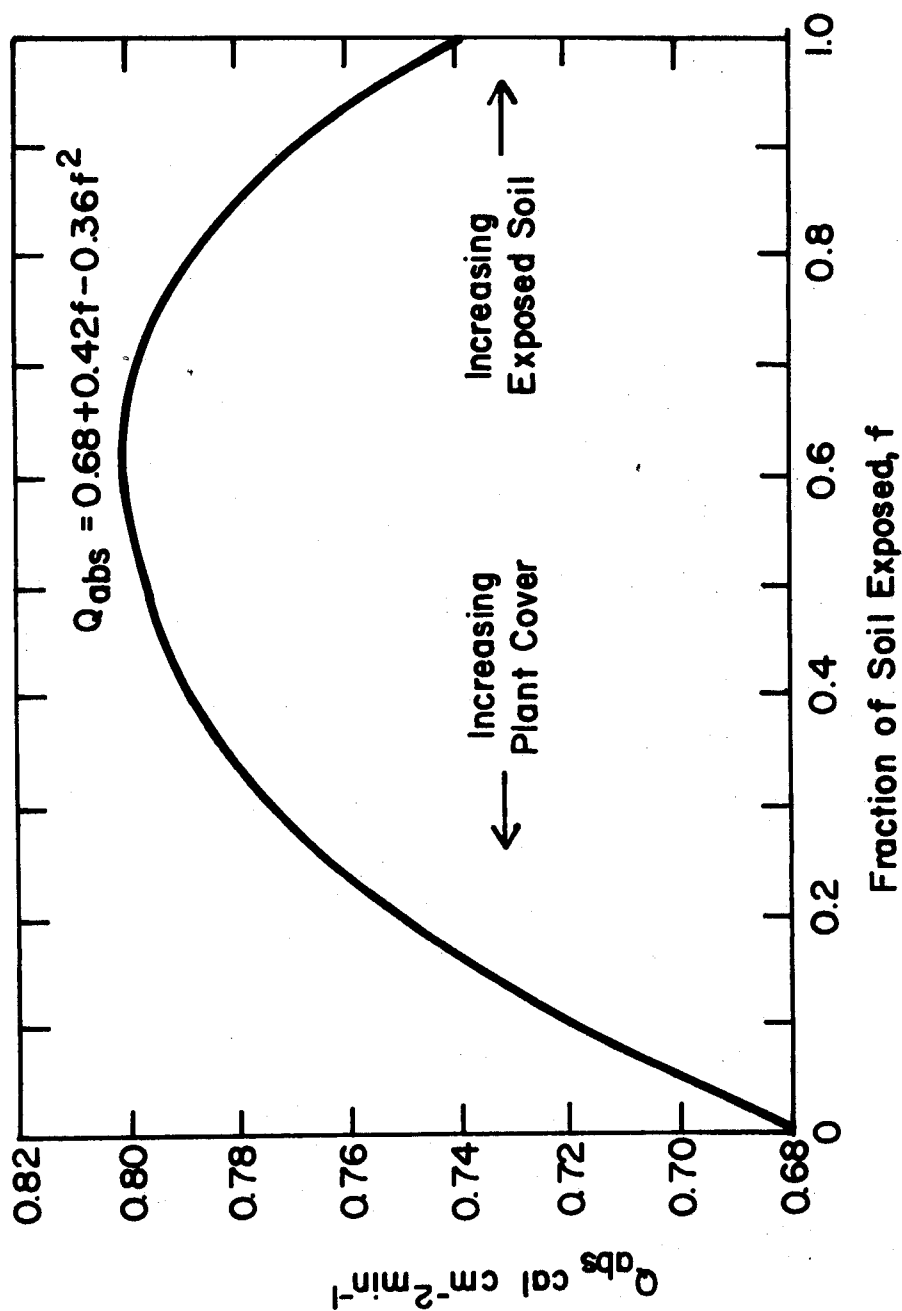


Figure 3. Energy absorbed by a plant canopy as a function of exposed soil (Gates, 1965).

The sum of the four component ratios should be one. This formula is valuable for its inclusion of the components of shaded leaves and soil in the radiation scheme. Variations in view angle, sun angle, and row direction are considered in this formulation of crop canopy radiance as detected by the instantaneous field of view of an airborne scanner.

A very thorough review of plant and soil reflective properties was conducted by Kumar (1972). This review contains a more detailed description of theoretical plant canopy models. Krumpe (1972) compiled a bibliography of over 850 references on remote sensing of terrestrial vegetation, covering most of the material published from 1955 to the present.

CHAPTER II

MATERIALS AND METHODS

Plot Location

During the summer of 1971 an experiment was carried out utilizing the facilities of the Laboratory for Applications of Remote Sensing (LARS) and the Purdue University Agronomy Farm to study the extent of vegetative cover of different growth stages in corn canopies. The objective was to observe and study the reflectance characteristics of corn canopies with both light and dark surface soil backgrounds. To this end, two plot locations were chosen at the Purdue University Agronomy Farm representing a light colored forest soil and dark colored prairie soil. Agronomy Farm plot number 15 was chosen as the site with a light surface soil, Russell silt loam, a well-drained alfisol with a dry Munsell color of 10 YR 6/2 and an organic matter content of about 3%. Agronomy Farm plot number 44 was chosen as the site with a dark surface soil, Chalmers silty clay loam, a very poorly drained mollisol with a dry Munsell color of 10 YR 4/1 and an organic matter content of about 6%.

The plots were located on the northern edges of plots 15 and 44, both bulk corn plots, so that shadowing problems would be minimized when data were taken from a Hi-Ranger bucket above the plots. The light

colored Russell soil site was very near the Agronomy Farm Weather Station, location of LARS ground reflectance panel deployment, and was thus in the path of several flights by the University of Michigan's multispectral scanner. The scanner plane did not fly over the dark colored Chalmers soil site.

Plot Design

In order to facilitate data collection and provide a wide range of ground covers on any given date of a scanner overflight or photographic mission, four different planting dates were used. Pioneer 3369A corn was planted in three replications at each site location on each of the following four dates: April 30, May 22, June 9, and June 30. This provided a spacing of 22, 18, and 21 days between planting dates, respectively.

Each plot extended 55 meters along the edge of the bulk corn fields and consisted of twelve sub-plots 4.57 by 4.57 meters in size. Each sub-plot contained six rows of corn, 4.57 meters long in 76 cm rows. Replications of planting dates were assigned randomly to the twelve sub-plots. Table 1 illustrates the layout of the two plots.

No special fertility treatments were used, and adequate fertility levels were maintained for the Agronomy Farm's bulk corn production. A plant population of about 49,400 plants per hectare was desired, and actual populations of from 43,200 to 50,700 plants per hectare were obtained. Actual plant counts were taken in each sub-plot for the calculation of leaf area within the sub-plot.

Table 1. Assignment of planting dates to field plots.

Planting Dates

A = April 30

B = May 22

C = June 9

D = June 30

RUSSELL PLOTS

Plot No.	1	2	3	4	5	6	7	8	9	10	11	12
	D	B	A	C	D	B	C	D	A	C	B	A

\updownarrow
 4.57 m
 $\leftarrow \rightarrow$
 4.57 m

CHALMERS PLOTS

Plot No.	1	2	3	4	5	6	7	8	9	10	11	12
	C	A	D	B	D	C	B	A	A	D	C	B

Data Collection

At the time of scanner overflights and photographic missions, field measurements of plant height and leaf area were made. Two plants were chosen at random from each sub-plot, and the plant height and leaf area were calculated from the average of these measurements. Leaf area was calculated using the method of McKee (1964) in which the length and width of each leaf on the corn plant are measured and multiplied together times a factor of 0.73 to account for the non-rectangular form of the corn leaf. Leaf area index is then calculated from the average leaf area per plant and the plant population per unit area of soil.

On the four dates, July 13, July 21, August 3, and August 17, the LARS Hi-Ranger truck was used to obtain vertical photographs over the sub-plots from an altitude of approximately 10 meters. Color and color infrared photography were taken on these dates with two Nikkormat 35 mm cameras. A typical frame of photography contained four full rows of each sub-plot, so that border effects could be eliminated.

Numerous multispectral scanner overflights were available from the summer of 1971, but only two of these were selected for analysis. The University of Michigan's multispectral scanner collected spectral data in eleven channels in the reflective wavelength range of 0.46 to 2.60 μm from overflights on July 12 and July 21, 1971. Both flights were at an altitude of about 305 meters and were flown in a north-south flight path directly over the Agronomy Farm Weather Station. The scanner data tapes were converted from analog to digital form and were reformatted for processing on the LARS IBM 360/67 digital computer.

CHAPTER III

LOW ALTITUDE PHOTOGRAPHY OF CORN CANOPIES

Problem Definition

Numerous investigators have examined the usefulness of color and color infrared photography of plant canopies in determining percent ground cover (Hoffer, 1967; McCree, 1968; Miller, 1969). Color film is generally felt to be best for ground cover determination on light colored soil backgrounds. Color infrared film has been of value in ground cover determination on dark colored soil backgrounds.

Characteristics of color and color infrared film prevent the researcher from obtaining quantifiable spectral information about plant canopies from these film types. Relative spectral measurements can be made, however, by photographic separation of the dye layers of the film and microdensitometry of these color separations. Computer analysis of digitized photography provides a means for distinguishing between the components of green vegetation and bare soil by analysis of spectrally separable classes. Digitization of low altitude photography thus provides a useful technique for analysis of the spectral and spatial relationships in plant canopies.

Procedures

Photographic Data Collection and Ground Measurements

Vertical photographs were obtained from the 24 individual sub-plots on four dates: July 13, July 21, August 3, and August 17, 1971. The LARS Hi-Ranger truck was used to take the photographs from an altitude of about 10 meters. Color (Kodak Ektachrome-X and Kodachrome II) and color infrared (Kodak Ektachrome Infrared Type 2443) transparency films were used in two Nikkormat 35 mm cameras with 50 mm focal length lenses to obtain the photographic data. A Kodak Wratten No. 12 filter was used with the Kodak Ektachrome Infrared film, and a skylight filter was used with the Kodak Ektachrome-X and Kodachrome II films. Simultaneous photographs were taken of each plot with the two cameras in such a way that four corn rows filled the field of view. The resulting scale on the 35 mm transparencies was 1:200.

Within one day of the photographic data collection, ground measurements were made of plant height and leaf area. Two plants were chosen at random from the sub-plots for these measurements, and leaf area was determined by the method described in the previous chapter. No attempt was made to measure actual percent ground cover since the geometry of the canopy prohibited anything but rough estimation of ground cover from ground level. Leaf area index determinations were preferable because of the ease and non-subjectivity of measurement. Percent ground cover estimates were limited to measurements taken from the low-altitude photography using the dot grid system described in the next section.

Estimation of Percent Ground Cover by Point Grid System

Thirty photographs were selected for percent ground cover estimation by a point grid technique. This included 12 Kodachrome II photographs of the Russell plots taken July 13, 12 Ektachrome-X photographs of the Russell plots taken July 21, 3 Ektachrome-X photographs of the Russell plots taken August 3, and 3 Ektachrome Infrared photographs of the Chalmers plots taken on July 13. These particular photographs were chosen because of their high quality and because of the diversity of ground covers represented among them.

The 24 by 36 mm transparencies were projected onto a rear-viewing screen and enlarged 15 times to a size of 16 by 24 cm. This gave a scale of about 1:30 for the enlarged image. A point grid of 1 point per 5.6 mm was overlaid on the screen, and a rectangular sample of two corn rows from the center of the frame was outlined. All the points which fell on corn plants were tallied and expressed as a percent of the total number of points within the bounded area, resulting in an estimate of percent ground cover. Table 2 lists the 30 plots, their planting dates, observation dates, leaf area indices, and point grid estimates of percent ground cover. Regression analysis was performed to determine if percent ground cover could be related to leaf area index.

Analysis of Digitized Photography

Characteristics of Color Infrared Film. The range of spectral sensitivity of color infrared film is extended into the near infrared wavelength region, where vegetation typically has a very strong spectral response. Kodak Ektachrome Infrared Film Type 2443, is the latest

Table 2. Point grid estimates and leaf area index measurements for 30 ground cover plots.

<u>Plot</u>	<u>Planting Date</u>	<u>Observation Date</u>	<u>LAI</u>	<u>Estimated Percent Ground Cover</u>
RP1	June 30	July 13	0.01	3.3
RP2	May 22	July 13	2.89	87.2
RP3	April 30	July 13	3.48	93.8
RP4	June 9	July 13	1.30	60.0
RP5	June 30	July 13	0.01	3.3
RP6	May 22	July 13	2.34	88.8
RP7	June 9	July 13	1.11	52.8
RP8	June 30	July 13	0.04	7.6
RP9	April 30	July 13	3.10	87.2
RP10	June 9	July 13	1.17	42.8
RP11	May 22	July 13	2.93	83.2
RP12	April 30	July 13	3.81	91.8
RP1	June 30	July 21	0.11	3.5
RP2	May 22	July 21	3.00	94.6
RP3	April 30	July 21	4.28	89.5
RP4	June 9	July 21	2.31	81.5
RP5	June 30	July 21	0.12	4.8
RP6	May 22	July 21	3.57	89.1
RP7	June 9	July 21	2.15	78.2
RP8	June 30	July 21	0.17	12.2
RP9	April 30	July 21	3.38	93.9
RP10	June 9	July 21	2.10	72.7
RP11	May 22	July 21	3.45	88.5
RP12	April 30	July 21	4.06	94.7
RP1	June 30	August 3	0.57	29.0
RP5	June 30	August 3	0.63	23.8
RP8	June 30	August 3	0.93	34.8
CP9	April 30	July 13	4.44	96.5
CP11	June 9	July 13	1.31	70.7
CP12	May 22	July 13	2.93	90.3

RP = Russell Plot

CP = Chalmers Plot

version of Kodak's multi-emulsion color infrared film. Fritz (1971) illustrates the wavelengths of spectral sensitivity for the film's three emulsion layers as well as the cutoff point for the Kodak Wratten No. 12 filter (Figure 4).

Knipling (1969) describes the spectral sensitivities of color infrared film and the image forming processes. The film has three dye layers: 1. a cyan forming layer sensitive to the near infrared wavelengths, 2. a magenta forming layer sensitive to the red visible wavelengths, and 3. a yellow forming layer sensitive to the green visible wavelengths. All three emulsions are sensitive to radiation below $0.5\ \mu\text{m}$, but these wavelengths are eliminated using the deep yellow Wratten No. 12 filter. Thus, color infrared film has two dye layers sensitive to visible light excluding the blue, and one dye layer sensitive to the near infrared. It is stressed that this film is not sensitive to the thermal, but rather is sensitive only up to $0.89\ \mu\text{m}$ in the shorter wavelength infrared. Ektachrome Infrared Film Type 2443 is sensitive to wavelengths from 0.47 to $0.89\ \mu\text{m}$ as compared to Ektachrome-X or Kodachrome II which are sensitive to wavelengths from 0.40 to $0.71\ \mu\text{m}$. The $0.72\ \mu\text{m}$ wavelength is generally considered to be the boundary between the visible and infrared wavelength regions.

Color Separation. Twenty color and color infrared transparencies were chosen for color separation and microdensitometry. Sixteen color and four color infrared transparencies were among those used. Before the color and color infrared multi-emulsion films could be densitometered, they had to be separated by a standard commercial process into the three emulsion layers and reproduced as black and white positive transparencies.

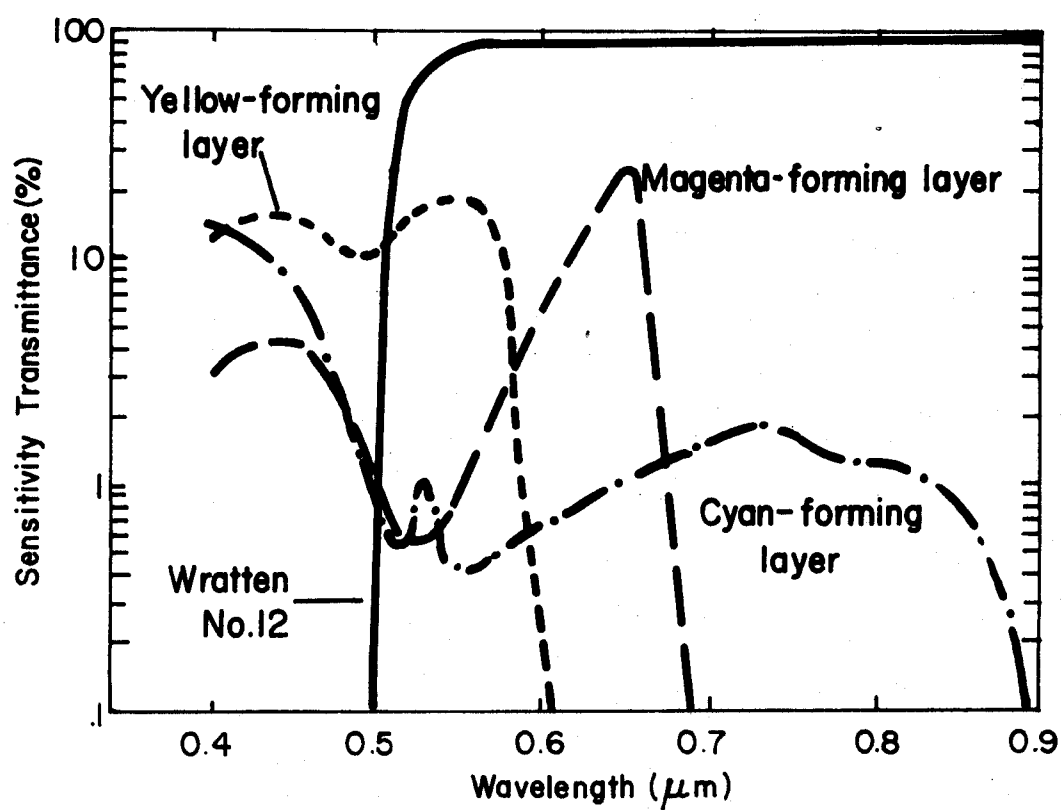


Figure 4. Spectral sensitivity curves for Kodak Ektachrome Infrared film type 2443, and the spectral transmittance of Kodak Wratten filter No. 12 (Fritz, 1971).

Hoffer, Anuta, and Phillips (1971) describe this separation process as well as all the other steps in digitization of photography. Kodak Wratten No. 47b blue, No. 61 green, and No. 23a red filters were used for the separations. Eastman Kodak Pamphlet No. E-59 (1968) describes the use of Wratten filters for emulsion layer separation of color films. Table 3 lists the bands of spectral sensitivity of the black and white transparencies upon separation by the three filters. Photographic separation of dye layers produces three separate black and white transparencies which must be run through the microdensitometer individually.

Microdensitometry. A scanning microdensitometer was utilized to obtain film density measurements of the black and white transparencies. This technique permits the rapid scanning density measurement of many small adjacent lines in sequence. An Optronics Inc. P-1000 digitizing, rotating-drum microdensitometer was used in this study. This unit scans transparencies by way of a rotating drum on which the film is mounted. A light source and optical system are used to project a beam through the film, and a photo cell mounted below the drum senses the transmitted light. The electrical signal representing transmitted light is sampled and converted to numerical form on a logarithmic density scale from 0 to 2. The digital density samples are recorded on magnetic tape with a precision of 2^8 , thus utilizing a 0 to 255 density range compatible with the LARS processing system.

A spatial resolution of 50 μ m was used, which allowed for a point on the film to be resolved which represented about 1.5 cm on the ground. Over 300,000 individual density measurements were transformed to a numerical data format from a typical 24 by 36 mm frame of photography.

Table 3. Spectral bands from color separation of color and color infrared film.

<u>Film Type</u>	<u>Separation Filters</u>		
	<u>Wratten No. 47b</u>	<u>Wratten No. 61</u>	<u>Wratten No. 23a</u>
Kodak Ektachrome-X and Kodak Kodachrome II	(0.40-0.47 μ m) Blue	(0.47-0.61 μ m) Green	(0.59-0.71 μ m) Red
Kodak Ektachrome Infrared Type 2443	(0.47-0.61 μ m) Green	(0.59-0.71 μ m) Red	(0.68-0.89 μ m) Infrared

The system has an accuracy of about 2% in density measurements.

The recorded film transmission values used are proportional to scene reflectance although the exact relationship is not known. Anuta and MacDonald (1971) reported that optical film density is a function of incoming radiance, film characteristics, filters used, optical system characteristics, and the film development process. Densitometry of film cannot eliminate characteristics inherently variable in photography, and, therefore, is not a calibrated procedure.

Reformatting and Data Registration. The individual scans were stored as separate data sets on tape. In order to analyze the data utilizing the information from all three emulsions of the original film, the data had to be reformatted in such a manner that each scene point was in geometrical coincidence in all three wavelength bands. A software system was developed at LARS (Anuta and MacDonald, 1971) to register or "overlay" multiple images of the same scene. The system combined the individual scans onto one data set with the image points stored in such a way that any scene ground point could be addressed by a line and column coordinate pair and a channel pointer. The digital film data storage tape was then available for analysis using the LARSYS processing system.

Data points within a field or any rectangular region could be identified by extracting line and column coordinates of the corners of that area and punching them on computer cards. Each 24 by 36 mm frame of photography had about 450 lines and 700 columns of data available for analysis.

Digital Display Imagery. The LARS Digital Video Display Unit was used in a preliminary checkout of the data. This device reproduces a pictorial representation of the digitized imagery by dividing the data up equally into 16 bins for gray level display. A typewriter terminal and keyboard are used to control program execution and display functions. A light pen is available for selection of coordinate points in the imagery. Photocopies of the displayed imagery can be made from a slave photocopy unit which is part of the system.

An initial checkout was made of all 20 frames of digitized photography. It became evident that a problem had been encountered in digitization of the 16 frames of color film since their digital display images contained portions which were highly oversaturated. Bright portions of the imagery had exceeded the scale of 0 to 255 and had "turned over" to low digitization values. The 16 frames of digitized color film were not used in analysis because of the apparent failure of the microdensitometer to accommodate the full range of density values represented on the color film.

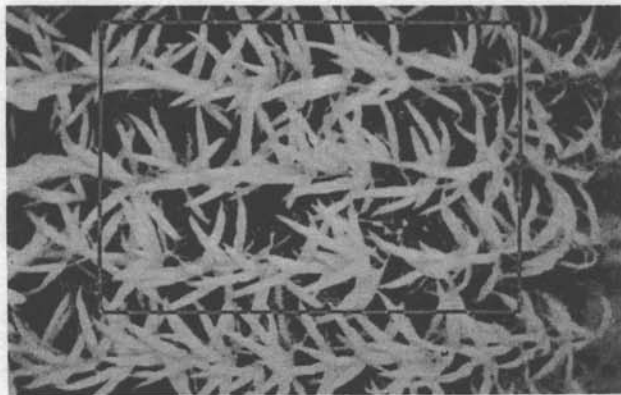
Three frames of digitized color infrared film appeared to be of high image quality and were chosen for detailed analysis. The light pen was used to select a set of data from each frame of digitized photography for ground cover analysis. Boundaries were drawn equidistant between rows for two or three rows in the frame so that the outlined area could be used for an accurate estimation of percent ground cover. Figure 5 shows the digital display images of the three frames of digitized color infrared photography and the areas outlined for detailed study in each of them. The imagery for Chalmers plots 9 and 11 is that of the 0.68 to



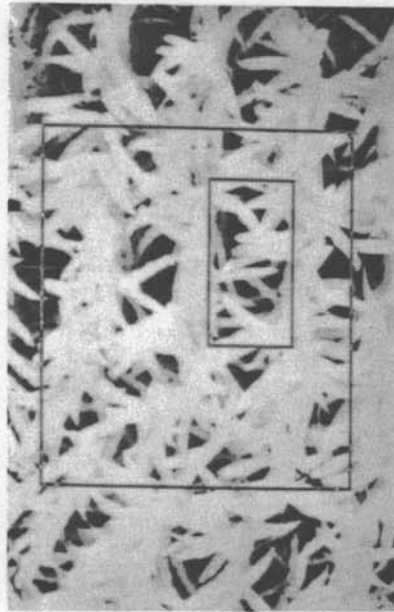
CP 12 Green Separation



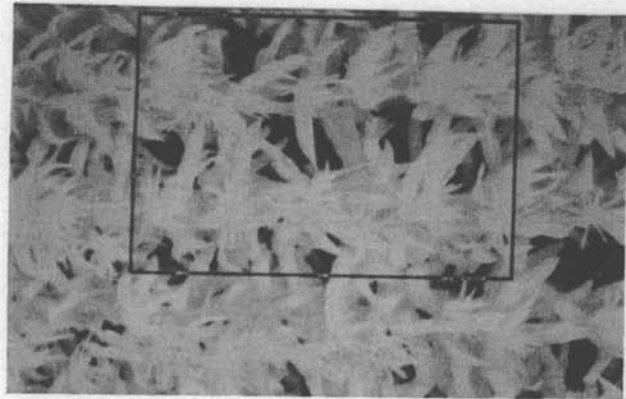
CP 12 Red Separation



CP 11 Infrared Separation



CP 12 Infrared Separation

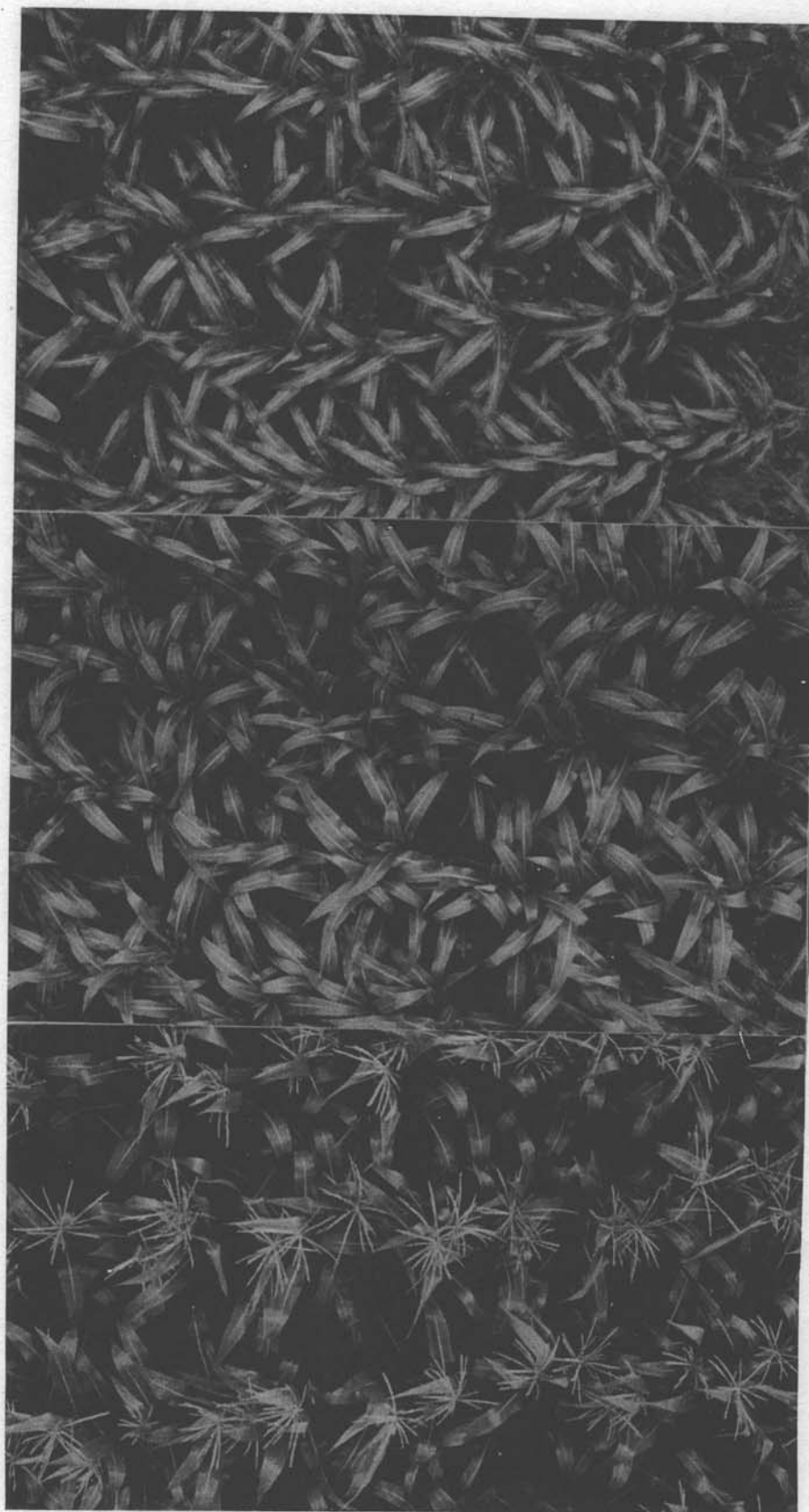


CP 9 Infrared Separation

Figure 5. Digital display images from 3 color separations of color IR film taken over 3 Chalmers plots.

0.89 μm near infrared wavelength band. All three wavelength bands (green, red, and near infrared) are shown for Chalmers plot 12. A smaller subset area has been outlined in the imagery for Chalmers plot 12. This subset area received very detailed study because of the complex vegetative cover represented therein. Figure 6 shows prints from the color and color infrared transparencies taken over these three plots. The digitized color infrared photography was obtained from these same color infrared transparencies. The high quality of the digitized imagery is striking, and one might easily mistake it for the original photographic imagery.

Training Class Analysis - Clustering. Analysis of the digitized photography was intended mainly as an attempt to distinguish between the components of green vegetation and bare soil in the imagery. This involved the determination of separable classes in the data set. The statistical pattern recognition analysis system LARSYSAA was used for classification purposes. This system uses a maximum likelihood ratio based on the Gaussian assumption to classify statistically separable classes (Fu, Landgrebe, and Phillips, 1969). "Training sample areas" must be provided to supply the LARSYSAA processor with statistics for recognition of spectral patterns of density values for similar conditions in the photograph. A useful technique for selection of training sample areas or training classes is the clustering method described by Wacker and Landgrebe (1970). The clustering program utilizes a process of iteration to minimize the Euclidean distance between relative density vectors (in the case of digitized photography) and the "cluster center" for a given class. Image points are grouped around these cluster



Chalmers Plot 9, 4.44 LAI
Ektachrome-X Color Film

Chalmers Plot 12, 2.93 LAI
Ektachrome-X Color Film

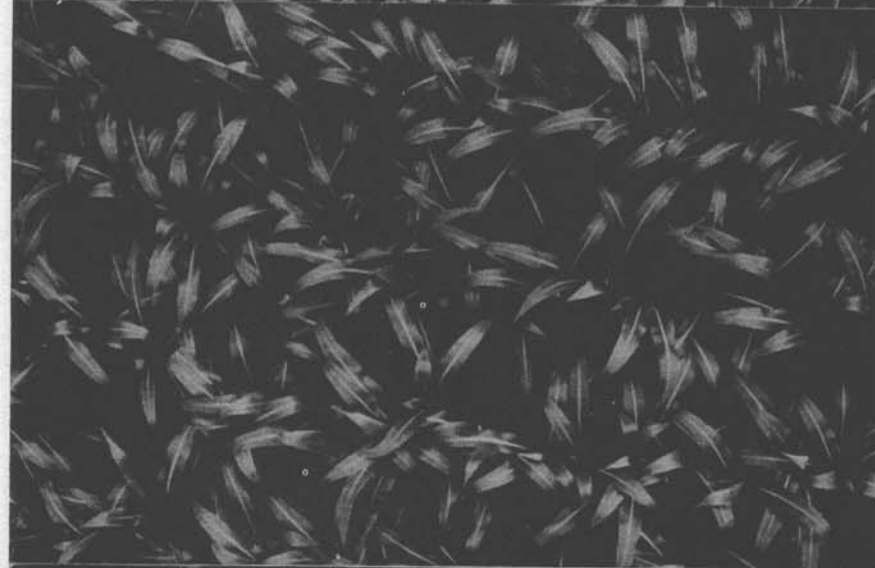
Chalmers Plot 11, 1.31 LAI
Ektachrome-X Color Film

Figure 6. Color prints from color and color infrared photographs taken over 3 Chalmers plots.

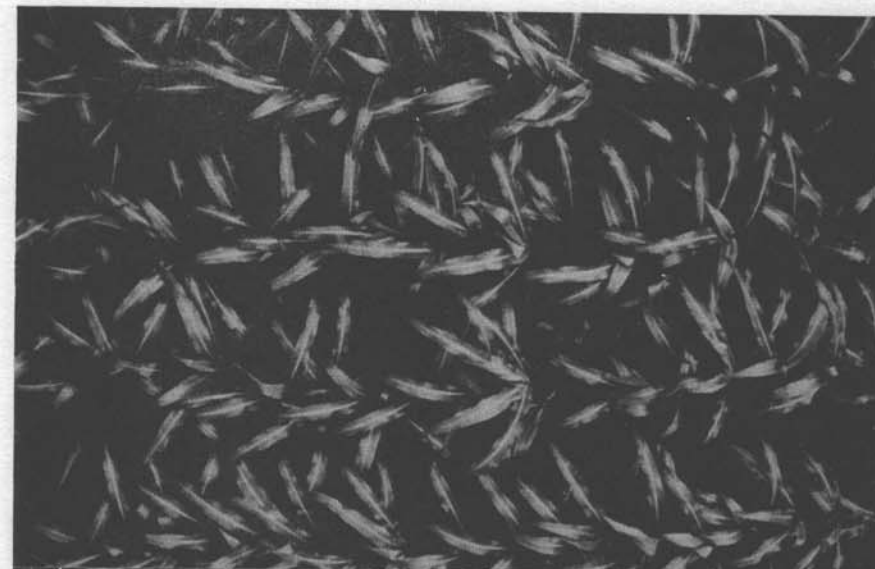
Figure 6, cont.



Chalmers Plot 9, 4.44 LAI
Ektachrome Infrared Film



Chalmers Plot 12, 2.93 LAI
Ektachrome Infrared Film



Chalmers Plot 11, 1.31 LAI
Ektachrome Infrared Film

centers such that the overall variance of the resultant "clusters" is minimized.

The clustering program permits calculation of a requested number of cluster classes in any desired combination of wavelength bands. For the purposes of this study, ten cluster classes were requested from each set of data and only the 0.68 to 0.89 μm near infrared wavelength band was used for vector analysis. Selection of the near infrared wavelength band for clustering purposes was based on the visual observation that this band provided better separation of the green vegetation-bare soil complex. Ten cluster classes were anticipated to represent sufficiently all of the spectrally separable ground features present in a frame of digitized photography.

An area of 100 lines by 100 columns was selected from the center of the outlined area on all three frames of digitized photography. This area was clustered as described above, and ten spectrally separable classes were produced from the imagery from Chalmers plots 9 and 11. The clustering program could not distinguish ten spectrally separable classes in the imagery from Chalmers plot 12, so it decremented the number of classes until it found five cluster centers to which the data could be assigned. Checking back to the digital display imagery for the three frames of photography, it could be seen that only one cluster class from each frame was necessary to characterize the training class component for bare soil. Most of the variability in the digitized photography was in the green vegetation, and all the remaining cluster classes were assigned as training classes for green vegetation.

Coordinates of uniform blocks of data representing each cluster class were selected by hand from the clustered array map of the clustering program. These coordinates were punched on cards, and decks were compiled representing training classes for input into the pattern classification processor.

Classification. The smaller subset area outlined on the digital display image for Chalmers plot 12 (Figure 5) was chosen for detailed analysis and determination of the best wavelength bands for classification. The five cluster classes produced from the clustering of Chalmers plot 12 were used for training the pattern classifier. The statistics processor of the LARSYSAA pattern classification system was used to compute the training statistics for each of the five cluster classes. These statistics consist of means and covariance matrices to be used by the Gaussian maximum likelihood classifier.

The coincident spectral plot of means plus and minus one standard deviation for the five cluster classes in all three wavelength bands of the digitized photography are shown in Figure 7. Cluster classes 1 through 4 represent green vegetation while cluster class 5 represents bare soil. It can be seen that cluster class 5 (represented by "E" on the printout) has a much lower mean in the 0.68 to 0.89 μm wavelength band than any of the other cluster classes, and the class representing bare soil should not be too hard to differentiate from the classes representing green vegetation. The situation in the 0.47 to 0.61 μm and 0.59 to 0.71 μm wavelength bands is quite different, however. The means and standard deviations of cluster class 5 in these two wavelength bands overlap with the means and standard deviations for several other

LARSYSAA
VERSION 2
LABORATORY FOR APPLICATIONS OF REMOTE SENSING
PURDUE UNIVERSITY
CHALMERS PLOT 12 JULY 13 2-93 LAI STATISTICS FOR THREE BANDS

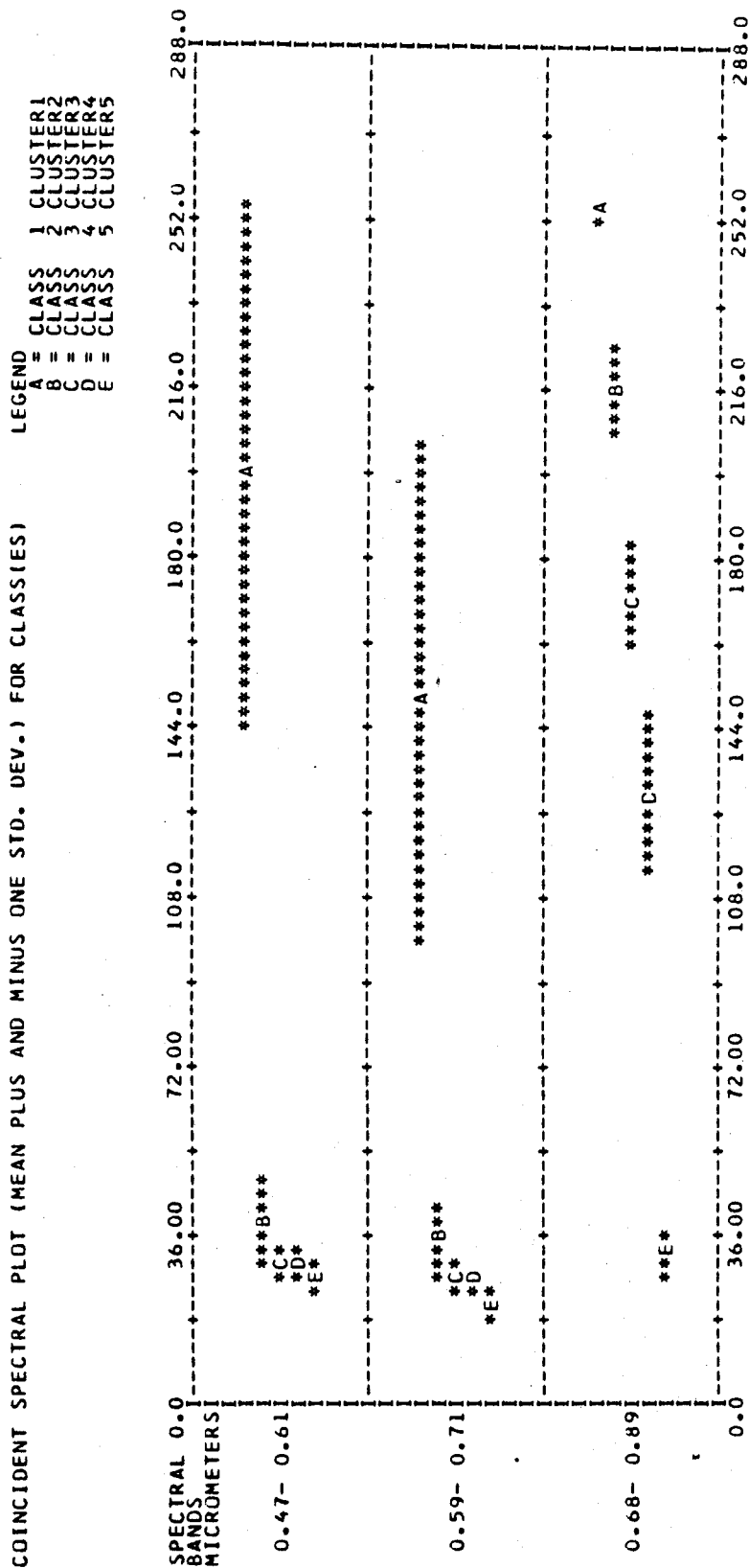


Figure 7. Coincident spectral plot for 5 cluster classes from digitized photography of Chalmers plot 12.

cluster classes. Examination of the coincident spectral plot seemed to indicate that the 0.68 to 0.89 μm near infrared wavelength band would be far better than the other two in discrimination between bare soil and green vegetation.

The LARSYSAA classification processor was then used to classify each image point into one of the five defined classes using statistics from any desired combination of wavelength bands. Three classifications were made using the three wavelength bands by themselves, and a fourth classification was made using the statistics from all three wavelength bands. Green vegetation classes and display symbols were pooled for pictorial displays of corn versus bare soil as well as for calculation of the percent area occupied by green vegetation.

Based on preliminary information indicating that the near infrared wavelength band was the most useful for classification purposes, the other two frames of digitized color infrared photography (Chalmers plots 9 and 11) were classified using the 0.68 to 0.89 μm band.

Results and Discussion

Relating Estimated Percent Ground Cover to Leaf Area Index

A regression analysis was performed on the data from the 30 frames of photography analyzed for percent ground cover by the point grid system. The data in Table 2 for estimated percent ground cover were plotted against leaf area index (LAI). The resulting relationship can be seen in Figure 8. It was desired to see if the ground level measurement of LAI could be used in this situation to estimate percent ground cover as determined from a view above the canopy. If such a relationship exists

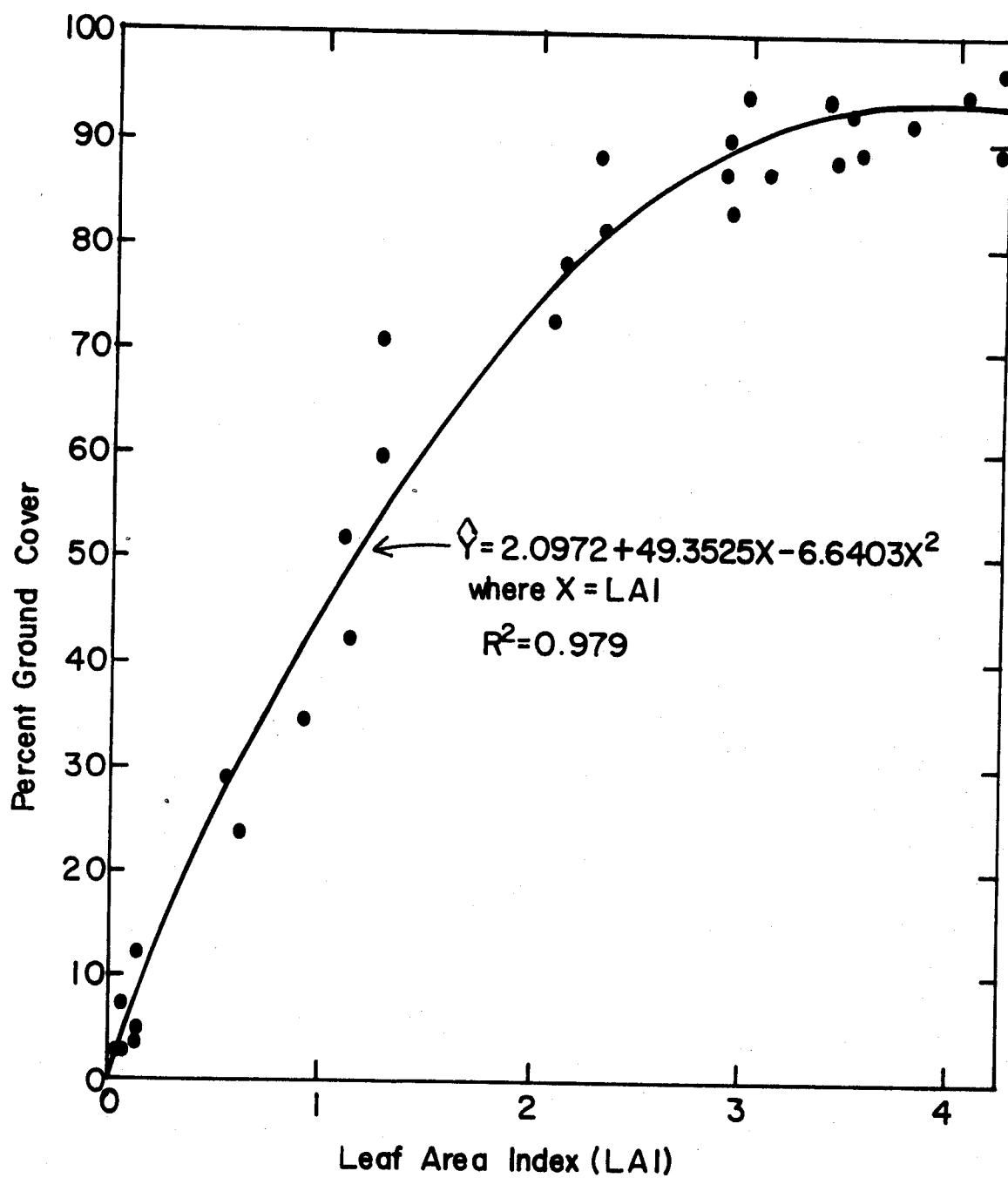


Figure 8. Percent ground cover plotted against leaf area index for 30 observations.

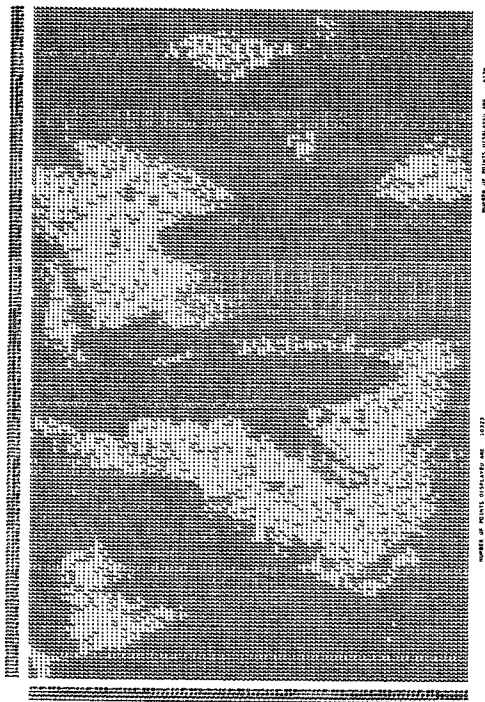
it would greatly aid the ground based observer whose job it is to collect supporting information on ground cover for remote sensing overflights.

In this problem percent ground cover was considered the dependent variable and leaf area index the independent variable. From the graph of the relationship (Figure 8) it was felt that a second order term may be needed to help explain variations in the dependent variable, so the squared term for LAI was also entered into the regression analysis. A stepwise regression program was run, and the linear term for LAI was entered first into the regression, followed by the squared term for LAI. The variation about the mean percent ground cover explained by the resulting regression was 97.9%. The line of fit is plotted in Figure 8, and the regression equation, $\hat{Y} = 2.0972 + 49.3525X - 6.6403X^2$ is given. For this particular situation, leaf area index appears to be useful in explaining variations in percent ground cover.

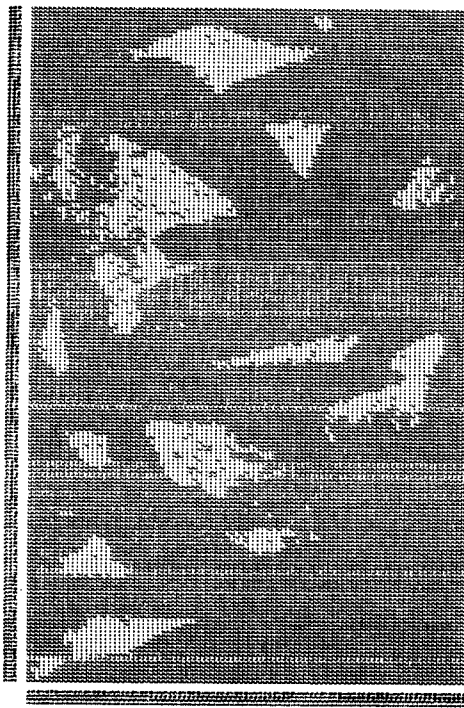
It is evident from Figure 8 that as LAI increases beyond a certain point (LAI = 3 in this case) percent ground cover does not increase very greatly. A ground cover of 100% was never observed from the low altitude photography. Cuellar (1971) found it difficult to estimate cover from the ground as ground cover approached 100%. If a prediction equation like the one calculated were available for different row widths and plant populations of corn, estimation of cover from LAI measurements would not be unreasonable, even as cover approached 100%.

Results of Classifications Using Three Color Separations

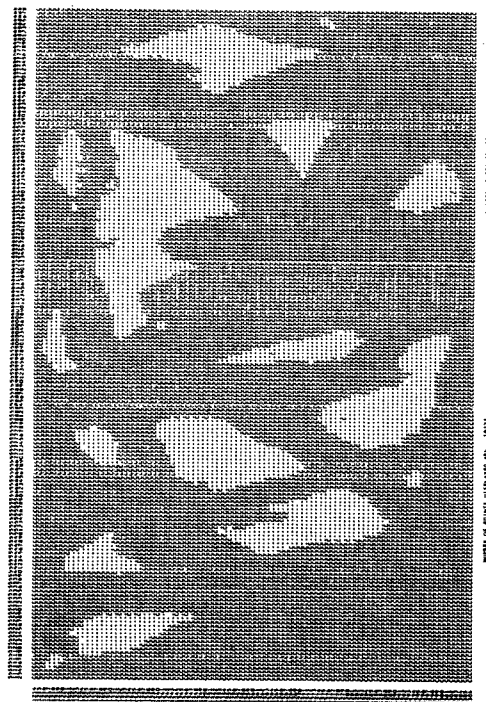
Display maps of the classified subset area for the digitized photography from Chalmers plot 12 are shown in Figure 9. Four display maps are shown, representing classifications in the green, red, and near



Green Wavelength Band



Red Wavelength Band



Near Infrared Wavelength Band



All Three Wavelength Bands

Figure 9. Computer display maps for 4 ground cover classifications of Chalmers Plot 12.

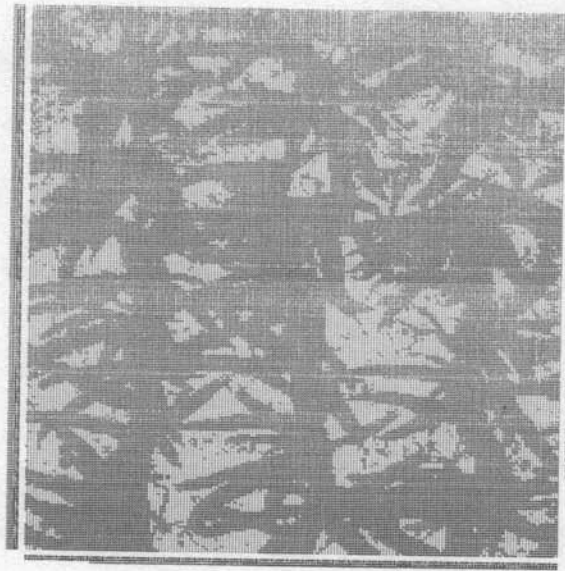
infrared wavelength bands separately and all three bands in combination. Green vegetation is displayed as a "C" and bare soil is displayed as a ".". The classification using the near infrared wavelength band was the best one for determination of percent ground cover in the subset area of Chalmers plot 12. The classification display map of this area in the near infrared wavelength band represents most closely the actual ground cover situation when compared with the original photography (Figure 6) and the digital display imagery (Figure 5).

The tabulated results of percent ground cover for the subset area of Chalmers plot 12 as determined by the four classifications are listed in Table 4. It can be seen that percent ground cover was overestimated in the classification using the red wavelength separation, while it was slightly underestimated in the classification using the green wavelength separation. The classification using all three wavelength bands in combination very greatly underestimated percent ground cover as is evident from the display map in Figure 9, as well as the results in Table 4. About one-third of the points in the map display for the multi-band classification were thresholded and are displayed as blanks. A threshold level of 0.1 % was applied to prevent assignment of a point to a particular class when membership in that class was not highly probable.

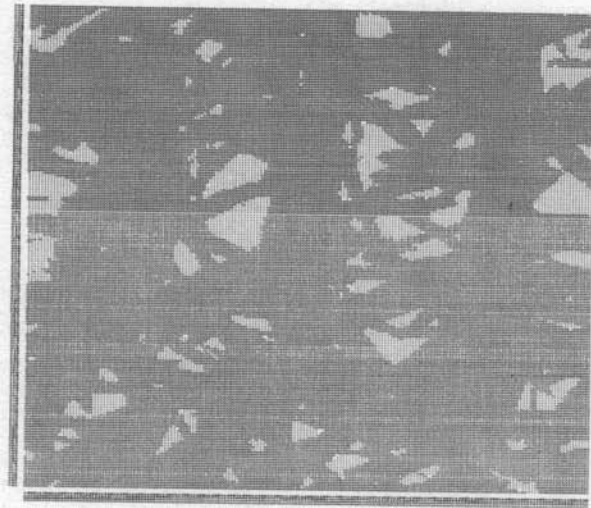
Classifications using the near infrared wavelength band were made from the digitized photography for Chalmers plots 9 and 11. A larger area from Chalmers plot 12 was also classified for percent ground cover determination. Figure 10 shows the display maps for these three plots. From the display map for Chalmers plot 11 it can be seen that even some green weeds in the plot were classified as green vegetation. The

Table 4. Percent ground cover determinations from 4 classifications of Chalmers plot 12.

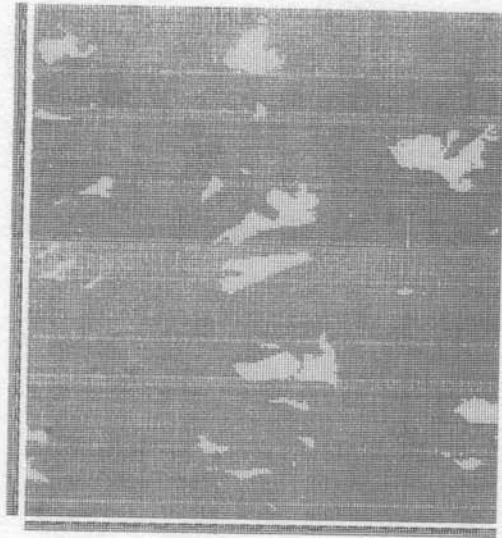
<u>Classification Bands</u>	<u>Wavelength Bands Used in Classification</u>	<u>Percent Classified as Green Vegetation</u>	<u>Percent Thresholded (0.1 % level)</u>
Near Infrared	0.68-0.89 μ m	81.6	0.2
Red	0.59-0.71 μ m	87.6	0
Green	0.47-0.61 μ m	78.9	0
Combination	$\left\{ \begin{array}{l} 0.68-0.89 \mu\text{m} \\ 0.59-0.71 \mu\text{m} \\ 0.47-0.61 \mu\text{m} \end{array} \right\}$	48.4	33.6



Chalmers Plot 11



Chalmers Plot 12



Chalmers Plot 9

Figure 10. Computer display maps for ground cover classifications of Chalmers Plots 9, 11, and 12, using near infrared color separations for classification.

classification results from these three plots and the corresponding leaf area indices are given in Table 5.

Evaluation of Color and Color Infrared Film in Determining Ground Cover

The color and color infrared photographs (Figure 6) show the differing usefulness of each in estimating ground cover on a dark soil. The color photographs are not as valuable as the color infrared photographs mainly because of the difficulty in distinguishing leaves in the shaded areas between the rows. This is in agreement with the findings of Hoffer (1967) who noted that increasing canopy on dark soils resulted in higher response on infrared film. Gerbermann, Gausman, and Wiegand (1969) likewise, found that the influence of crop shadows and sunlit furrows could be detected on color infrared film.

On the light colored Russell plots color film seemed to be the most useful for estimating ground cover when the percent cover was less than about 75% and the soil was in a typical dry surface condition. If the surface soil of the Russell plots was very moist and the ground cover was greater than about 75%, however, color infrared film seemed to be best for estimating ground cover. Often when a corn canopy reaches 75% ground cover, the evaporation from the surface soil is lessened, and the surface soil appears darker. If this is the case, color infrared film would be preferable in either a dark or light soil background situation in which the percent ground cover is greater than about 75%.

Table 5. Percent ground cover determinations from classifications of three Chalmers plots in the near infrared.

<u>Plot</u>	<u>Planting Date</u>	<u>Number of Cluster Classes used in Analysis</u>	<u>LAI</u>	<u>Percent Classified as Green Vegetation</u>
Chalmers plot #11	June 9	10	1.31	78.9
Chalmers plot #12	May 22	5	2.93	89.5
Chalmers plot #9	April 30	10	4.44	93.2

Need for More Quantifiable Information

Differences in exposure, development, and manufacturing of photographic films prevent simple quantitative calibration of photography to reflectance values. Although reflectance calibration of photographic film has been attempted by the use of gray scale step wedges and ground reflectance panels (Silvestro, 1969), it is not at all practical for the type of experiment described here. Very little information as to the actual reflectance values could be obtained from the photography taken in this study.

Microdensitometry and digitization of photographic film can be a precise and quantitative process with known allowable error. Unfortunately, however, the photographic film from which the data is obtained is subject to many sources of variation as listed above. Digitized photography is only as good as the original photograph.

Photography is limited to the wavelength region of about 0.4 to 0.9 μm . There may very well be other wavelength regions which may be more useful in estimating ground cover and which may be determined only by non-photographic sensors. Multispectral airborne scanners and portable field spectroradiometers may be able to cover the entire reflective wavelength range while obtaining more quantifiable information on ground cover.

Summary and Conclusions

Color infrared film is potentially useful for ground cover determination from low altitude photography. The near infrared dye layer of this film was the most useful for separation of the green vegetation and

bare soil components of the corn canopy. Digitization of low altitude photography of plant canopies provides a valuable method for computer assisted determination of percent ground cover.

Color film is of value in ground cover determination from low altitude photography of corn canopies if the soil background is light and the ground cover is less than about 75%. For dark soil backgrounds and ground covers of greater than 75% in corn canopies, color infrared film would be more valuable.

Percent ground cover as determined from low altitude photography can be related to leaf area index of a corn canopy for a given row width and plant population. Leaf area index is easy to measure from the ground and gives more information as to the actual crop biomass than does percent ground cover.

Low altitude photography of corn canopies is useful for spatial characterization of ground cover, but quantifiable spectral information is limited due to variability between frames of photography. Micro-densitometry and digitization of color and color infrared film provide quantitative techniques for analyzing density differences which may be related to components of green vegetation and bare soil in the scene.

Since the near infrared color separation of color infrared film seemed to be the most useful in ground cover determination, it may be just as valuable to use black and white infrared film filtered to the near infrared for photography of corn canopies. Color infrared film is still of value even without having its three dye layers photographically separated.

CHAPTER IV

AIRBORNE MULTISPECTRAL SCANNER DATA FROM CORN CANOPIES

Problem Definition

Airborne multispectral scanner data provide an extended view of the reflective properties of plant canopies. Information may be obtained in the wavelength range from 0.4 μm to 2.6 μm in this manner. Comparisons of scanner data values in the various discrete wavelength bands or channels of the multispectral scanner allow for investigation of the spectral differences between various plant canopy covers.

Kristof and Baumgardner (1970) found a ratio technique to be useful in relating multispectral scanner data values to extent of ground cover. In particular, the ratios of scanner data values from the near infrared and chlorophyll absorption regions of the spectrum appear to be of great value in expressing changes in ground cover. These ratios can be related to a ground based measurement of ground cover such as leaf area index. Prediction equations can then be formulated for estimation of leaf area index from ratios of multispectral scanner data values.

Procedures

Multispectral Scanner Data Collection

Two flight missions by the University of Michigan's airborne multispectral scanner were used in this study. The flight path for both missions was a north-south flightline directly over the Purdue University Agronomy Farm's Weather Station. Corn plots of various ground covers planted on a Russell silt loam soil were located in the flight path in close proximity to the weather station. The weather station was the location of placement of a set of eight ground reflectance panels whose use in standardizing scanner response over time will be described later. Figure 11 shows the placement of the panels with respect to the weather station.

July 12 and July 21, 1971 were the dates for the two scanner overflights. The July 12 flight was at 1401 hours EST while the July 21 flight was at 1305 hours EST. Both overflights were at an altitude of 305 m and both took place on clear, cloud-free days.

The University of Michigan's multispectral scanner collected spectral data in the 0.46 to 2.60 μm reflective wavelength range, as well as the 9.3 to 11.7 μm thermal infrared wavelength range. Only the reflective wavelength bands or channels were used in this study. Table 6 lists the 12 channels of data collected by the University of Michigan scanner and the corresponding wavelength bands.

The aircraft scanner data were recorded in analog form and converted to a digital format for analysis by the LARSYS processing system. Two flightlines of interest were digitized at a sample rate of 450 samples

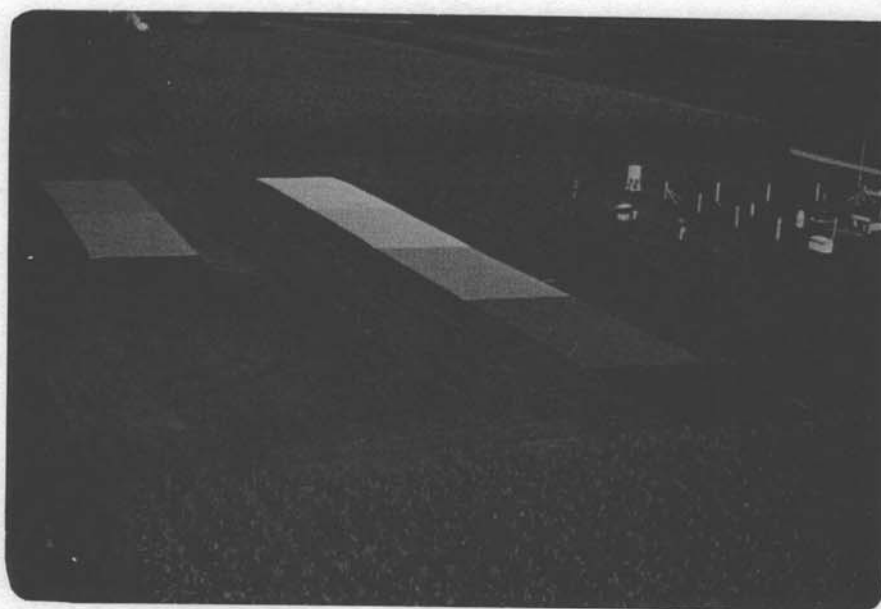


Figure 11. Ground reflectance panel placement at the Purdue University Agronomy Farm Weather Station, August 17, 1971.

Table 6. The 12 channels and corresponding wavelength bands for the University of Michigan multispectral scanner.

Limits of Spectral Bands (μm)

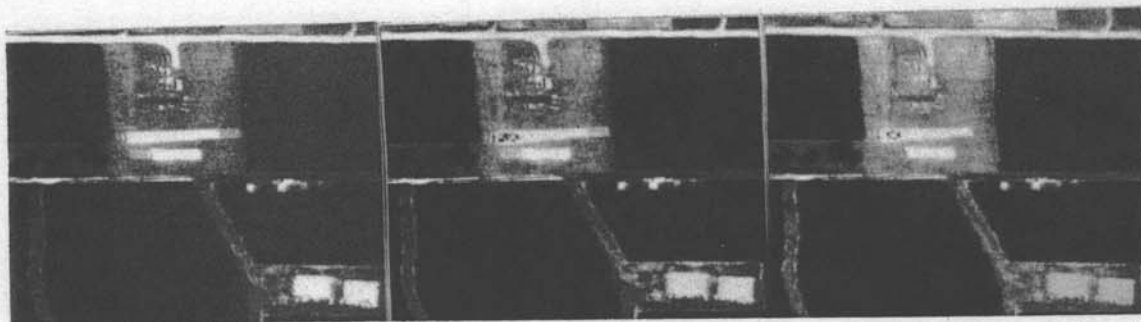
<u>Channel</u>	<u>Lower</u>	<u>Upper</u>	<u>Wavelength Region</u>
1	0.46	0.49	Visible
2	0.48	0.51	Visible
3	0.50	0.54	Visible
4	0.52	0.57	Visible
5	0.54	0.60	Visible
6	0.58	0.65	Visible
7	0.61	0.70	Visible
8	0.72	0.92	Near Infrared
9	1.00	1.40	Near Infrared
10	1.50	1.80	Near Infrared
11	2.00	2.60	Near Infrared
12	9.30	11.70	Thermal Infrared

per scan line of data. This meant that every line of analog scanner data was sampled in the digitization process. Each resolution unit represented an area about 1 m by 1 m on the ground. The digitized data were reformatted into a form compatible with data processing programs at LARS.

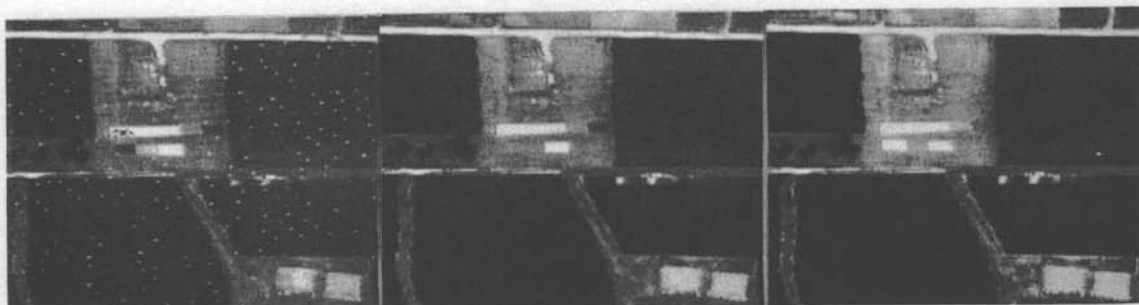
Digital Display Imagery

The LARS Digital Video Display Unit was used to display the digitized scanner data imagery in the twelve wavelength bands of the multispectral scanner. The digital display images for the July 12 scanner flight in the twelve wavelength channels for the area near the Purdue University Agronomy Farm's Weather Station are shown in Figure 12. These display images were obtained from black and white Polaroid photographs taken from the photocopy unit which is part of the digital display system. The images are composed of sixteen gray levels which were produced by dividing all the data points in the displayed area into sixteen equal bins of data. Even though the images look like normal panchromatic photographs, it must be remembered that each image represents the relative response values only in the wavelength band corresponding to that channel (Figure 6).

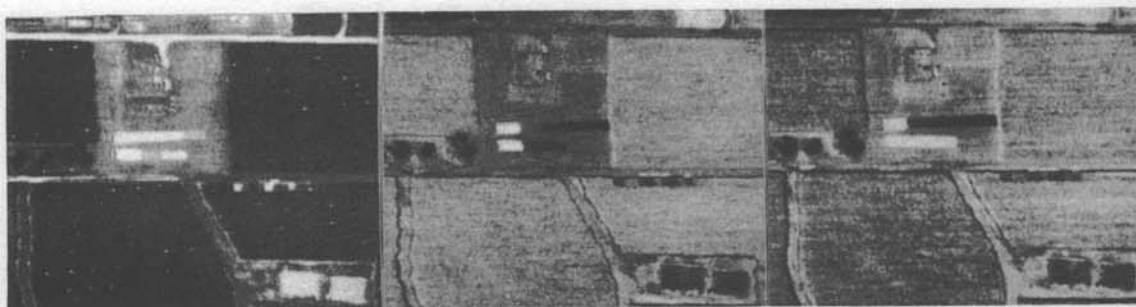
The ground reflectance panels can be seen in the center of the imagery. These panels are 6.1 m by 12.2 m standard reflectance canvases painted with special reflecting paints. The gray reflectance panels have a relatively constant percent reflectance throughout the reflective wavelength range, and are useful for visual comparisons with ground features in the nearby area. The reflectance panels for the July 12 flight were arranged in the same order as in Figure 11 (taken August 17) except that



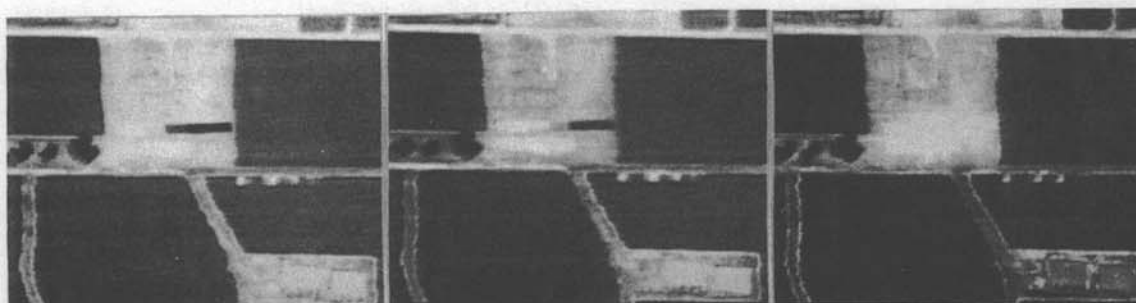
Channel 1 (0.46-0.49 μ m) Channel 2 (0.48-0.51 μ m) Channel 3 (0.50-0.54 μ m)



Channel 4 (0.52-0.57 μ m) Channel 5 (0.54-0.60 μ m) Channel 6 (0.58-0.65 μ m)



Channel 7 (0.61-0.70 μ m) Channel 8 (0.72-0.92 μ m) Channel 9 (1.0-1.4 μ m)



Channel 10 (1.5-1.8 μ m) Channel 11 (2.0-2.6 μ m) Channel 12 (9.3-11.7 μ m)

Figure 12. Digital display imagery of Russell plots and panels, July 12 scanner flight.

the three color panels for July 12 were arranged green-blue-red from east to west.

Locating Plots and Obtaining Mean Scanner Data Values

The approximate area of the Russell plots was outlined on the digital display screen using the light pen, and the coordinates of the area were recorded by the field selection processor. This area was then clustered utilizing the data from all twelve wavelength bands of the multispectral scanner with ten cluster classes being requested. The resulting cluster array map was of value in locating the twelve sub-plots within the Russell plots. Sub-plots that were planted on the same date and were of approximately the same ground cover were grouped into the same cluster classes by the clustering program, thus facilitating the selection of data blocks representing each sub-plot.

Each sub-plot was slightly larger than 4 by 4 ground resolution units or data points. A square block of four data points was selected from the northeast portion of each sub-plot in order to eliminate any shadowing effects from bordering sub-plots. Statistics were then obtained from these data blocks for all of the sub-plots on both dates of scanner overflights.

At the time of the July 21 scanner overflight, photographic data were being obtained from the LARS Hi-Ranger truck over Russell plot 2. The location of the Hi-Ranger truck in relation to the Russell plots can be seen in Figure 13. This print is from a black and white photograph taken by the scanner airplane, coincident with the scanner data. It became evident upon cluster analysis of the Russell plots for the July 21 scanner overflight that the Hi-Ranger truck was having an effect on the

£4	32	16	8	4
----	----	----	---	---

Red	Blue	Green
-----	------	-------

Hi-Ranger Truck

Russell Plois



↑ N ↓

Figure 13. Black and white scanner coincident photograph filtered to the red wavelength region, taken July 21, 1971 over the Purdue University Agronomy Farm Weather Station.

spectral response of three of the sub-plots. For this reason, Russell plots 2, 3, and 4 were discarded from further analysis of the scanner data from July 21.

The LARSYS statistics processor was used to obtain mean scanner data values for the sub-plots for the two flight dates. These mean values were obtained without any attempt made to calibrate scanner response between flights. The normal procedure used at LARS for obtaining statistics from multispectral scanner data was used, which takes into account zero reference drift or the drift in the scanner system response to a black or zero signal level. More about calibration procedures for multispectral scanner data will be presented in the next chapter. The mean scanner data values obtained for the twelve sub-plots in the eleven reflective wavelength bands for the two dates are given in Table 7.

Ratio Techniques for Relating Scanner Response Ratios to Leaf Area Index

Kristof and Baumgardner (1971) used the ratio of scanner data values in the 0.58 to 0.62 μm wavelength band to the relative reflectance in the 0.80 to 1.00 μm wavelength band to observe increases in ground cover. Considerations of the reflectance properties of green vegetation and soil would seem to favor a ratio of these two wavelength regions for characterizing ground cover. Chlorophyll absorbs at 0.65 μm in the visible wavelengths, and it is reasonable to assume that as a crop canopy becomes more dense it would absorb more strongly (and hence, reflect less) in this region. The 0.72 to 1.3 μm wavelength range is the region in which little absorption takes place in green vegetation and in which almost all incident light is transmitted or reflected. Multiple leaf layer experiments

Table 7. Uncalibrated mean scanner data values for 12 Russell plots in 11 reflective wavelength bands for two flight dates.

July 12, 1971 Multispectral Scanner Flight

RP#	Channels										
	1	2	3	4	5	6	7	8	9	10	11
1	103.61	154.02	138.75	102.11	111.05	132.14	139.14	77.64	106.67	171.00	183.59
2	58.36	78.52	82.75	68.36	66.80	57.89	58.37	94.89	114.92	138.50	108.09
3	53.11	73.02	73.50	59.61	59.80	51.89	52.87	96.89	115.42	117.25	100.34
4	65.61	83.52	90.75	72.61	67.80	66.89	68.87	78.39	102.42	128.75	125.09
5	106.61	154.02	142.00	99.36	109.30	125.39	132.12	76.14	105.67	179.25	186.59
6	64.61	88.52	88.75	72.36	69.55	60.39	64.12	96.64	114.42	141.50	108.84
7	62.11	88.77	91.25	69.36	66.80	67.39	67.37	80.89	102.17	128.25	116.59
8	77.36	105.52	104.50	73.86	77.80	91.89	98.62	62.39	92.67	140.25	154.84
9	55.11	70.27	71.75	62.11	58.80	51.89	55.62	93.39	112.42	116.50	98.09
10	62.36	87.27	88.50	68.85	67.30	66.89	66.62	81.64	106.17	125.75	120.84
11	58.36	78.02	79.75	67.61	64.80	59.39	58.12	94.14	113.67	129.00	107.59
12	54.86	74.27	74.00	62.86	60.80	54.39	54.87	96.14	114.92	123.00	100.09

Table 7, cont.

July 21, 1971 Multispectral Scanner Flight

RP#	Channels										
	1	2	3	4	5	6	7	8	9	10	11
1	74.38	93.09	63.39	113.38	75.49	96.93	94.27	105.75	88.65	108.84	112.50
2											
3	Missing Data - interference from Hi-Ranger Truck										
4											
5	75.38	95.09	62.64	112.38	75.74	95.93	94.02	102.25	88.65	110.09	114.00
6	38.88	38.59	36.14	54.63	40.74	42.18	39.27	106.25	81.65	62.84	58.50
7	40.88	44.34	38.64	61.88	47.24	45.93	44.27	105.75	83.15	69.84	63.50
8	69.13	85.09	58.64	102.88	70.49	87.43	87.77	100.75	86.40	99.59	103.25
9	40.13	41.59	38.39	55.13	41.74	43.93	41.27	106.50	80.65	62.09	53.50
10	41.88	44.09	39.89	61.38	45.24	46.18	44.02	106.75	81.65	67.84	58.00
11	39.38	40.09	36.64	53.38	40.99	41.43	39.52	105.25	82.15	63.09	55.25
12	38.13	38.34	35.89	51.38	39.24	41.18	39.27	105.00	81.65	57.84	53.25

have shown that reflectance in this 0.72 to 1.3 μm wavelength region increases with increasing leaf layers (Myers et al., 1966). Therefore, the reflectance of a crop canopy may be expected to increase in the 0.72 to 1.3 μm wavelength range as green vegetative cover increases. Soil reflectance generally increases in going from the red wavelength region to the near infrared wavelength region, the amount of increase for a particular soil depending mainly on the soil moisture content.

The scanner wavelength band configuration was changed from that at the time of the study of Kristof and Baumgardner (1971), the chlorophyll absorption band now falling in the 0.61 to 0.70 μm wavelength band of channel 7. Two near infrared wavelength bands were now available in the region of high reflectance of green vegetation: the 0.72 to 0.92 μm wavelength band of channel 8, and the 1.0 to 1.4 μm band of channel 9.

Ratios of scanner data values (Table 7) were calculated by dividing the scanner data values from channels 8 or 9 by the scanner data values from channel 7 (hereafter referred to as the ratios of channels 8/7 or 9/7). These ratios were then plotted against leaf area index, as measured at the time of the overflights. The ratios of channels 8/7 and 9/7 for the two flight dates and the corresponding LAI's for all of the sub-plots are listed in Table 8. Stepwise multiple regression analysis was run on the data to see if either of the two ratios of near infrared to red wavelength scanner data response could be related to leaf area index.

Table 8. Ratios of uncalibrated scanner data values and leaf area indices for 12 Russell plots for two flight dates.

July 12, 1971 Multispectral Scanner Flight

Russell Plot No.	LAI	Ratio Channels 8/7	Ratio Channels 9/7
1	0.01	0.56	0.76
2	2.89	1.63	1.97
3	3.48	1.83	2.18
4	1.30	1.14	1.49
5	0.01	0.58	0.80
6	2.34	1.51	1.78
7	1.11	1.20	1.52
8	0.04	0.63	0.94
9	3.10	1.68	2.02
10	1.17	1.23	1.59
11	2.93	1.62	1.96
12	3.82	1.75	2.09

July 21, 1971 Multispectral Scanner Flight

1	0.11	1.21	0.94
2	3.00	{ Missing Data }	{ Missing Data }
3	4.28		
4	2.31		
5	0.12	1.09	0.94
6	3.57	2.71	2.08
7	2.15	2.39	1.88
8	0.17	1.15	0.98
9	3.38	2.58	1.95
10	2.10	2.42	1.85
11	3.45	2.66	2.08
12	4.06	2.67	2.08

Results and Discussion

Visual Comparisons of Digital Display Imagery

The photographs obtained from the LARS Digital Video Display Unit in the twelve wavelength bands of the multispectral scanner are shown in Figure 12. The Russell sub-plots are rather small to be able to pick out each one individually, but the low ground cover plots do stand out and serve as reference points. The speckled appearance of the imagery in channels 4 and 7 was caused by problems in digitization of the multispectral scanner data, but this problem does not seem to have affected any of the ground features of interest. The bulk corn plots to the east, west, and south of the reflectance panels are of special interest when viewed in all wavelength bands. These bulk corn plots were planted near May 1, and had a very dense cover by this date.

In channels 1-7 the bulk corn fields have a very low reflectance when compared to the gray reflectance panels. It can be seen that the bulk corn fields are reflecting even less than the black reflectance panel except in the peak of the green wavelengths in channel 4 (0.52 to 0.57 μm). This black reflectance panel has a measured percent reflectance of not more than 4% throughout the reflective wavelength range according to DK-2 spectrophotometer measurements. If the black reflectance panel is indeed reflecting less than 4% in the field, then the corn canopies are apparently reflecting even less than 4% in all but channel 4 of the visible wavelengths. This would tend to be in agreement with Knipling (1969) who estimated that the visible wavelength reflectance from a complete canopy may be 3 to 5 percent reflectance.

In channels 8 and 9, the bulk corn fields are reflecting somewhere between the reflectance of the white and the light gray panels. DK-2 spectrophotometer measurements of the white and light gray panels indicate that they reflect 56% and 27% respectively in the wavelength region of channels 8 and 9. If these panel reflectances are similar in the field, the bulk corn canopies are reflecting between 27% and 56%. This is also in agreement with Knipling's estimate that the near infrared reflectance from a complete canopy would be about 35%.

The reflectance of the bulk corn plots decreases in channel 10 from the high reflectances in channels 8 and 9, and then decreases in channel 11 from the reflectance in channel 10. The reflectance of the corn plots follows the same general response as that of green vegetation studied in the laboratory (Hoffer and Johannsen, 1969). The reflectance panels do not have standard thermal properties, but it can be seen from the imagery in channel 12 that all of the panels seem to be quite warmer than their surroundings, especially the relatively cool cornfields.

Scanner Response Ratios and Leaf Area Index for Two Flight Dates

The ratios of scanner data values in channels 9/7 for the July 12 and July 21 flight dates were plotted against leaf area index (Figure 14). The points seemed to indicate that a rather good relationship existed between the ratio of scanner data in channels 9/7 and LAI. A stepwise multiple regression analysis indicated that 96.8% of the variation about the mean LAI could be explained by the second order regression equation, $\hat{Y} = 1.0751 - 2.8756X + 1.9442X^2$, where X is equal to the ratio of scanner data values in channels 9/7. This indicated that ratios of multispectral

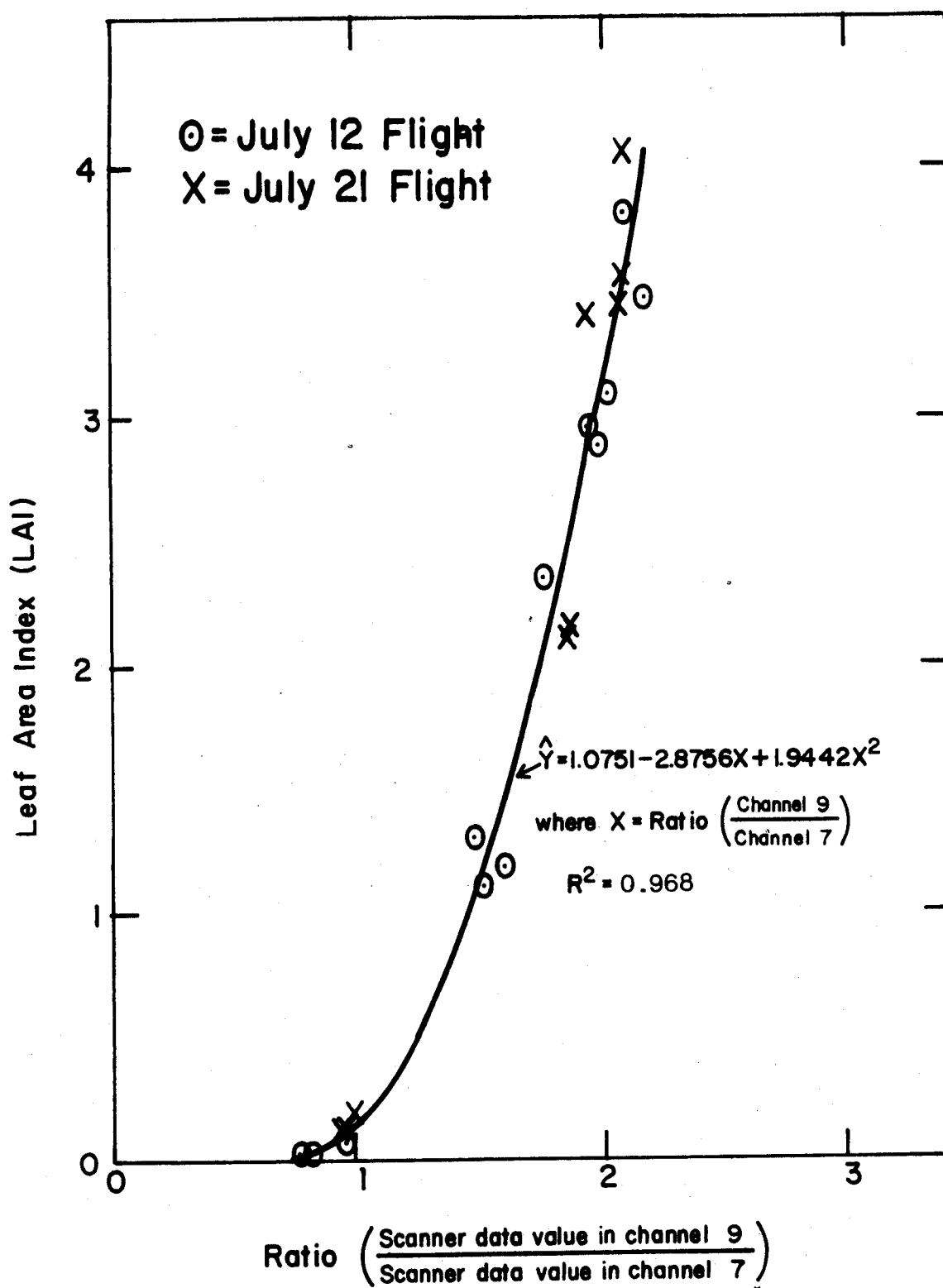


Figure 14. Leaf area index versus the ratio of scanner data values in channels 9/7 for two flight dates.

scanner data may, as hoped for, be related to some ground based measurement of ground cover. It was interesting to note that the ratios of scanner data values for both dates compared quite well even without any calibration of scanner response between the two dates.

It was expected that the ratios of scanner data values in channels 8/7 should also show a good relationship with LAI. The ratios of scanner data values in channels 8/7 for the July 12 and July 21 flight dates were plotted in Figure 15. It very soon became obvious that two separate relationships existed for the two multispectral scanner flights. Step-wise multiple regression analysis indicated that 98.1% of the variation in LAI could be explained by the second order regression equation, $\hat{Y} = -0.48754 + 1.26899X^2$, where X equals the ratio of scanner data values in channels 8/7 for the July 12 scanner flight. For the July 21 scanner flight a linear relationship was indicated which was able to account for 93.0% of the variation in LAI. The regression equation for July 21 was $\hat{Y} = -2.4611 + 2.18245X$, where X equals the ratio of scanner data values in channels 8/7 for the July 21 scanner flight.

A relationship did seem to exist between the ratio of scanner data values in channels 8/7 and LAI, but the same relationship did not hold between flight dates. Apparently a change had taken place between July 12 and July 21 in the way in which the multispectral scanner was recording data in channel 8. This indicated that raw scanner data could be highly unreliable in any attempts to use a ratio technique over time (between flight dates).

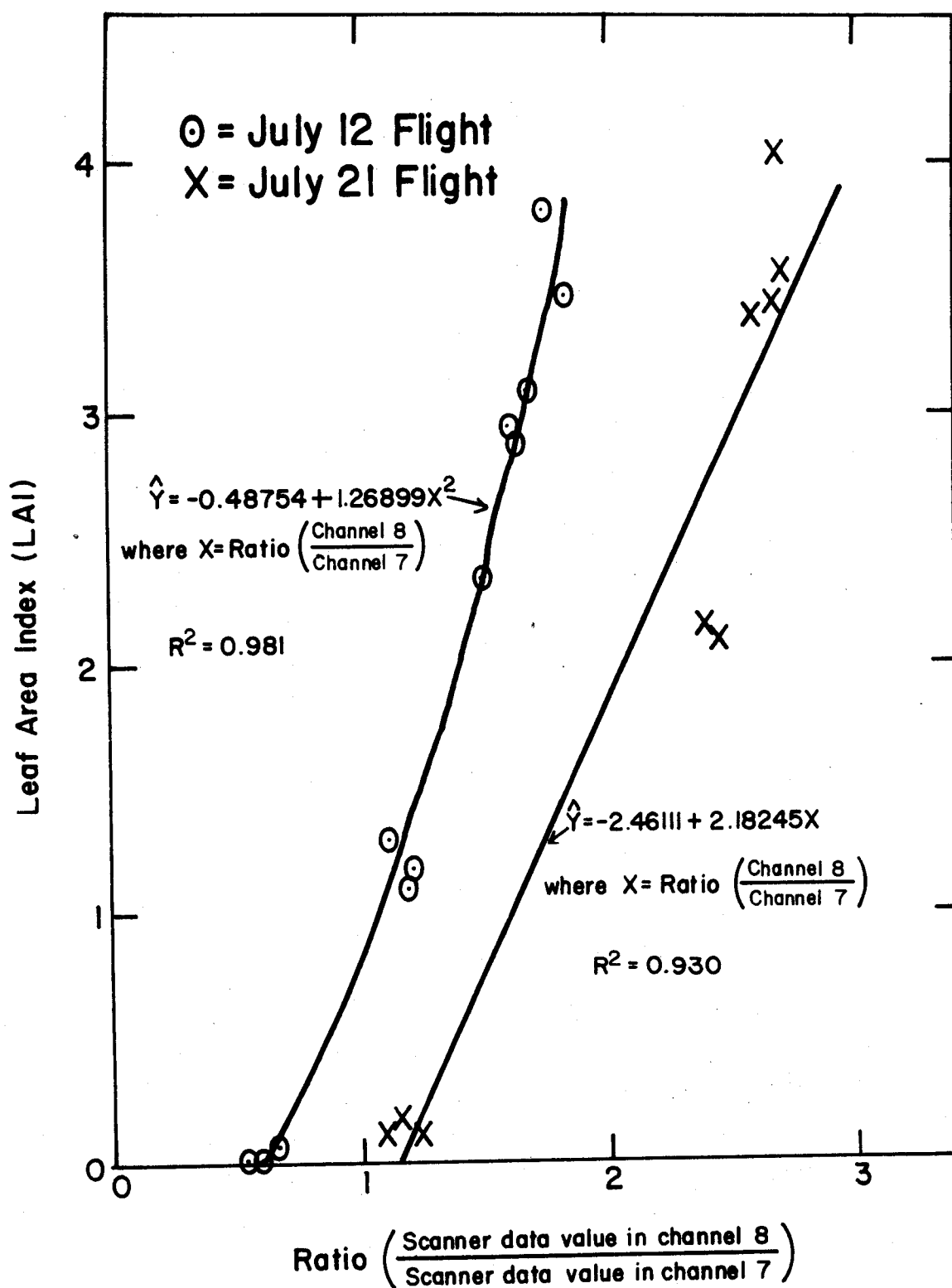


Figure 15. Leaf area index versus the ratio of scanner data values in channels 8/7 for two flight dates.

Problems in Evaluating Scanner Data Over Time

Comparisons of multispectral scanner data between flight dates have always been difficult because of the many variable factors involved. Weather and atmospheric conditions, scene illumination intensity as a function of wavelength, time of day, and angle of illumination can always be counted on to complicate comparisons between multispectral scanner flights.

Not only are there natural phenomena to contend with, but there are also many involving the scanner system itself. Data values for the same ground target have been observed to change from one side of the flightline to the other and from the beginning of a flightline to the end. Changes in scanner response over time within the same flightline may occur due to drift in zero level reference as well as gain changes in the system. Gain changes are often made in one channel and not in another, thus it becomes difficult to make any comparisons between channels over time.

Many potential applications of remote sensing depend on the ability to view repeatedly a target of interest and characterize the spectral properties of that target over time. Ground cover sensing is certainly an area in which this ability is needed. A more sophisticated calibrated airborne spectrophotometer is needed to increase the capability to compare scanner data over time.

Summary and Conclusions

Multispectral scanner data from corn canopies provide more quantitative spectral information on ground cover than does photography. Ratios of uncalibrated scanner data can be used within a given scanner mission to estimate changes in vegetative cover as measured by leaf area index. The peak reflectance wavelengths for green vegetation (0.72 to 1.3 μm) and the region of strong chlorophyll absorption (0.65 μm) seem to provide the best information on changing ground cover.

Regression equations can be evolved relating leaf area index in corn canopies to the ratios of scanner data values from channels 8 and 9 (0.72 to 0.92 μm and 1.0 to 1.4 μm) to scanner data values from channel 7 (0.61 to 0.70 μm). This can only be done within a given flight mission unless the investigator is certain that there were no changes in scanner system gain between flights.

Visual observation of digital display imagery of the ground reflectance panels and nearby cornfields indicated that dense corn canopies reflected less than 4% in most visible wavelength bands. In the 0.72 to 1.4 μm wavelength range, the dense corn canopies reflected between 27% and 56% when compared to the ground reflectance panels. These values were within the expected ranges of reflectance estimated by Knipling (1969).

CHAPTER V

NORMALIZED SPECTRAL RESPONSE OF CORN CANOPIES FROM AIRBORNE MULTISPECTRAL SCANNER DATA

Problem Definition

Airborne multispectral scanner data allow for examination of the spectral differences between various plant canopy covers. Ratios of scanner data response can be related to the ground based measurement of leaf area index. It is desirable to be able to compare results from more than one flight date. In this way the theorized relationships between ratios of scanner data values and leaf area index can be tested.

Variations in scanner system response between flight dates have prevented direct comparison of scanner data over time. Internal calibration standards within the multispectral scanner and reference to ground reflectance panels permit normalization of scanner response between flight dates. The objective of this study was to attempt to normalize the spectral response of corn canopies as detected by an airborne multispectral scanner.

Procedures

Internal Calibration - Black Level and Calibration Lamp

The University of Michigan multispectral scanner records three calibration sources for every scan line of data in the reflective wavelength region. These three calibration values are stored on the Laboratory for Applications of Remote Sensing (LARS) aircraft data storage tape and may be called upon by the data analyst to effect internal calibration of scanner response. The three calibration sources are: 1. CO, a black or dark level reference which gives a measure of black or zero signal level, 2. C1, a constant light source filtered to approximate closely the spectral energy curve of solar illumination, and 3. C2, a sun sensor which measures the solar illumination incident upon the top of the aircraft. These three sources have the potential to permit comparison of multispectral scanner data collected at different times. The black level source, CO, and the precision calibration lamp source, C1, should remain constant with the passage of time, but the sun sensor source, C2, will vary according to solar illumination.

The black level, CO, and precision calibration lamp, C1, are completely internal standards whereas the sun sensor, C2, depends on conditions external to the scanner. The sun sensor records the solar illumination at aircraft altitudes, which may or may not be the same as the solar illumination of the target. Sun sensor calibration becomes particularly undependable on cloudy days when clouds may be shadowing the sun sensor but not the ground target. For purposes of this study, only the CO and C1 calibration sources were used.

The calibration lamp values recorded with the scanner data represent a precise luminous energy source which varies only with the lamp current, lamp age, and lamp filter used. Use of the calibration lamp values compensates for gain changes in the scanner system.

The conversion of analog scanner data to digital form is performed at LARS with the aim of utilizing the maximum dynamic range of the data system. The amplifier gain changes necessary to utilize this dynamic range and the characteristics of the scanner system itself, result in the fact that the data values in each channel are unrelated to those in other channels. Within a channel, however, data values are directly related to scene reflectance by some unknown function.

A linear calibration function is used in the LARSYS processing system (a computer software system developed at LARS for analysis of aircraft scanner data) which delivers data to the statistics processor. Phillips (1969) describes the implementation of this function in the calibration procedure. The calibration function is:

$$D_D = A_C \cdot D_T + B_C$$

where

D_D = Data delivered to the statistics processor

D_T = Data stored on the aircraft data storage tape

A_C and B_C = Calibration values

A_C and B_C are calculated for each scan line of data and are used throughout the entire scan line for which they have been calculated. For this study, A_C and B_C were set to the values for the black level and the

calibration lamp, thus utilizing a two point calibration capable of removing low frequency bias level drift and amplification changes from the system. A_C and B_C could have been set to any of seven combinations of the three calibration sources, but this particular combination was chosen because the system drift and gain were known to vary from one end of the flightline to another.

The calibration values for A_C and B_C in the above equation were extracted from the values for C0 and C1 in the identification record for the particular flightline. The average C0 and C1 values for channels 1 through 11 were calculated and recorded for the July 12 and July 21, 1971 flight dates (Table 9). These C0 and C1 values were used to obtain two point internal calibration of the scanner data response from the Russell silt loam test plots and from the set of ground reflectance panels.

External Calibration - Ground Reflectance Panels

Locating Panels and Obtaining Mean Scanner Data Values. Eight ground reflectance panels were available on the two flight dates (Figure 11). The set consisted of 5 gray level panels of nominal reflectances of 4%, 8%, 16%, 32%, and 64% as well as red, green, and blue panels. These panels served as a form of external calibration providing a ground to aircraft link capable of removing the effect of atmospheric scattering (Silvestro, 1969). Use of the panels allows estimation of gain correction factors for approximation of actual scene reflectance in each channel. Hasell and Larsen (1968) describe the use of these eight reflectance panels in calibrating the output of the University of Michigan multispectral scanner.

Table 9. Internal calibration values for two flight dates.

July 12, 1971 Run No. 71029401

<u>Channel</u>	<u>CO Value</u>	<u>Cl Value</u>
1	24.36	71.08
2	28.27	105.90
3	23.25	94.83
4	29.86	66.63
5	22.05	76.64
6	21.64	92.50
7	28.37	90.10
8	19.64	79.14
9	23.92	33.31
10	19.50	68.89
11	23.84	93.54

July 21, 1971 Run No. 71054401

<u>Channel</u>	<u>CO Value</u>	<u>Cl Value</u>
1	21.87	55.60
2	21.79	78.51
3	23.55	48.40
4	18.24	63.75
5	26.88	66.60
6	21.79	75.04
7	28.72	75.40
8	27.11	68.63
9	23.51	26.10
10	20.36	33.49
11	22.47	40.53

Calibration to ground reflectance panels permits normalization of scanner data to scene reflectance when the area of interest is in environmental proximity to the reflectance panels. Environmental proximity in this case means an area of the same illumination, the same sun angle, the same aircraft altitude, and the same atmospheric conditions as the area from which scanner data are collected for ground reflectance panels.

The approximate locations of the reflectance panels in both flight-lines were determined by outlining the areas with the light pen on the digital display screen. These areas were then clustered using the data from channels 2,4,6,8,10, and 12. Ten cluster classes were requested in each area, but the clustering program decremented the number of cluster classes until only the same number of cluster classes as panels remained. The coordinates of the ground reflectance panels were then obtained from the cluster array map. Each panel was represented by about 100 data points.

The LARSYS statistics processor was used to obtain internally calibrated mean scanner data values for the panels for both flight dates. The values for C0 and C1 in the identification record for each run were used for two point calibration of the scanner response in order to reduce variations caused by gain changes and drift in scanner response throughout the flightline. For the purposes of this study, all C0 values were set equal to zero, and C1 values were calculated by subtracting the identification record values of C0 from the identification record values of C1. This was done in order to set the black level or zero radiation standard to zero response, since the black level standard always has the

lowest response of any object viewed by the scanner. The dynamic range between the identification record values of C0 and C1 was thus retained, the only difference being the scaling-down of the range so that black level response was set to a scanner response of zero. From the resulting scanner data values for the eight ground reflectance panels for the two flight dates, it can be seen that some of the values for the lighter panels saturated or "turned over" because of failure of the scanner system to respond correctly to these high reflectance values (Table 10). The saturated data values could not be used in analysis.

The scanner data values for the ground reflectance panels (Table 10) were later used in relating scanner response to actual scene reflectance. The next step in the procedure involved the laboratory measurement of the percent reflectance of the ground reflectance panels.

Laboratory Measurements of Spectral Reflectance of Panels. It is assumed that the ground reflectance panels behave as perfectly diffuse or Lambertian reflectors of incident illumination; that is, they exhibit a uniform spatial distribution of radiance, independent of the geometry of illumination. Another assumption which had to be made was that laboratory DK-2 spectroradiometer measurements of percent reflectance could be related to percent reflectance in a field situation. No field spectroradiometer was available to measure actual directional reflectance of the panels in the field so the DK-2 spectroradiometer was used to characterize the reflectance of the eight panels.

Differences exist between the DK-2 spectroradiometer and field or airborne spectroradiometers in the way in which they measure percent reflectance. In the DK-2 spectroradiometer, illumination is normal to

Table 10. Scanner data values for ground reflectance panels, calibrated to CO and Cl.

July 12, 1971 Scanner Flight, Run No. 71029401

<u>Channel</u>	<u>64% Gray</u>	<u>32% Gray</u>	<u>16% Gray</u>	<u>8% Gray</u>	<u>4% Gray</u>	<u>Red</u>	<u>Green</u>	<u>Blue</u>
1	saturated	223.62	156.39	90.74	55.84	60.83	154.27	222.28
2	saturated	saturated	226.31	130.58	84.53	85.23	220.10	226.89
3	saturated	230.15	193.56	112.64	73.79	77.83	224.75	209.13
4	saturated	171.23	97.29	55.01	37.17	39.09	144.45	71.57
5	231.26	198.16	112.75	64.47	47.46	60.59	119.51	59.20
6	231.71	218.91	123.83	71.02	52.52	169.55	87.86	65.42
7	229.21	208.59	119.21	65.63	50.72	218.82	69.69	69.21
8	117.04	66.34	41.30	26.68	24.70	137.64	44.20	52.41
9	151.61	82.49	56.90	41.90	43.72	178.24	181.10	183.77
10	239.23	142.13	98.16	71.79	74.13	231.88	239.64	239.64
11	234.44	148.01	102.43	72.58	71.18	225.72	227.72	230.76

Table 10, cont.

July 21, 1971 Scanner Flight, Run No. 71054401

<u>Channel</u>	<u>64% Gray</u>	<u>32% Gray</u>	<u>16% Gray</u>	<u>8% Gray</u>	<u>4% Gray</u>	<u>Red</u>	<u>Green</u>	<u>Blue</u>
1	saturated	222.65	160.76	92.17	52.34	58.02	180.73	224.22
2	saturated	saturated	218.03	130.81	76.76	81.02	221.56	221.34
3	209.03	173.79	97.05	55.35	34.04	36.01	189.69	109.72
4	saturated	220.78	164.10	94.34	62.30	67.47	219.53	119.97
5	215.24	209.84	119.82	69.67	46.68	60.91	139.78	65.88
6	210.96	216.69	131.97	75.10	52.59	163.75	94.71	71.19
7	210.89	207.41	123.46	70.14	49.93	192.21	70.85	75.72
8	122.63	67.56	40.50	26.76	24.33	136.87	40.63	53.39
9	59.66	32.44	22.75	16.93	16.88	71.49	72.38	72.30
10	97.34	52.57	34.67	24.96	21.42	97.66	114.63	116.67
11	81.90	48.55	33.63	25.37	25.12	88.98	97.46	103.37

the sample, and total reflectance is measured in an integrating sphere. Percent reflectance is determined as the ratio of energy reflected from the sample compared to a standard reflectance material (usually MgO). In the field or airborne situation, illumination is more or less hemispherical, and radiance is measured from a single detector location, approximately normal to the panel. At the present time no information is available as to the magnitude of differences between laboratory and field reflectance measurements, and the assumption was made in this study that the differences between the two would not be too great.

Two different sets of color panels were available for the two flight dates. On the July 12 scanner flight date, a set of eight reflectance panels from the University of Michigan's Willow Run Laboratories were deployed at the Purdue University Agronomy Farm. Sample patches of each reflectance panel were taken on July 12, and DK-2 spectral response in the 0.35 to 2.6 μm wavelength range was determined for each sample patch. The set of eight reflectance panels used at the time of the July 21 flight was that belonging to LARS. The LARS reflectance panels were new at the time of the July 21 flight, and the manufacturer's curves for DK-2 spectral response in the 0.35 to 2.6 μm wavelength range were used. The spectral response curves for the LARS red, green, and blue color panels in the 0.35 to 2.0 μm wavelength range as determined by the DK-2 spectroradiometer were plotted (Figure 16). The DK-2 spectroradiometer measurements indicate that the gray reflectance panels have a relatively constant percent reflectance over the wavelength range from 0.35 to 2.0 μm , (Figure 17) whereas the color panels peak sharply in certain wavelength regions.

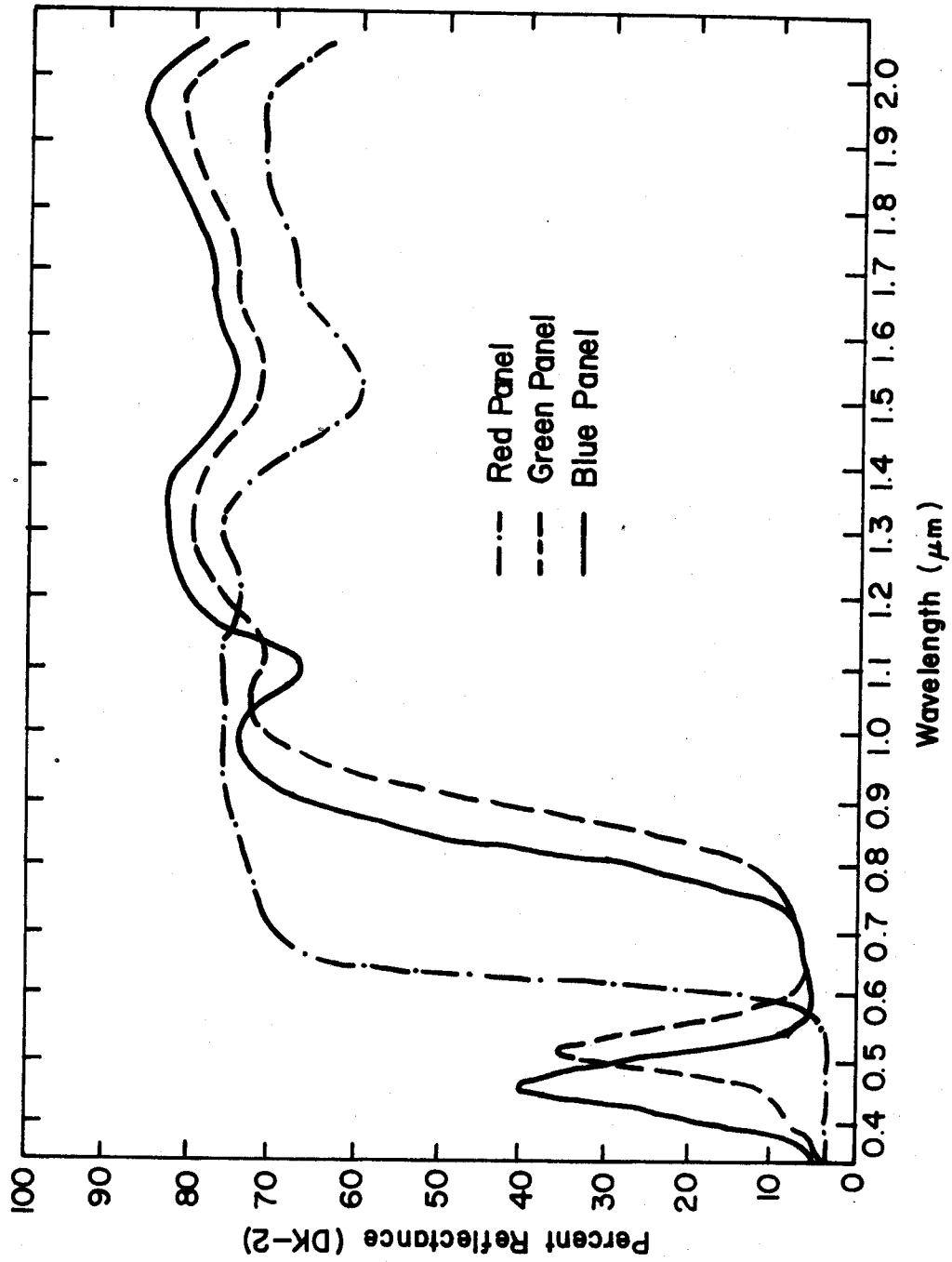


Figure 16. DK-2 spectral reflectance for red, green, and blue LARS color panels.

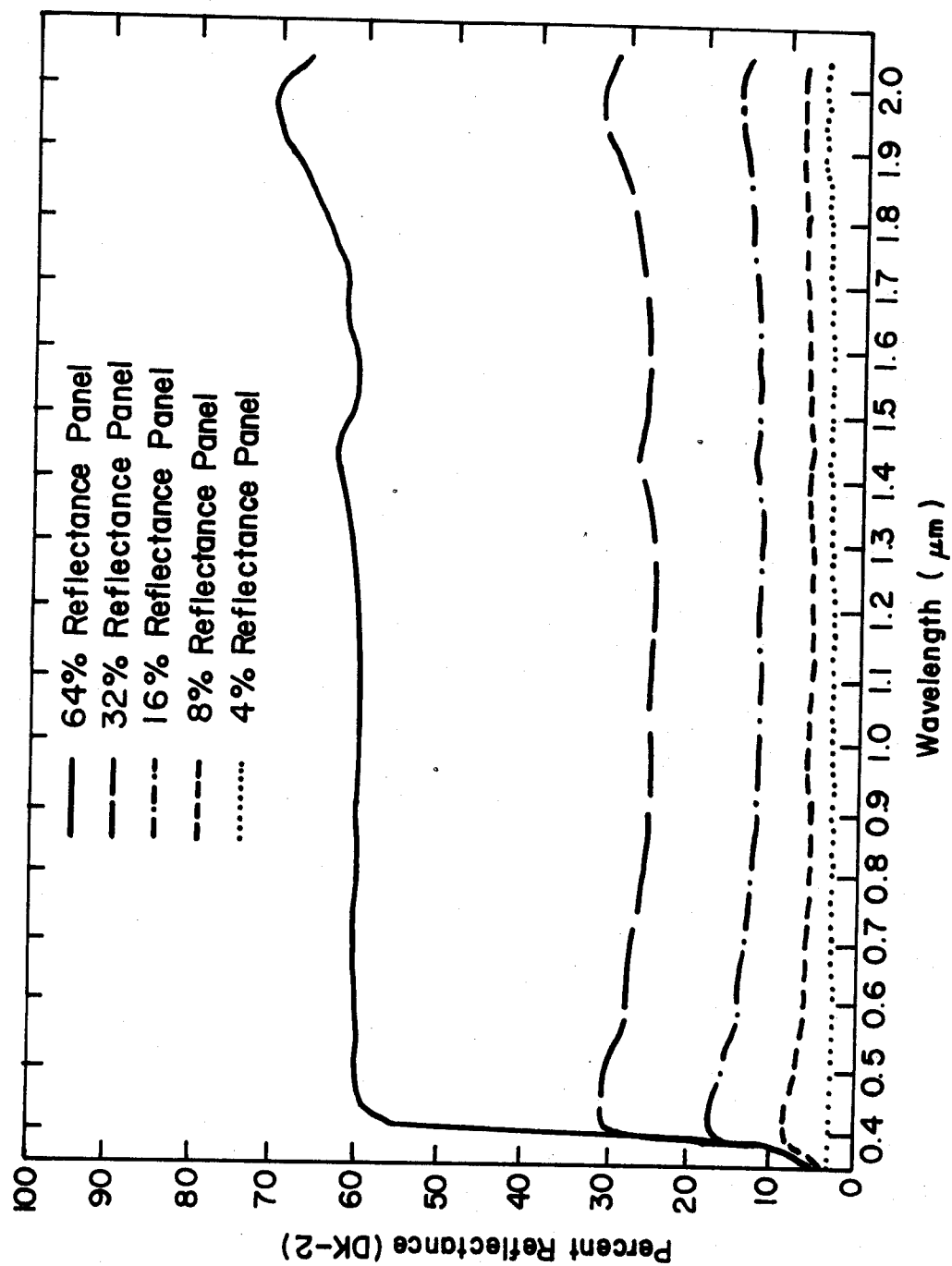


Figure 17. DK-2 spectral reflectance for 5 LARS gray scale panels.

Segments corresponding to the eleven wavelength bands of the multi-spectral scanner were designated on the DK-2 spectral response curves for the reflectance panels. The percent reflectance for each panel was determined at the midpoint of the wavelength band. The percent reflectance values for the eight reflectance panels for both the Michigan and LARS panels were determined and recorded (Table 11). Percent reflectance for the color panels was difficult to determine from the DK-2 spectral curves in wavelength bands in which spectral response changed notably. Therefore, some of the reflectance values for the color panels were questionable, and these particular color panels in certain wavelength bands were not used in relating scanner response to panel reflectance.

Evolving Prediction Equations for Relative Reflectance from Scanner Data Values

Plots were made of percent reflectance (Table 11) versus scanner data values (Table 10) of the reflectance panels for all eleven wavelength bands for both flight dates. Certain panel values were deleted from consideration because of saturation of scanner data values or difficulty in estimating DK-2 reflectance in certain wavelength bands. Specific panels were selected for use in evolving prediction equations for relative reflectance from scanner data values (Table 12).

Percent reflectance (from DK-2 data) versus scanner data values for channel 7 of the July 21 flight were plotted (Figure 18). Five panels were selected to describe the relationship between percent reflectance and scanner data values. Three regression models were theorized:

1. linear equation through the origin,
2. linear equation with negative Y intercept,
- and 3. second order equation forced through the origin. The

Table 11. DK-2 percent reflectance for two sets of color panels in the wavelength regions corresponding to channels of the multi-spectral scanner.

Michigan Reflectance Panels - Used on July 12 Overflight

<u>Channel</u>	<u>Gray Scale Panels</u>					<u>Color Panels</u>		
	<u>64% Gray</u>	<u>32% Gray</u>	<u>16% Gray</u>	<u>8% Gray</u>	<u>4% Gray</u>	<u>Red</u>	<u>Green</u>	<u>Blue</u>
1	46	29	15	8	4	4	21	29
2	47	29	15	8	4	4	30	21
3	48	29	15	8	4	4	31	13
4	49	28	14	7	4	5	23	7
5	50	28	14	7	4	11	17	6
6	51	28	14	7	5	46	10	6
7	52	28	14	7	5	55	9	7
8	55	28	14	7	5	71	26	37
9	58	26	14	8	6	75	77	73
10	55	25	14	8	7	63	70	71
11	39	23	14	9	7	45	51	54

LARS Reflectance Panels - Used on July 21 Overflight

<u>Channel</u>	<u>Gray Scale Panels</u>					<u>Color Panels</u>		
	<u>64% Gray</u>	<u>32% Gray</u>	<u>16% Gray</u>	<u>8% Gray</u>	<u>4% Gray</u>	<u>Red</u>	<u>Green</u>	<u>Blue</u>
1	62	31	18	9	3	3	17	39
2	61	31	17	8	3	3	28	29
3	61	30	17	8	3	3	34	16
4	61	29	16	8	3	4	30	9
5	60	28	15	7	3	7	18	6
6	60	27	14	7	3	30	8	5
7	60	27	14	7	3	62	9	6
8	61	26	13	6	3	73	26	37
9	62	25	12	6	4	75	77	73
10	62	27	13	7	4	64	74	76
11	62	30	15	6	5	50	60	65

Table 12. Reflectance panels selected for regression analysis on two flight dates.

July 12, 1971 Scanner Flight

<u>Channel</u>	<u>No. of Observations</u>	<u>Reflectance Panels Used</u>					
1	6	4%	8%	16%	32%	Red	Blue
2	6	4%	8%	16%	32%	Red	Blue
3	5	4%	8%	16%	32%	Red	
4	6	4%	8%	16%	32%	Red	Green
5	6	4%	8%	16%	32%	Green	Blue
6	6	4%	8%	16%	32%	Green	Blue
7	5	4%	8%	16%	32%	Blue	
8	5	4%	8%	16%	32%	Red	
9	5	4%	8%	16%	32%	Red	
10	5	4%	8%	16%	32%	Red	
11	5	4%	8%	16%	32%	Red	

July 21, 1971 Scanner Flight

<u>Channel</u>	<u>No. of Observations</u>	<u>Reflectance Panels Used</u>					
1	5	4%	8%	16%	32%	Red	
2	4	4%	8%	16%		Red	
3	5	4%	8%	16%	32%	Red	
4	5	4%	8%	16%	32%	Red	
5	6	4%	8%	16%	32%	Green	Blue
6	6	4%	8%	16%	32%	Green	Blue
7	5	4%	8%	16%	32%	Blue	
8	6	4%	8%	16%	32%	64%	Red Green Blue
9	8	4%	8%	16%	32%	64%	Red Green Blue
10	8	4%	8%	16%	32%	64%	
11	6	4%	8%	16%	32%	64%	

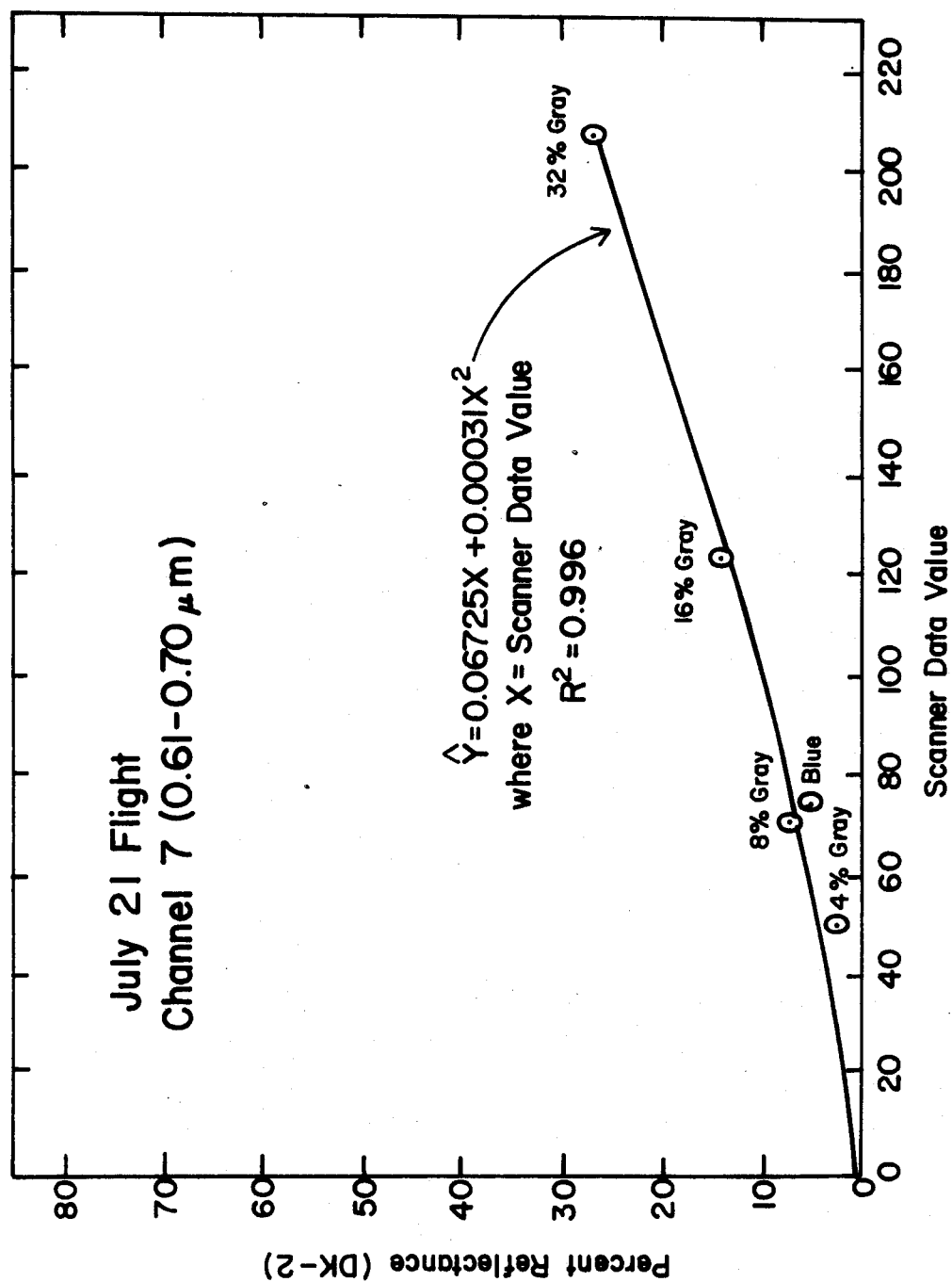


Figure 18. Percent reflectance versus scanner data values in channel 7 for 5 panels, July 21 scanner flight.

first model had a logical basis in the fact that it included the point where scanner data value equaled percent reflectance which equaled 0, but first order regression through the origin failed to provide a satisfactory fit to the five data points. The second model provided a satisfactory fit to the five data points, but resulted in negative estimates of percent reflectance for scanner data values below 31 (of which there were two cases among the July 21 Russell plot scanner data values). The third model provided a satisfactory fit to the five data points, and provided reasonable estimates of percent reflectance for the ground cover plots. A second order regression model, forced through the origin, was used to describe the relationship between percent reflectance and scanner data values for channels 1 through 7 in the visible spectral region.

In the near infrared channels a much different relationship was apparent. Percent reflectance versus scanner data values for channel 9 of the July 21 flight were plotted (Figure 19). A linear regression equation best described this relationship, as it did for all the channels in the reflective infrared.

Prediction equations were determined separately for all eleven channels for both flight dates (Table 13). These prediction equations could be used to determine the relative reflectance, normalized to ground reflectance panels, for ground targets in environmental proximity to the panels.

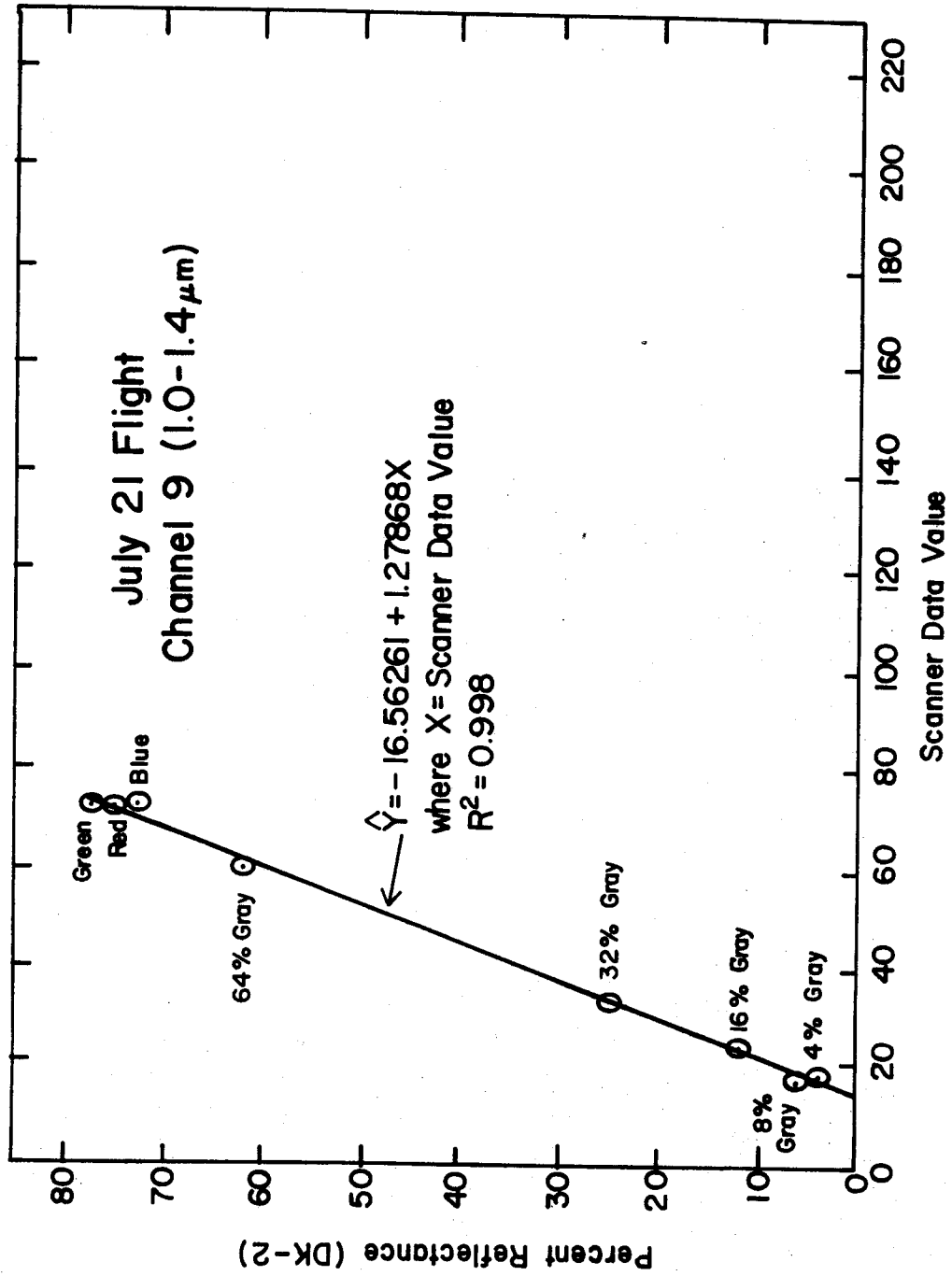


Figure 19. Percent reflectance versus scanner data values in channel 9 for 8 panels, July 21 scanner flight.

Table 13. Prediction equations for percent reflectance (relative to ground reflectance panels) from scanner data values calibrated to C0 and C1.

July 12, 1971 Scanner Flight

$$\hat{Y} = \beta_1 X + \beta_{11} X^2$$

<u>Channel</u>	<u>β_1</u>	<u>β_{11}</u>
1	0.04411	0.00038
2	0.01522	0.00035
3	0.00985	0.00046
4	0.11166	0.00031
5	0.09953	0.00022
6	0.08980	0.00018
7	0.09053	0.00021

$$\hat{Y} = \beta_0 + \beta_1 X$$

<u>Channel</u>	<u>β_0</u>	<u>β_1</u>
8	-9.50851	0.58162
9	-14.67859	0.50190
10	-19.30879	0.34549
11	-9.85590	0.23758

July 21, 1971 Scanner Flight

$$\hat{Y} = \beta_1 X + \beta_{11} X^2$$

<u>Channel</u>	<u>β_1</u>	<u>β_{11}</u>
1	0.04423	0.00043
2	0.02194	0.00026
3	0.12514	-0.00029
4	0.02836	0.00046

Table 13, cont.

<u>Channel</u>	<u>β_1</u>	<u>β_{11}</u>
5	0.08857	0.00023
6	0.05831	0.00031
7	0.06725	0.00031

$$\hat{Y} = \beta_0 + \beta_1 X$$

<u>Channel</u>	<u>β_0</u>	<u>β_1</u>
8	-11.79622	0.60379
9	-16.56261	1.27868
10	-12.58878	0.76388
11	-19.13257	0.99577

Determining Relative Reflectance of Plots Normalized to Panels

In order to apply the prediction equations (Table 13) to the ground cover plots, the scanner data values for the plots had to be obtained using CO-C1 calibration. Mean scanner data values were obtained for the plots in the same manner in which they were obtained for the ground reflectance panels (Table 14).

These prediction equations were then applied to each channel of data for each of the Russell plots listed in Table 14. Percent reflectance values relative to the ground reflectance panels were determined for the ground cover plots. Normalized reflectance values were calculated and recorded (Table 15).

Ratio Techniques for Relating Normalized Reflectance to Leaf Area Index

The same ratio techniques described in the previous chapter were applied to the normalized reflectance data. The ratios of normalized reflectance in channels 8/7 and 9/7 were taken from the values listed in Table 15 and related to leaf area index. These ratios and the corresponding values of LAI were compared (Table 16). Stepwise multiple regression analysis was run on the data to determine the relationship of ratios of normalized reflectance to LAI for the ground cover plots.

Results and Discussion

Evaluation of Normalized Reflectance Curves of Corn Plots

In order to understand the spectral response from corn canopies it is first helpful to get some idea of the individual spectral response of corn leaves and the soil background. DK-2 spectral reflectance curves

Table 14. Mean scanner data values calibrated to C0 and C1 for 12 Russell plots for two flight dates.

July 12, 1971 Multispectral Scanner Flight - Run 71029401

Plot No.	<u>Channels</u>										
	1	2	3	4	5	6	7	8	9	10	11
1	78.78	126.78	114.83	71.80	88.34	111.86	112.58	58.49	97.13	155.89	161.37
2	33.80	50.66	59.15	38.26	44.42	36.70	30.36	75.89	106.81	122.45	85.10
3	28.58	45.12	49.96	29.57	37.47	30.62	24.79	77.90	107.40	100.58	77.28
4	41.00	55.70	67.11	42.48	45.41	45.81	40.98	59.25	92.14	112.41	102.28
5	81.76	126.78	118.06	69.07	86.60	105.02	104.99	56.98	95.95	164.38	164.40
6	40.01	60.74	65.12	42.24	47.15	39.23	36.18	77.65	106.22	125.53	85.86
7	37.53	60.99	67.60	39.25	44.42	46.31	39.47	61.77	91.85	111.90	93.69
8	52.68	77.88	80.78	43.73	55.33	71.11	71.09	43.11	80.70	124.25	132.33
9	30.57	42.34	48.22	32.05	36.48	30.62	27.58	74.37	103.88	99.81	75.00
10	37.77	59.48	64.87	38.76	44.91	45.81	38.71	62.53	96.54	109.33	97.98
11	33.80	50.16	56.17	37.52	42.43	38.21	30.11	75.13	105.34	112.67	84.60
12	30.32	46.38	50.45	32.79	38.46	33.15	26.82	77.15	106.81	106.50	77.02

Table 14, cont.

July 21, 1971 Multispectral Scanner Flight - Run 71054401

Plot No.	<u>Channels</u>										
	1	2	3	4	5	6	7	8	9	10	11
1	115.78	179.61	85.13	162.54	134.29	166.80	170.29	75.35	48.71	84.85	79.61
2											
3	Missing Data - interference from Hi-Ranger Truck										
4											
5	116.85	178.27	84.83	159.83	133.19	164.90	168.94	74.89	47.27	79.66	76.38
6	30.28	44.35	24.54	56.27	40.51	37.88	32.15	67.89	42.59	38.22	30.93
7	35.01	53.41	29.15	73.06	51.46	48.57	39.93	76.89	44.61	42.45	37.63
8	93.80	144.64	70.25	136.92	111.99	136.77	140.44	70.05	44.68	72.51	62.24
9	29.23	43.96	24.85	55.03	38.77	36.85	31.04	76.20	41.15	33.85	26.86
10	40.64	59.87	32.98	73.14	52.80	53.17	47.24	69.74	41.30	40.34	35.07
11	31.24	44.98	23.93	54.72	37.67	37.16	31.91	66.43	41.15	36.40	29.42
12	25.94	37.89	20.55	46.98	33.97	32.25	27.71	63.66	39.14	31.44	24.68

Table 15. Normalized reflectance (relative to ground reflectance panels) of Russell ground cover plots for two flight dates.

July 12, 1971 Multispectral Scanner Flight - Run 71029401

Plot No.	<u>Channels</u>										
	1	2	3	4	5	6	7	8	9	10	11
1	5.83	7.56	7.20	9.62	10.51	12.30	12.85	24.51	34.07	34.55	28.48
2	1.92	1.67	2.19	4.73	4.86	3.54	2.94	34.63	38.93	23.00	10.36
3	1.57	1.40	1.64	3.57	4.04	2.92	2.37	35.80	39.23	15.44	8.50
4	2.45	1.93	2.73	5.30	4.97	4.49	4.06	24.95	31.57	19.53	14.44
5	6.15	7.56	7.57	9.19	10.27	11.42	11.82	23.63	33.48	37.48	29.20
6	2.37	2.22	2.59	5.27	5.18	3.80	3.55	35.65	38.63	24.06	10.54
7	2.19	2.23	2.77	4.86	4.86	4.54	3.90	25.42	31.42	19.35	12.40
8	3.38	3.31	3.80	5.48	6.18	7.30	7.50	15.56	25.82	23.62	21.58
9	1.70	1.27	1.54	3.90	3.92	2.92	2.66	33.75	37.46	15.17	7.96
10	2.21	2.14	2.57	4.79	4.91	4.49	3.82	26.86	33.77	18.46	13.42
11	1.92	1.64	2.01	4.63	4.62	3.69	2.92	34.19	38.19	19.62	10.24
12	1.69	1.46	1.67	3.99	4.15	3.17	2.58	35.36	38.93	17.49	8.44

Table 15, cont.

July 21, 1971 Multispectral Scanner Flight - Run 71054401

Plot No.	<u>Channels</u>										
	1	2	3	4	5	6	7	8	9	10	11
1	10.89	12.33	12.75	16.76	16.04	18.35	20.44	33.70	45.72	52.23	60.14
2											
3	Missing Data - interference from Hi-Ranger Truck										
4											
5	11.04	12.17	12.70	16.28	15.88	18.04	20.21	33.42	43.88	48.26	56.92
6	1.73	1.48	3.25	3.05	3.97	2.65	2.48	29.20	37.90	16.61	11.67
7	2.08	1.91	3.89	4.53	5.17	3.56	3.18	34.63	40.48	19.84	18.34
8	7.93	8.61	10.22	12.51	12.80	13.77	15.56	30.50	40.57	42.80	42.84
9	1.66	1.47	3.29	2.95	3.78	2.57	2.39	34.21	36.06	13.27	7.61
10	2.51	2.25	4.44	4.54	5.32	3.98	3.87	30.21	36.25	18.23	15.79
11	1.80	1.51	3.16	2.93	3.66	2.59	2.46	28.31	26.06	15.22	10.16
12	1.44	1.20	2.69	2.35	3.27	2.20	2.10	26.64	33.48	11.43	5.44

Table 16. Ratios of normalized reflectance in channels 8/7 and 9/7 for Russell plots on two flight dates.

July 12, 1971 Scanner Flight

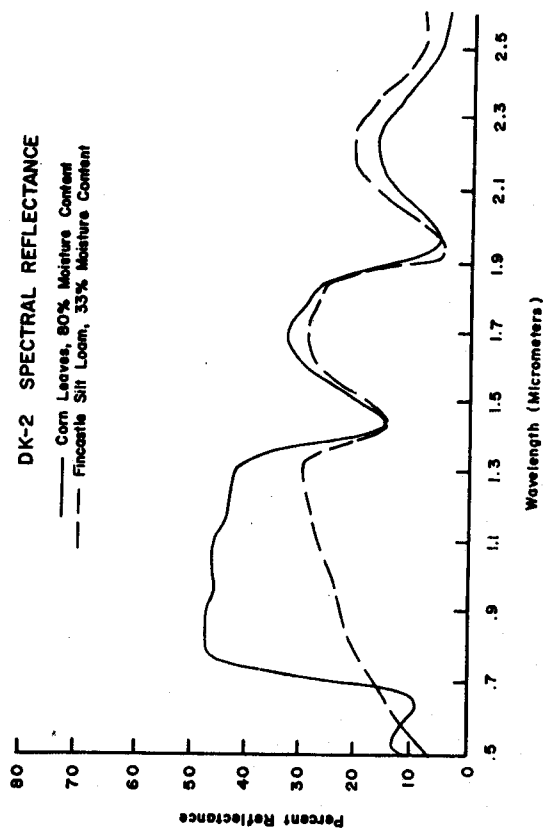
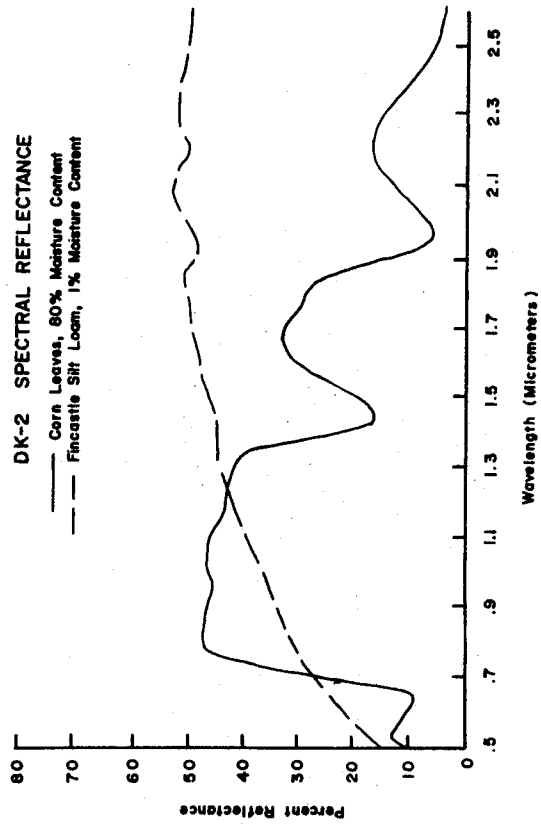
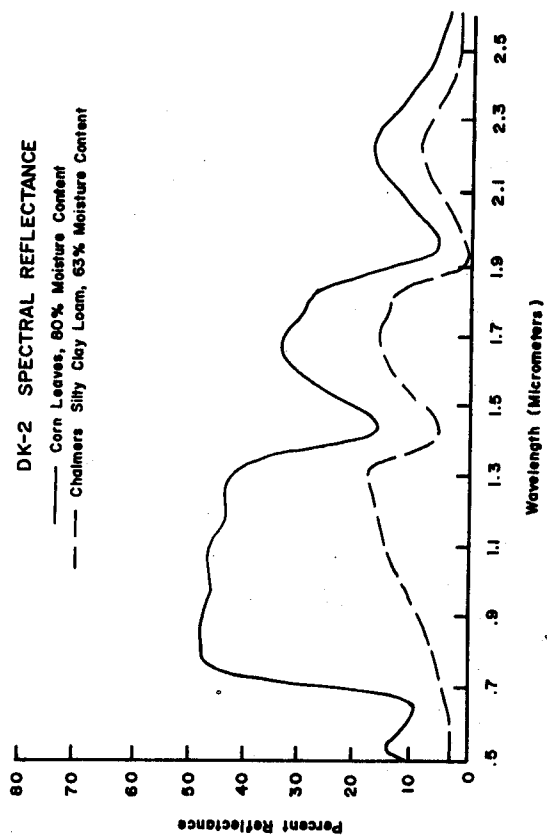
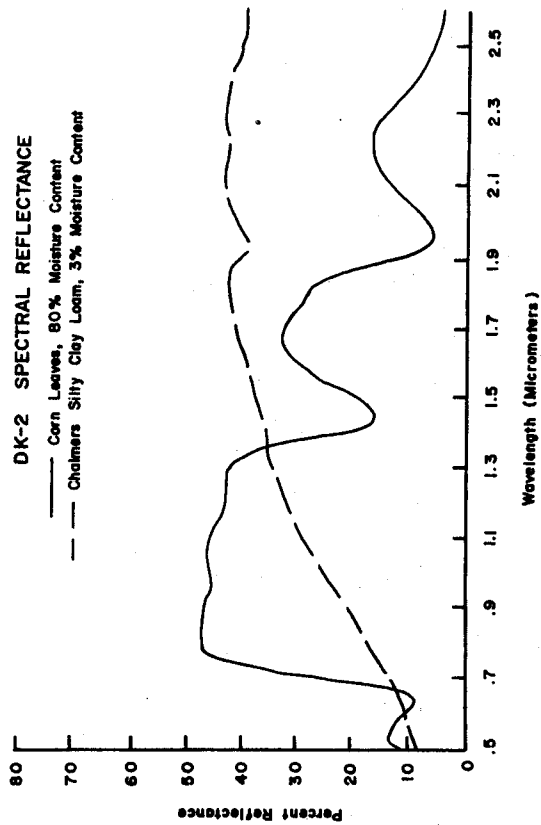
<u>Plot No.</u>	<u>LAI</u>	<u>Ratio Channels 8/7</u>	<u>Ratio Channels 9/7</u>
1	0.01	1.91	2.65
2	2.89	11.78	13.24
3	3.48	15.11	16.55
4	1.30	6.15	7.78
5	0.01	2.00	2.83
6	2.34	10.04	10.88
7	1.11	6.77	8.06
8	0.04	2.07	3.44
9	3.10	12.69	14.08
10	1.17	7.03	8.84
11	2.93	11.71	13.08
12	3.82	13.71	15.09

July 21, 1971 Scanner Flight

<u>Plot No.</u>	<u>LAI</u>	<u>Ratio Channels 8/7</u>	<u>Ratio Channels 9/7</u>
1	0.11	1.65	2.24
2	3.00	{ Missing Data }	{ Missing Data }
3	4.28		
4	2.31		
5	0.12	1.65	2.17
6	3.57	11.77	15.28
7	2.15	10.89	12.73
8	0.17	1.96	2.61
9	3.38	14.31	15.09
10	2.10	7.83	9.37
11	3.45	11.51	14.66
12	4.06	12.69	15.94

for corn leaves with 80% moisture content, and two soils in saturated and air dry conditions were obtained (Figure 20). The spectral response curves for Chalmers silty clay loam, a dark surface soil, and Fincastle silt loam, a light surface soil, are shown. Fincastle silt loam is the somewhat poorly drained member of the catena of which Russell silt loam is the well drained member. The spectral curves for the Russell soil should be very similar to those illustrated for the Fincastle soil since they have the same surface color and texture and about the same organic matter content. It is obvious that moisture content of the soil can greatly affect the spectral response of the soil. The surface soil condition in a field situation would probably be closer to the spectral response illustrated for the air dry soil than that for the saturated soil (Hoffer and Johannsen, 1969).

The curves of scanner data values versus wavelength for three of the Russell plots on the July 12 flight date were plotted (Figure 21). The plots represent three greatly different ground cover conditions. The scanner data values used are the uncalibrated scanner response values from the July 12 multispectral scanner mission over the Agronomy Farm (Table 7). The wavelength scale is incremented in micrometers on the bottom of the graph, with the corresponding midpoints of the channel wavelength bands being displayed at the top of the graph. It can be seen that there is no relationship between adjacent channels and that the shape of the spectral response curves can in no way be related to any familiar response curves for green vegetation or bare soil.



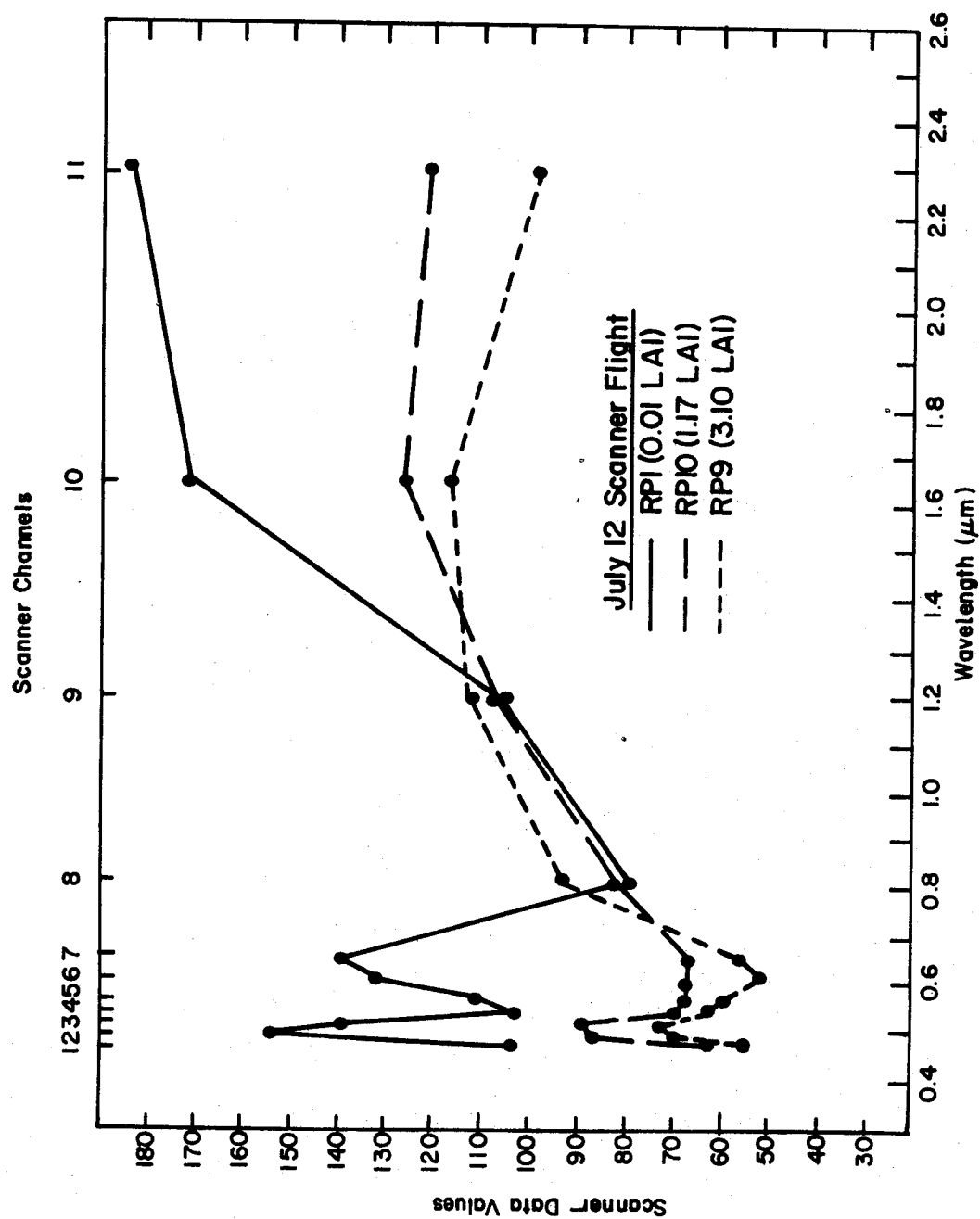


Figure 21. Uncalibrated scanner response curves for 3 Russell plots, July 12.

Normalized spectral response curves for three different ground cover situations were plotted for two scanner flight dates (Figures 22 and 23). The normalized response curves of Figure 22 are of the same three ground cover plots shown in Figure 21. The same original data were used for plotting these curves. The only difference is that the scanner data values in the latter have been normalized to relative reflectance, using the ground reflectance panels. The relative reflectance values for Figures 22 and 23 were obtained from Table 15. The curves in Figure 22 resemble the DK-2 spectral response curves for green vegetation and bare soil. They have the familiar peaks in the green and near infrared wavelengths for green vegetation and the relatively smoothly increasing curve for bare soil (Figure 20). The plot with the higher leaf area index has a higher response in the 0.72 to 1.3 μm wavelength region and a lower response in the 0.65 μm chlorophyll absorption region than does the plot with a lesser LAI. The response curve in Figure 22 for Russell plot 1, with an LAI of 0.01 (essentially bare soil) resembles quite closely the response curve in Figure 20 for air dry Fincastle soil.

In the plots of normalized spectral response curves (Figures 22 and 23) it is observed that the plots with high percent ground cover have a lower response in channels 10 and 11 than plots with lesser ground cover. This is probably a result of the spectral response of vegetation from the medium ground cover plots being "mixed" with the spectral response of the bare soil.

The normalized response curve for Russell plot 8 (Figure 23) shows much higher response throughout the 0.46 to 2.6 μm wavelength range than for Russell plot 1 (Figure 22), even though the ground cover was slightly

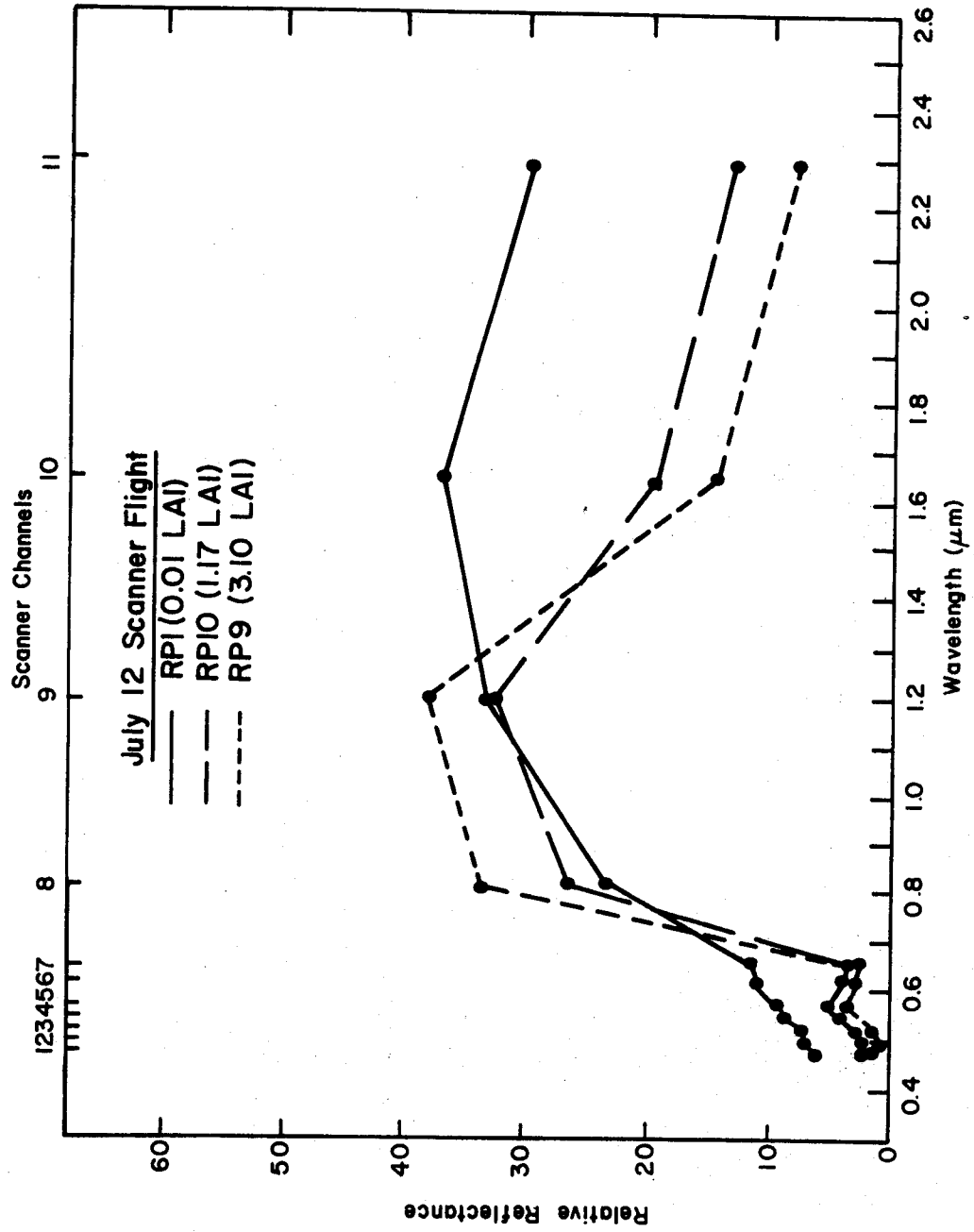


Figure 22. Normalized spectral response curves for 3 Russell plots, July 12.

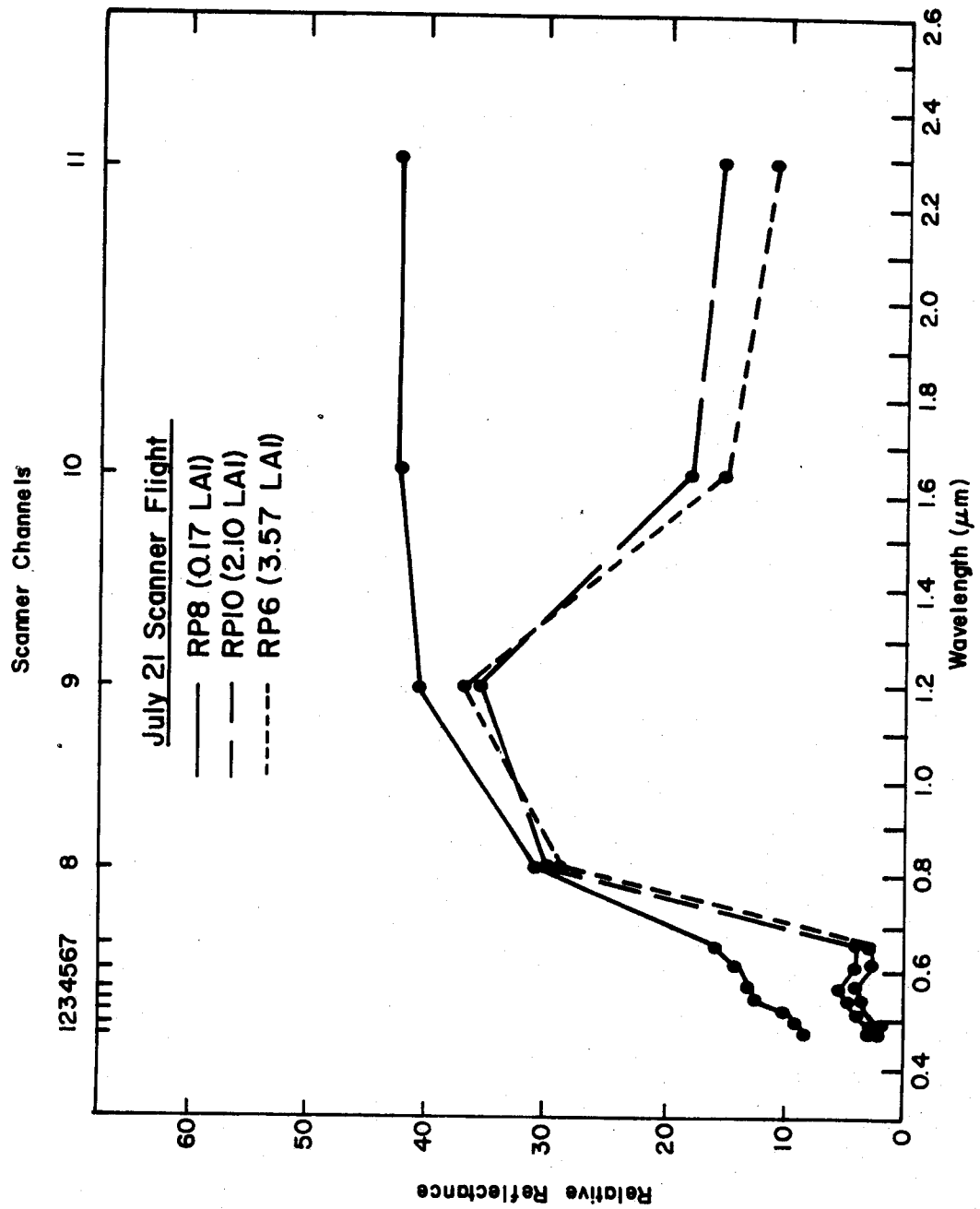


Figure 23. Normalized spectral response curves for 3 Russell plots, July 21.

higher on Russell plot 8. Upon further investigation it was theorized that the great differences in spectral response between these two plots were not accountable only to ground cover differences. Examination of the Hi-Ranger photography taken over these two plots on July 13 and July 21 showed that the soil background appeared much lighter on the July 21 photography of Russell plot 8. Weather records from the Agronomy Farm Weather Station indicated that a long dry period preceded the July 21 flight while a rather substantial rain fell the day before the July 12 flight. It is likely then, that the great differences observed in the spectral response of the low ground cover plots on the two flight dates were accountable more to moisture differences than differences in ground cover.

Relative Reflectance Ratios and Leaf Area Index for Two Flight Dates

The ratios of normalized reflectance in channels 8/7 and 9/7 were calculated for the two flight dates (Table 16). These ratios were then plotted against leaf area index (Figures 24 and 25). Stepwise multiple regression indicated a linear relationship between LAI and both ratios. Using the ratio of 9/7 for normalized data, 96.4% of the variation in LAI could be explained by the regression equation, $\hat{Y} = -0.7245 + 0.2735X$. For the ratio of 8/7 for normalized data, 94.1% of the variation in LAI could be explained by the regression equation, $\hat{Y} = -0.5117 + 0.2971X$.

A considerable improvement occurred in the use of the ratio of normalized data in channels 8/7 to predict LAI over the use of uncalibrated scanner data values in these channels. The procedure of normalizing the reflectance of the plots to the ground reflectance panels apparently was successful in eliminating variations in scanner response between flight dates.

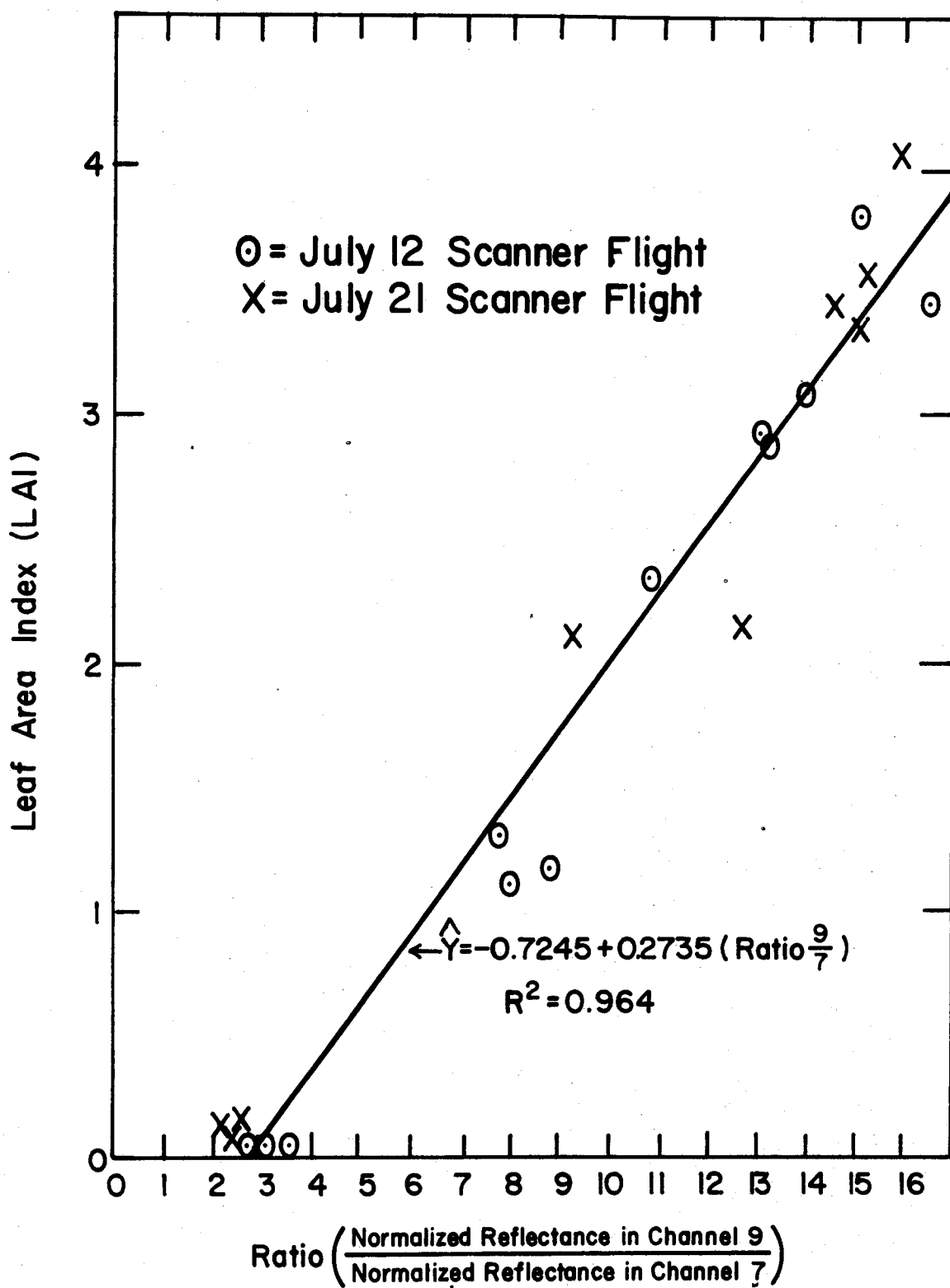


Figure 24. Leaf area index versus the ratio of normalized reflectance in channels 9/7 for two flight dates.

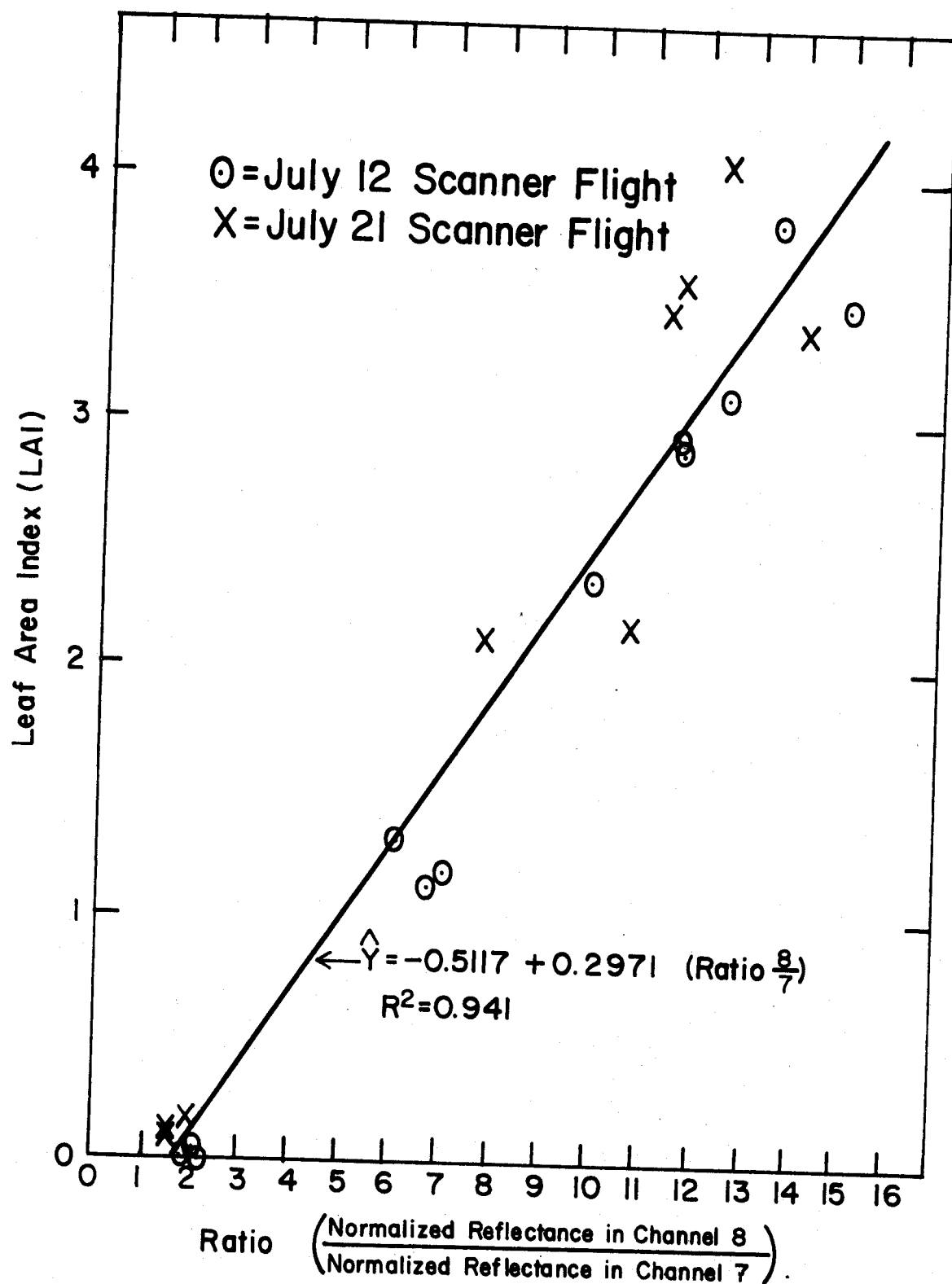


Figure 25. Leaf area index versus the ratio of normalized reflectance in channels 8/7 for two flight dates.

Summary and Conclusions

Multispectral scanner response can be related to the reflectance of ground reflectance panels in arriving at prediction equations for relative reflectance from scanner data values. This normalization of scanner data to ground reflectance panels allows for extension over time of ratio techniques for predicting leaf area index. Regression equations can be evolved relating leaf area index to the ratios of scanner data values from channels 8 and 9 to scanner data values from channel 7.

Spectral response curves for corn canopies can be determined from the derived prediction equations relating panel reflectance to scanner response. The spectral response curves for different ground cover plots from normalized scanner data show that the various ground cover response curves represent a "mixing" of the spectral response from the green vegetation and bare soil components.

The normalized spectral response curves for the ground cover plots indicate an increase in reflectance in the 0.72 to 1.3 μm near infrared wavelength region with increasing leaf area index. A decrease in reflectance was observed for the 0.65 μm chlorophyll absorption band with increasing leaf area index.

Moisture differences apparently had a strong effect on the spectral response of the corn canopies on the two flight dates. Soil moisture differences greatly affect the spectral response from low ground cover plots.

The use of ground reflectance panels aids in arriving at normalized reflectance values for corn canopies. One drawback is the lack of a reflectance panel whose reflectance in the visible wavelength region is as low as that of a dense corn canopy. For this reason, extrapolation of data below the known reflectance value of the 4% reflectance panel is necessary. This may introduce error in estimating the normalized reflectance of dense corn canopies in the visible wavelength region.

The practical implications of using ratio techniques for analysis of ground cover are certain to become apparent in future efforts in remote sensing. The orbital perspective of the Earth Resources Technology Satellite (ERTS) and SKYLAB will provide a general view of agricultural crops. With the extremely high altitude and coarse resolution from space platforms such as these, it is likely that differences in vegetative cover will provide the strongest means of discriminating between various healthy green agricultural crops. Ratio techniques utilizing information from the near infrared and chlorophyll absorption regions should prove useful in analyzing relative vegetative cover.

BIBLIOGRAPHY

1. Allen, W. A., and A. J. Richardson. 1968. Interaction of light with a plant canopy. *J. Opt. Soc. Amer.* 58:1023-1028.
2. Anuta, P. E., and R. B. MacDonald. 1971. Crop surveys from multi-band satellite photography using digital techniques. *Remote Sensing of Environment.* 2:53-67.
3. Baumgardner, M. F., S. J. Kristof, C. J. Johannsen, and A. L. Zachary. 1969. Effects of organic matter on the multispectral properties of soils. *Proc. of the Indiana Acad. of Sci.* 79:413-422.
4. Bouyoucos, G. J. 1913. An investigation of the soil temperature and some of the most important factors influencing it. *Mich. Agr. Exp. Sta. Tech. Bull. No. 17.* pp. 1-196.
5. Bowers, S. A., and R. J. Hanks. 1965. Reflectance of radiant energy from soils. *Soil Sci.* 100(2):130-138.
6. Breece, H. T. III, and R. A. Holmes. 1971. Bidirectional scattering characteristics of healthy green soybean and corn leaves in vivo. *Applied Optics.* 10:119-127.
7. Cipra, J. E., M. F. Baumgardner, E. R. Stoner, and R. B. MacDonald. 1971. Measuring radiance characteristics of soil with a field spectroradiometer. *Soil Sci. Soc. Amer. Proc.* 35:1014-1017.
8. Condit, H. R. 1970. The spectral reflectance of American soils. *Photogrammetric Engineering.* 36:955-966.
9. Cuellar, J. A. 1971. Correlation of ground cover estimated from aerial photos with ground observations. *Spectral Survey of Irrigated Region Crops and Soils.* 1971 Annual Report, USDA, Weslaco, Texas. pp. IV.13.-IV.17.
10. Eastman Kodak Company. 1968. *Practical Densitometry.* Kodak Pamphlet No. E-59. Rochester, New York. 23pp.

11. Fritz, N. L. 1971. New color films for aerial photography. Proceedings of the Third Biennial Workshop on Aerial Color Photography in the Plant Sciences. A. Anson (ed.) (Amer. Soc. of Photogrammetry, Florida Dept. Agr., Univ. of Florida and USDA) Gainesville, FL. pp. 45-68.
12. Fu, K. S., D. A. Landgrebe, and T. L. Phillips. 1969. Information processing of remotely sensed agricultural data. Proceedings of the IEEE. 57:639-653.
13. Gates, D. M. 1962. Energy Exchange in the Biosphere. New York: Harper and Row, Publishers. 151 pp.
14. Gates, D. M. 1963. The energy environment in which we live. American Scientist. 51:327-348.
15. Gates, D. M. 1965. Characteristics of soil and vegetated surfaces to reflected and emitted radiation. Proc. 3rd Symp. Remote Sensing of Environment. Univ. of Michigan, Ann Arbor, MI. pp. 573-600.
16. Gates, D. M., H. F. Keegan, J. C. Schleter, and V. R. Weidner. 1965. Spectral properties of plants. Applied Optics. 4:11-20.
17. Gausman, H. W., W. A. Allen, and R. Cardenas. 1969. Reflectance of cotton leaves and their structures. Remote Sensing of Environment. 1:19-22.
18. Gerbermann, A. H., H. W. Gausman, and C. L. Wiegand. 1969. Shadow and other background effects on optical density of film transparencies. In Aerial Color Photography in the Plant Sciences. Knipling, E. B. (ed.) (Florida Dept. Agr., Univ. Florida and USDA) Gainesville, FL. pp. 127-129.
19. Hasell, P. G. Jr., and L. M. Larsen. 1968. Calibration of an airborne multispectral optical sensor. Technical Report ECOM-00013-137, Willow Run Laboratories, Institute of Science and Technology, Univ. of Michigan, Ann Arbor, MI. 87 pp.
20. Hoffer, R. M. 1967. Interpretation of remote multispectral imagery of agricultural crops. Report of the Laboratory for Agricultural Remote Sensing, Purdue University Agr. Exp. Sta. Res. Bull. 831. pp. 18-30.
21. Hoffer, R. M., and C. J. Johannsen. 1969. Ecological principles in spectral signature analysis. In Remote Sensing in Ecology. Univ. of Georgia Press, P. Johnson (ed.), Athens, GA. pp. 1-16.

22. Hoffer, R. M., P. E. Anuta, and T. L. Phillips. 1971. Applications of ADP techniques to multiband and multiemulsion digitized photography. LARS Information Note 091071, Laboratory for Applications of Remote Sensing, Purdue University. 19 pp. Accepted for publication in Photogrammetric Engineering.
23. Holmes, R. A., and R. B. MacDonald. 1969. The physical basis of system design for remote sensing in agriculture. Proceedings of the IEEE. 57:629-639.
24. Idso, S. B., D. G. Baker, and D. M. Gates. 1966. The energy environment of plants. Advances in Agronomy. 18:171-216.
25. Idso, S. B., and C. T. deWit. 1970. Light relations in plant canopies. Applied Optics. 9:177-184.
26. Johannsen, C. J. 1969. The detection of available soil moisture by remote sensing techniques. Ph.D. Thesis. Purdue Univ. (Library Call No. 22744). Univ. Microfilms. Ann Arbor, MI, (order no. 70-8909). 287pp.
27. Knipling, E. B. 1969. Leaf reflectance and image formation on color infrared film. In Remote Sensing in Ecology. Univ. of Georgia Press, P. Johnson (ed.) Athens, GA. pp. 17-29.
28. Knipling, E. B. 1970. Physical and physiological basis for the reflectance of visible and near-infrared radiation from vegetation. Remote Sensing of Environment. 1:155-160.
29. Kristof, S. J., and M. F. Baumgardner. 1970. Changes of multi-spectral soil patterns with increasing crop canopy. Abstract in Proceedings of the Indiana Academy of Science for 1970. 80:443.
30. Krumpe, P. F. 1972. Remote sensing of terrestrial vegetation: a comprehensive bibliography. Forestry Remote Sensing Laboratory, Univ. of California, Berkeley, CA. 69pp.
31. Kumar, R. 1972. Radiation from plants - reflection and emission: a review. Publication No. 72-2-2 of the School of Aeronautics, Astronautics, and Engineering Sciences, Purdue University. 105 pp.
32. Laboratory for Agricultural Remote Sensing (LARS). 1967. Remote Multispectral Sensing in Agriculture. Vol. II (Annual Report). Purdue University Agr. Exp. Sta. Res. Bull. 832. pp. 13-24.
33. Laboratory for Agricultural Remote Sensing (LARS). 1968. Remote Multispectral Sensing in Agriculture. Vol. III (Annual Report). Purdue Univ. Agr. Exp. Sta. Res. Bull. 844. pp. 53-58.

34. Laboratory for Agricultural Remote Sensing (LARS). 1970. Remote Multispectral Sensing in Agriculture. Vol. IV (Annual Report). Purdue Univ. Agr. Exp. Sta. Res. Bull. 873. pp. 80-86.
35. McCree, K. J. 1968. IR sensitive film for spectral measurements under plant canopies. Agr. Meteorol. 5:203-208.
36. McKee, G. W. 1964. A coefficient for computing leaf area in hybrid corn. Agron. J. 56:240-241.
37. Miller, L. D. 1969. Measurement of resource environments with airborne thermal mappers - where do we stand? Proceedings of the Purdue Centennial Year Symposium on Information Processing. Purdue Univ. pp. 746-763.
38. Miller, L. D. and R. L. Pearson. 1971. Areal mapping program of the IBP grassland biome: remote sensing of the productivity of the short-grass prairie as input into biosystem models. Proceedings of the Seventh Symposium on Remote Sensing of Environment. Univ. of Mich. Ann Arbor, MI. pp. 165-205.
39. Myers, V. I., C. L. Wiegand, M. D. Heilman, and J. R. Thomas. 1966. Remote sensing in soil and water conservation research. Proceedings of the Fourth Symposium on Remote Sensing of Environment. Univ. of Mich., Ann Arbor, MI. pp. 801-813.
40. Myers, V. I. 1970. Soil, water, and plant relations. In Remote Sensing with Special Reference to Agriculture and Forestry. National Academy of Sciences, J. R. Shay (ed.), Washington, D.C. pp. 253-297.
41. Null, W. S. 1969. Photographic interpretation of canopy density - a different approach. Journal of Forestry. 67:175-177.
42. Phillips, T. L. 1969. Calibration of scanner data for operation processing programs at LARS. LARS Information Note 071069. Laboratory for Applications of Remote Sensing, Purdue University, 7 pp.
43. Silvestro, F. B. 1969. Multispectral photographic determination of reflectance. Photogrammetric Engineering. 35:259-262.
44. Sinclair, T. R. 1968. Pathway of solar radiation through leaves. Master's Thesis, Purdue University.
45. Vinogradov, B. W. 1969. Remote sensing of the arid zone vegetation in the visible spectrum for studying the productivity. Proceedings of the Sixth Symposium on Remote Sensing of Environment. Univ. of Mich., Ann Arbor, MI. pp. 1237-1250.

46. Wacker, A. G., and D. A. Landgrebe. 1970. Boundaries in multi-spectral imagery by clustering. Proceedings of the Ninth IEEE Symposium on Adaptive Processes XI. pp. 4.1-4.8.

UNCLASSIFIED

Security Classification

DOCUMENT CONTROL DATA - R & D

(Security classification of title, body of abstract and indexing annotation must be entered when the overall report is classified)

1. ORIGINATING ACTIVITY (Corporate author) School of Agriculture Purdue University		2a. REPORT SECURITY CLASSIFICATION unclassified	
3. REPORT TITLE Multispectral Determination of Vegetative Cover in Corn Crop Canopy		2b. GROUP	
4. DESCRIPTIVE NOTES (Type of report and inclusive dates) scientific report			
5. AUTHOR(S) (First name, middle initial, last name) Eric R. Stoner Marion F. Baumgardner			
6. REPORT DATE June, 1972		7a. TOTAL NO. OF PAGES 126	7b. NO. OF REFS
8a. CONTRACT OR GRANT NO. NASA Grant NGR 15-005-112		9a. ORIGINATOR'S REPORT NUMBER(S)	
b. PROJECT NO.		9b. OTHER REPORT NO(S) (Any other numbers that may be assigned this report) LARS Print #111072	
c.			
d.			
10. DISTRIBUTION STATEMENT unlimited			
11. SUPPLEMENTARY NOTES		12. SPONSORING MILITARY ACTIVITY NASA	
13. ABSTRACT This research was designed to study the relationship between different amounts of vegetative ground cover and the energy reflected by corn canopies. Low altitude photography and an airborne multispectral scanner were used to measure this reflected energy. Field plots were laid out, representing four growth stages of corn. Two plot locations were chosen--on a very dark and a very light surface soil. Color and color infrared photographs were taken from a vertical distance of 10 m. Estimates of ground cover were made from these photographs and were related to field measurements of leaf area index. Ground cover could be predicted from leaf area index measurements by a second order equation. Color infrared photography proved helpful in determining ground cover on dark soil backgrounds, as long as the ground cover did not exceed about 75%. Microdensitometry and digitization of the three separated dye layers of color infrared film showed that the near infrared dye layer is most valuable in ground cover determinations. Computer analysis of the digitized photography provided an accurate method of determining percent ground cover. Multispectral scanner data were collected in two flights over the light soil background plots at an altitude of 305 m. Energy in eleven reflective wavelength bands from 0.46 to 2.6 um was recorded by the scanner. A set of eight ground reflectance panels was in close proximity to the ground cover plots and was used to try to normalize the scanner data over time. Ratio techniques were used to relate uncalibrated scanner response to leaf area			

-over-

UNCLASSIFIED

Security Classification

UNCLASSIFIED

Security Classification

14. KEY WORDS	LINK A		LINK B		LINK C	
	ROLE	WT	ROLE	WT	ROLE	WT
<p>13. ABSTRACT (from previous page)</p> <p>index. The ratios of scanner data values for the 0.72 to 0.92 um band over the 0.61 to 0.70 um band and the 1.0 to 1.4 um band over the 0.61 to 0.70 um band were calculated for each plot. The ratios related very well to leaf area index for a given scanner flight date, but could not be generalized between flights because of uncertainty in scanner response over time.</p> <p>Ground reflectance panels were used to relate laboratory reflectance measurements to scanner response. Separate prediction equations were obtained for both flight dates for all eleven reflective wavelength bands of the multispectral scanner. In this way, scanner response was normalized to ground panel reflectance. Ratios of normalized scanner data could be related to leaf area index over time.</p> <p>The normalized scanner response was used to plot relative reflectance versus wavelength for the ground cover plots. Spectral response curves resulted which were similar to those for bare soil and green vegetation as determined by laboratory measurements. The spectral response of different ground cover plots represented a "mixing" of the spectral response curves for the bare soil and green vegetation components of the scene.</p> <p>The spectral response curves from the normalized scanner data indicated that reflectance in the 0.72 to 1.3 um wavelength range increased as leaf area index increased. A decrease in reflectance was observed in the 0.65 um chlorophyll absorption band as leaf area index increased. This confirmed the validity of using the ratio of the response from a near infrared wavelength band to that of the red wavelength band in relating multispectral scanner data to leaf area index in corn.</p>						

UNCLASSIFIED

Security Classification